The 2017 Chesapeake Bay Water Quality and Sediment Transport Model

A Report to the US Environmental Protection Agency Chesapeake Bay Program

May 2017 Draft

Carl F. Cerco
Mark R. Noel

US Army Engineer Research and Development Center, Vicksburg MS

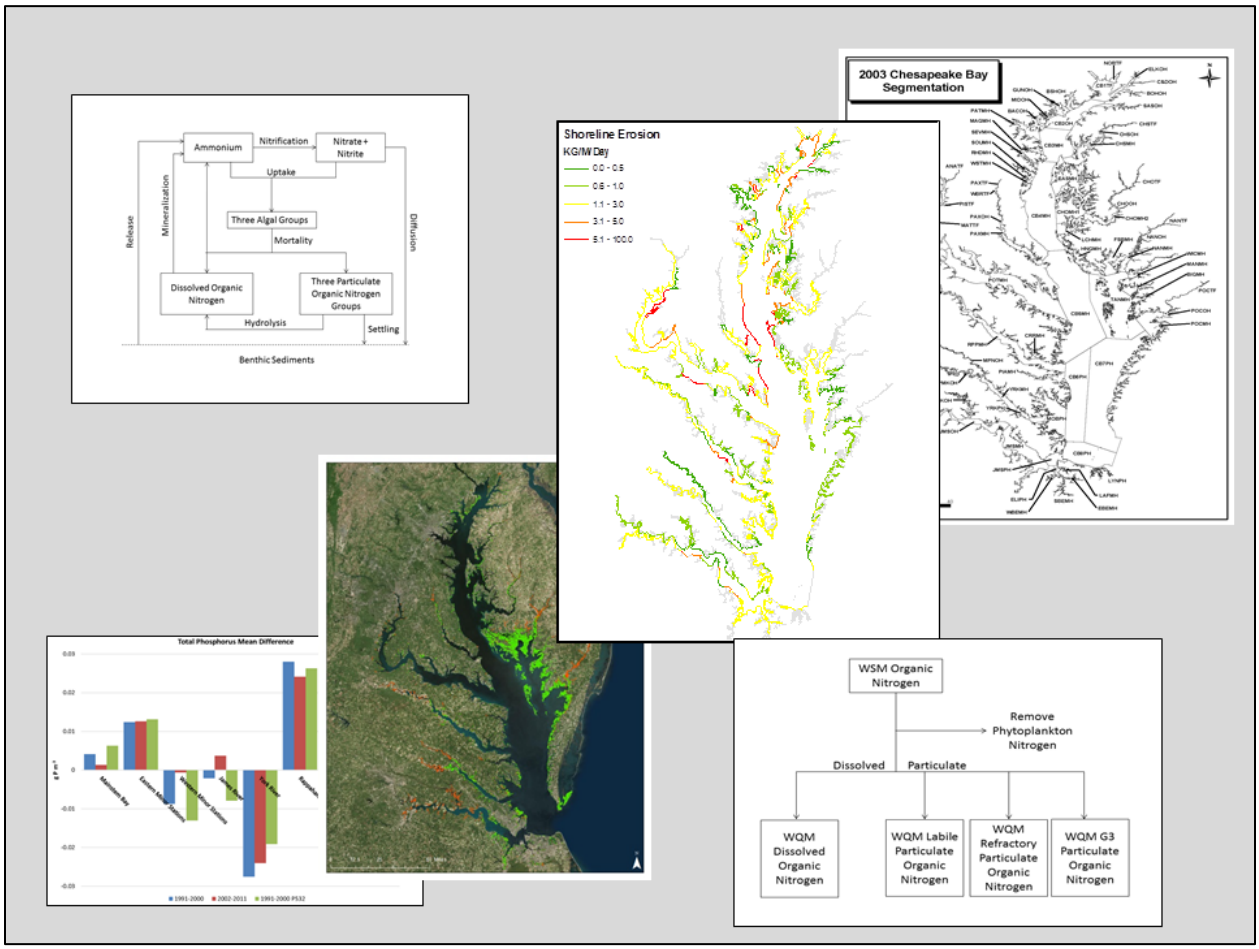

Abstract

This report provides draft documentation for the 2017 version of the Chesapeake Bay Water Quality and Sediment Transport Model (WQSTM). This model version is intended to provide support for the 2017 Midpoint Assessment of the 2010 Chesapeake Total Maximum Daily Loads (TMDL). The model is calibrated to the years 1991-2000 and validated with an independent data set from 2002-2011. Watershed loads for the application period are provided by a "Beta 4" version of the Phase 6 Chesapeake Bay Watershed Model (WSM). These loads will be replaced by a final version of Phase 6 loads at which time the WQSTM will undergo final calibration. Major changes to the WQSTM structure are not anticipated although an improved WQSTM calibration is expected.

The first section of this report summarizes changes from previous versions of the WQSTM. Notably, a wetlands module has been introduced and three particulate organic matter classes are now specified in the water column, corresponding to the three classes in the sediment diagenesis model. The second section of the report details model kinetics which are largely based on the original kinetics developed in 1992. Silica and zooplankton state variables have been deleted, however, due to data limitations and no evidence they influence the TMDL standards being evaluated. This model version reinstitutes a partial-attenuation model for the computation of light attenuation, as detailed in Chapter 3. The partial attenuation model relaxes data requirements which limited application of the preceding optical model. The new wetlands module is described in Chapter 4. The next section describes loads to the water column from shoreline erosion. This model version incorporates nutrient loads as well as suspended solids. The processes for linking the WQSTM to loads from the watershed, point-sources, and atmosphere are described in Chapter 6. The mapping of WSM variables into WQSTM variables is detailed. The report concludes with a statistical summary of model results. At present, the model computations of total nitrogen are in excess of observations. We expect this excess will be corrected through implementation of a final set of WSM loads followed by final calibration of the WQM. Time-series and spatial comparisons of the model to observations are provided in appendices for the calibration and verification. The comparisons emphasize model variables critical to the TMDL which focuses on dissolved oxygen, chlorophyll, and water clarity.

Acknowledgements

Funding for this study was provided by the US EPA Chesapeake Bay Program through an Inter-Agency Agreement with the US Army Engineer District Baltimore. Modeling Coordinator at the Chesapeake Bay Program was Mr. Lewis Linker.

Point of Contact

Carl F. Cerco, PhD, PE
Research Hydrologist (retired)
US Army ERDC
3909 Halls Ferry Road
Vicksburg MS 39180
769-230-5543
carlcerco@outlook.com

1 Introduction

The study described here builds on a modeling framework established nearly 30 years ago and subjected to continuous revision since then. Four major study phases preceded this one. The first phase (Cerco and Cole 1994) provided modeling technology for the 1991 re-evaluation of the 1987 nutrient reduction goals. The second phase (Cerco et al. 2002) refined the computational grid to improve representation in the Virginia tributaries and introduced living resources into the computational framework. This phase provided computational tools for the Tributary Strategy management effort. The third phase (Cerco and Noel 2004a) continued the grid refinements and extended the model into still smaller tributaries. This version of the model provided verification for a 2003 agreement to cap average annual nitrogen and phosphorus loads to the bay. The fourth phase (Cerco et al. 2010) provided modeling technology to support development of the 2010 Total Maximum Daily Load (TMDL) for Chesapeake Bay.

The present model version is referred to as the 2015 Chesapeake Bay model. This phase of modeling has multiple objectives including:

- Extend the model application period to encompass recent observations including those collected in the Shallow Water Monitoring Program.
- Perform adjustments and re-calibration necessary to accommodate loads computed by Phase 6 of the Chesapeake Bay Program (CBP) Watershed Model (WSM).
- Provide modeling technology to support a 2017 Mid-Point Reassessment of the 2010 TMDL.

The final objective stated above is considered the most consequential and the schedule of the present study was specified to provide a 2017 product.

What's New, What's Not?

Each preceding model application employed a different combination of model features and required addition of capabilities to support project goals. The present study follows this precedent. This study breaks precedent by removing model features which are obsolete or no longer relevant. Brief descriptions of model revisions since the 2010 version are described below. More detailed descriptions of significant revisions are provided in succeeding chapters.

Application Period

The 2015 study introduces a new intensive calibration period from 2002 to 2011. Model application to this period is subject to the same graphical presentations and statistical comparisons to observations conducted for the preceding 1991-2000 calibration period. Examination and presentation of the 1991-2000 results are retained since the years 1993-1995 form the basis for the TMDL determination. The earlier years also provide a rich data set of living resource and process observations for comparison with relevant model results.

Model Kinetics

Particulate Organic Matter

The model of the water column was originally formulated (Cerco and Cole 1994) with two classes of particulate organic matter: labile and refractory. These classes were distinguished by their reaction rates. Labile material decomposed on a time scale of days to weeks while refractory material required more time. Labile and refractory state variables were defined for carbon, nitrogen, and phosphorus.

The sediment diagenesis model (DiToro and Fitzpatrick 1993) was formulated with three classes of organic matter: G1, G2, G3 (Westrich and Berner 1984). These classes indicate labile, refractory, and slow refractory material. Upon settling to the sediments, labile state variables in the water column were routed to the G1 sediment state variables. Refractory state variables in the water column were split between G2 and G3 sediment state variables. This arrangement proved unsatisfactory in the 2015 model. Problems occurred because the split into G2 and G3 occurred at the sediment-water interface. Distinctions in G2 and G3 content could not be assigned to refractory particles originating from different sources e.g. phytoplankton vs. shoreline erosion loads. The problem was alleviated by introducing a third reactive class of organic material to the suite of water column state variables. Labile, refractory, and G3 particles in the water are now routed directly to G1, G2, and G3 classes in the diagenesis model. Internal and external sources of particulate organic material are provided with individual, potentially distinct, particle composition.

Silica

Silica was included in the original model to allow for potential nutrient limitation of diatoms during the spring algal bloom in the Bay and lower tributaries. Two state variables were required: particulate biogenic silica (PBS) and dissolved silica (Dsil). Application of the silica sub-model was hindered from the onset by a shortfall of PBS observations. While Dsil was regularly monitored in the water column and at river inputs, only sporadic observations were available for specification of PBS loads and for calibration of PBS in the water column. Subsequent model applications indicated that phosphorus is the predominant limiting nutrient during the spring algal bloom. Consequently, silica has been eliminated from the 2015 model.

Zooplankton

Zooplankton were added to the model circa 2000 during the Virginia Tributary Refinements phase (Cerco et al. 2002). One motivation was an interest in direct computation of living resources e.g. submerged aquatic vegetation, zooplankton, and benthos. A second motivation was to improve computation of phytoplankton dynamics by improving predation terms. Two zooplankton classes were added: microzooplankton and mesozooplankton. Both classes preyed upon phytoplankton. The model formulation included an additional predation term to represent other planktivores including menhaden. Despite model limitations, credible representations of zooplankton biomass were obtained (Cerco and Myers 2000). During an effort to improve computations of primary production, however, we found the formulation of the additional predation term was more important than the zooplankton representation in determining primary production (Cerco and Noel 2004b). Interest in zooplankton results has diminished since they were introduced and their inclusion added little to the model. Consequently, zooplankton were eliminated from the 2015 model version.

Sediment Diagenesis Model

Testa et al. (2013) revised the denitrification formulation in the original diagenesis model. Their revision provided improved computations of sediment-water nitrate flux across a range of environments from freshwater to mesohaline. The revised formulation is incorporated in the 2015 model.

Deposit-feeding benthos were added to the diagenesis model at the same time living resources were added elsewhere (Cerco and Meyers 2000). The deposit feeders were living resource indicators but served no purpose in the model. Deposit feeders fed on and recycled sediment carbon. We found they influenced carbon cycling among various reactive classes in an unpredictable manner. In view of diminished interest and uncertain influence, deposit feeders were eliminated from the 2015 model.

Wetlands Module

Tidal wetlands exert a potentially large influence on the concentrations of dissolved and suspended materials in the adjacent open waters (references). Wetland processes can play a significant role, largely through removal processes, in estuarine nutrient and solids budgets (references). In recognition of wetland effects, protocols have been developed to provide nutrient and sediment mass reduction credits for shoreline management projects that include restoration of vegetation (Drescher and Stack 2015).

Wetlands respiration has been represented in the Chesapeake Bay model since the 2002 version (Cerco and Noel 2004a). Incorporation of wetlands respiration was required to reflect low dissolved oxygen concentrations observed in open waters adjacent to extensive tidal wetlands. Wetlands respiration is now incorporated into a more representative wetlands module. The module was developed largely in response to the potential credits allowed in the TMDL for wetlands restoration (Drescher and Stack 2015). The module also improves

model performance in regions with extensive wetlands. Development of a mechanistic biogeochemical wetlands model is a formidable task beyond the scope of this study. The module does, however, provide basic representations of relevant wetlands processes including burial of organic and inorganic particles, denitrification, and respiration.

Shoreline Erosion

State-of-the-art quantification of solids loads entering the Bay from shoreline erosion was conducted concurrent with the 2010 model study (Cerco et al. 2010). The loads were derived from long-term shoreline recession rates and accounted for structures and other local features. The quantification added previously-unavailable spatial detail to estimated solids loads. The solids loads from the 2010 model are retained in the 2015 version.

Shoreline erosion adds nutrients to the Bay as well as solids. Phosphorus, especially, contributed by erosion is a significant portion of the system total phosphorus load. Nutrients associated with shoreline erosion have been included in various model versions (Cerco and Noel 2004a) but were omitted from the 2010 version. The loads were omitted because no guidance existed as to how to incorporate them in the TMDL development. A recent panel report recognizes the potential for nutrient reduction credits associated with erosion management practices but withholds recommendations pending more information on nutrient availability/reactivity. In view of the recognized contribution of shoreline erosion to the Bay nutrient budget and the pending consideration of these nutrients in TMDL development, nutrient loads from shoreline erosion are restored to this model version.

Oysters

Bivalve filter feeders were added to the model as part of the Tributary Refinements phase (Cerco et al. 2002). The addition reflected the general interest in living resources as well as a specific mandate to investigate the impact of a ten-fold increase in oyster population on Bay water quality. The filter feeder module incorporated two freshwater bivalve groups as well as oysters. Investigation of a ten-fold increase in oyster population (Cerco and Noel 2007) led to the following conclusions:

- The contemporary oyster population had little effect on water quality.
- A ten-fold increase would improve conditions in the vicinity of oyster reefs but do little to alleviate hypoxia in deep channels of the Bay and tributaries.

Representation of oysters was operable in the 2010 model version but received limited attention. Effects of oyster restoration were not considered in the TMDL development. Oysters are receiving increased attention because of the rapid rise in aquaculture and the potential associated beneficial effects (references?). As a consequence of the increased interest, the oyster module has been updated to reflect contemporary populations on reefs and current aquaculture operations.

Light Attenuation

The initial versions of the bay model calculated light attenuation in the water column through various partial-attenuation models. Attenuation was the linear sum of contributions from water itself and from suspended particles. The 2010 model version incorporated an advanced optical model which calculated attenuation as a non-linear function of attenuation from color and attenuation and scattering from solids and chlorophyll. The advanced model added rigor to the calculation of light attenuation but at a cost. The model was demanding in data requirements for parameterization. The complex formulation rendered the model difficult to "tune" to improve agreement between predictions and observations. As a consequence, the 2015 model restores a partial attenuation relationship for calculation of light attenuation.

Submerged Aquatic Vegetation

Submerged aquatic vegetation (SAV) was added to the 2002 model version along with other living resources. The model is basically a representation of SAV production and loss on a unit-area basis. SAV biomass and fluxes between SAV and the surrounding water, on the unit-area basis, are multiplied by the SAV bed area associated with each cell in the model computational grid to obtain biomass and fluxes associated with the cell. Specification of bed area has been problematic since the initial model application (Cerco and Moore 2001), especially since the area changes in response to processes which are not entirely understood or predicable. The 2010 model defined SAV cells distinct from the water quality model computational grid. The extent of the SAV cells was determined by the largest historical observed bed area. The actual bed area within each cell was determined by light penetration to the bottom. The algorithm to determine area did not function well, largely because area was determined exclusively by light availability. Processes which allow or prevent SAV propagation to areas with sufficient illumination were absent. The 2015 model specifies bed area based on annual surveys. This specification enhances the computation of total SAV biomass and ensures the correct representation of mass fluxes between SAV and the Bay water column.

Hydrodynamics

The calculation of hydrodynamics via the CH3D hydrodynamic model is unchanged from the 2010 model version. The model application period has been extended to 2011 and hydrodynamic calculations have been updated as revised calculations of hydrology become available from the watershed model. Likewise, the calculation of surface waves and bottom shear stress for the sediment transport model are unchanged. The sediment transport model itself is exactly as parameterized and employed in the 2010 model. The reader is referred to the 2010 documentation for details.

References

Cerco, C.F. and Cole, T. M. (1994). "Three-dimensional eutrophication model of Chesapeake Bay," Technical Report EL-94-4, U.S. Army Engineer Waterways Experiment Station, Vicksburg MS.

Cerco, C., and Meyers, M. (2000). "Tributary refinements to the Chesapeake Bay Model," *Journal of Environmental Engineering*, 126(2), 164-174.

Cerco, C., and Moore, K. (2001). "System-wide submerged aquatic vegetation model for Chesapeake Bay," *Estuaries*, 24(4), 522-534.

Cerco, C., Johnson, B., and Wang, H. (2002). "Tributary refinements to the Chesapeake Bay model," ERDC TR-02-4, US Army Engineer Research and Development Center, Vicksburg, MS.

Cerco, C., and Noel, M. (2004a). "The 2002 Chesapeake Bay eutrophication model," EPA 903-R-04-004, Chesapeake Bay Program Office, US Environmental Protection Agency, Annapolis MD. (available at http://www.chesapeakebay.net/modsc.htm)

Cerco, C., and Noel, M. (2004b). "Process-based primary production modeling in Chesapeake Bay," *Marine Ecology Progress Series*, 282, 45-58.

Cerco, C., and Noel, M. (2007). "Can oyster restoration reverse cultural eutrophication in Chesapeake Bay?," *Estuaries and Coasts*, 30(2), 331-343.

Cerco, C., Kim, S.-C. and Noel, M. (2010). "The 2010 Chesapeake Bay eutrophication model," Chesapeake Bay Program Office, US Environmental Protection Agency, Annapolis MD. (available at http://www.chesapeakebay.net/publications/title/the_2010_chesapeake_bay_eutrophication_model1)

DiToro, D., and Fitzpatrick, J. (1993). "Chesapeake Bay sediment flux model," Contract Report El-93-2, US Army Corps of Engineers Waterways Experiment Station, Vicksburg MS.

Drescher, S., and Stack, B. (2015). "Recommendations of the expert panel to define removal rates for shoreline management projects," Chesapeake Bay Partnership. (available at http://www.chesapeakebay.net/documents/Shoreline_Management_Protocols_Final_Approved_07132015-WQGIT-approved.pdf)

Testa, J., Brady, D., DiToro, D., Boynton, W., Cornwell, J., and Kemp, W. (2013). "Sediment flux modeling: Simulating nitrogen, phosphorus, and silica cycles," *Estuarine, Coastal and Shelf Science*, 131, 245-263.

Westrich, J., and Berner, R. (1984). “The role of sedimentary organic matter in bacterial sulfate reduction: The G model tested,” *Limnology and Oceanography*, 29(2), 236-249.

2 Water Quality Model Formulation

Introduction

CE-QUAL-ICM was designed to be a flexible, widely-applicable eutrophication model. Initial application was to Chesapeake Bay (Cerco and Cole 1994). Subsequent additional applications included the Delaware Inland Bays (Cerco et al. 1994), Newark Bay (Cerco and Bunch 1997), San Juan Estuary (Bunch et al. 2000), Virginia Tributary Refinements (Cerco et al. 2002) and the 2002 (Cerco and Noel 2004) and 2010 (Cerco et al. 2010) Chesapeake Bay models. Each application employed a different combination of model features and required addition of system-specific capabilities. This chapter describes general features and site-specific developments of the model as presently applied to the water column of Chesapeake Bay.

Conservation of Mass Equation

The foundation of CE-QUAL-ICM is the solution to the three-dimensional mass-conservation equation for a control volume. Control volumes correspond to cells on the model grid. CE-QUAL-ICM solves, for each volume and for each state variable, the equation:

$$\frac{\delta V_j \cdot C_j}{\delta t} = \sum_{k=1}^{n} Q_k \cdot C_k + \sum_{k=1}^{n} A_k \cdot D_k \cdot \frac{\delta C}{\delta x_k} + \Sigma S_j \qquad (1)$$

in which:

V_j = volume of j^{th} control volume (m^3)
C_j = concentration in j^{th} control volume (g m^{-3})
t, x = temporal and spatial coordinates
n = number of flow faces attached to j^{th} control volume
Q_k = volumetric flow across flow face k of j^{th} control volume (m^3 s^{-1})
C_k = concentration in flow across face k (g m^{-3})
A_k = area of flow face k (m^2)
D_k = diffusion coefficient at flow face k (m^2 s^{-1})
S_j = external loads and kinetic sources and sinks in j^{th} control volume (g s^{-1})

Solution of Equation 1 on a digital computer requires discretization of the continuous derivatives and specification of parameter values. The equation is solved using the QUICKEST algorithm (Leonard 1979) in the horizontal plane and an implicit central-difference scheme in the vertical direction. Discrete time steps, determined by computational stability requirements, are $\approx$ 5 minutes.

State Variables

At present, the CE-QUAL-ICM model incorporates 24 state variables in the water column including physical variables, multiple algal groups, and multiple forms of carbon, nitrogen, and phosphorus (Table 1).

Algae

Algae are grouped into three model classes: freshwater, spring diatoms, and other green algae. The model formulations for the three groups are virtually identical. The definition of three groups provides flexibility in parameter evaluation to fit various regions of the Bay system. In particular, definition of a freshwater group allows maximum flexibility in parameter specification in freshwater portions of the system which vary greatly in terms of physical characteristics, loading, and surroundings. The spring diatoms are large phytoplankton which produce an annual bloom in the saline portions of the bay and tributaries. Algae which do not fall into the preceding two groups are lumped into the heading of green algae. The green algae represent the mixture that characterizes saline waters during summer and autumn, and freshwater regions in which a specific algal group is not defined. Non-bloom forming diatoms comprise a portion of this mixture.

Organic Carbon

Four organic carbon state variables are considered: dissolved, labile particulate, refractory particulate, and G3 particulate. Labile, refractory, and G3 distinctions are based upon the time scale of decomposition. Labile organic carbon decomposes on a time scale of days to weeks while refractory organic carbon requires more time. G3 particulate carbon is virtually inert in the water column. The three particulate organic carbon groups correspond to the three G groups in the sediment diagenesis model (DiToro and Fitzpatrick 1993) although the decay rates may differ between the water column and sediments.

Nitrogen

Nitrogen is first divided into available and unavailable fractions. Available refers to employment in algal nutrition. Two available forms are considered: reduced and oxidized nitrogen. Ammonium is the single reduced nitrogen form considered. Nitrate and nitrite comprise the oxidized nitrogen pool. Both reduced and oxidized nitrogen are utilized to fulfill algal nutrient requirements. The primary reason for distinguishing the two is that ammonium is oxidized by nitrifying bacteria into nitrite and, subsequently, nitrate. This oxidation can be a significant sink of oxygen in the water column and sediments.

Unavailable nitrogen state variables are dissolved organic nitrogen, labile particulate organic nitrogen, refractory particulate organic nitrogen, and G3 particulate organic nitrogen.

Phosphorus

As with nitrogen, phosphorus is first divided into available and unavailable fractions. Only a single available form, dissolved phosphate, is considered. Five forms of unavailable phosphorus are considered: dissolved organic phosphorus, labile particulate organic phosphorus, refractory particulate organic phosphorus, G3 particulate organic phosphorus, and particulate inorganic phosphorus.

Chemical Oxygen Demand

Reduced substances that are oxidized by abiotic processes are combined in the chemical oxygen demand pool. The primary component of chemical oxygen demand in saltwater is sulfide released from sediments. Oxidation of sulfide to sulfate may remove substantial quantities of dissolved oxygen from the water column. In freshwater, the primary component is methane which is also released from bottom sediments.

Dissolved Oxygen

Dissolved oxygen is required for the existence of higher life forms. Oxygen availability determines the distribution of organisms and the flows of energy and nutrients in an ecosystem. Dissolved oxygen is a central component of the water-quality model.

Salinity

Salinity is a conservative tracer that provides verification of the transport component of the model and facilitates examination of conservation of mass. Salinity also influences the dissolved oxygen saturation concentration and may be used in the determination of kinetics constants that differ in saline and fresh water.

Temperature

Temperature is a primary determinant of the rate of biochemical reactions. Reaction rates increase as a function of temperature although extreme temperatures may result in the mortality of organisms and a decrease in kinetics rates.

Fixed Solids

Fixed solids are the mineral fraction of total suspended solids. In previous model versions, fixed solids contributed to light attenuation and formed a site for sorption of dissolved inorganic phosphorus. The former role of fixed solids is now occupied by the four solids classes incorporated in the suspended

solids model. The fixed solids variable is retained but has no present function.

The remainder of this chapter is devoted to detailing the kinetics sources and sinks and to reporting parameter values. For notational simplicity, the transport terms are dropped in the reporting of kinetics formulations.

Algae

Equations governing the three algal groups are largely the same. Differences among groups are expressed through the magnitudes of parameters in the equations. Generic equations are presented below.

Algal sources and sinks in the conservation equation include production, metabolism, predation, and settling. These are expressed:

$$\frac{\delta}{\delta t}B = \left(G - BM - Wa \cdot \frac{\delta}{\delta z}\right)B - PR \qquad (2)$$

in which:

B = algal biomass, expressed as carbon (g C m^{-3})
G = growth (d^{-1})
BM = basal metabolism (d^{-1})
Wa = algal settling velocity (m d^{-1})
PR = predation (g C m^{-3} d^{-1})
z = vertical coordinate

Production

Production by phytoplankton is determined by the intensity of light, by the availability of nutrients, and by the ambient temperature.

Light

The influence of light on phytoplankton production is represented by a chlorophyll-specific production equation (Jassby and Platt 1976):

$$P^B = P^Bm \frac{I}{\sqrt{I^2 + Ik^2}} \qquad (3)$$

in which:

P^B = photosynthetic rate (g C g^{-1} Chl d^{-1})
P^Bm = maximum photosynthetic rate (g C g^{-1} Chl d^{-1})
I = irradiance (E m^{-2} d^{-1})

Parameter Ik is defined as the irradiance at which the initial slope of the production vs. irradiance relationship (Figure 1) intersects the value of $P^B m$

$$Ik = \frac{P^B m}{\alpha} \qquad (4)$$

in which:

α = initial slope of production vs. irradiance relationship (g C g^{-1} Chl (E m^{-2})$^{-1}$)

Chlorophyll-specific production rate is readily converted to carbon specific growth rate, for use in Equation 2, through division by the carbon-to-chlorophyll ratio:

$$G = \frac{P^B}{CChl} \qquad (5)$$

in which:

CChl = carbon-to-chlorophyll ratio (g C g^{-1} chlorophyll a)

Nutrients

Carbon, nitrogen, and phosphorus are the primary nutrients required for algal growth. Diatoms require silica, as well. Inorganic carbon and silica are usually available in excess and are not considered in the model. The effects of the remaining nutrients on growth are described by the formulation commonly referred to as "Monod kinetics" (Figure 2; Monod 1949):

$$f(N) = \frac{D}{KHd + D} \qquad (6)$$

in which:

f(N) = nutrient limitation on algal production ($0 \leq f(N) \leq 1$)
D = concentration of dissolved nutrient (g m^{-3})
KHd = half-saturation constant for nutrient uptake (g m^{-3})

Temperature

Algal production increases as a function of temperature until an optimum temperature or temperature range is reached. Above the optimum, production declines until a temperature lethal to the organisms is attained. Numerous functional representations of temperature effects are available. Inspection of growth versus temperature data indicates a function similar to a Gaussian probability curve (Figure 3) provides a good fit to observations:

$$f(T) = e^{-KTg1 \cdot (T - Topt)^2} \quad when \quad T \le Topt$$
$$= e^{-KTg2 \cdot (Topt - T)^2} \quad when \quad T > Topt \qquad (7)$$

in which:

T = temperature (^oC)
Topt = optimal temperature for algal growth (^oC)
KTg1 = effect of temperature below Topt on growth ($^oC^{-2}$)
KTg2 = effect of temperature above Topt on growth ($^oC^{-2}$)

Constructing the Photosynthesis vs. Irradiance Curve

A production versus irradiance relationship is constructed for each model cell at each time step. First, the maximum photosynthetic rate under ambient temperature and nutrient concentrations is determined:

$$P^Bm(N,T) = P^Bm \cdot f(T) \cdot \frac{D}{KHd + D} \qquad (8)$$

in which:

P^Bm(N,T) = maximum photosynthetic rate under ambient temperature and nutrient concentrations (g C g^{-1} Chl d^{-1})

The single most limiting nutrient is employed in determining the nutrient limitation.

Next, parameter Ik is derived from Equation 4. Finally, the production vs. irradiance relationship is constructed using P^Bm(N,T) and Ik. The resulting production versus irradiance curve exhibits three regions (Figure 4). For I >> Ik, the value of the term $I / (I^2 + Ik^2)^{½}$ approaches unity and temperature and nutrients are the primary factors that influence production. For I << Ik, production is determined solely by α and irradiance I. In the region where the initial slope of the production versus irradiance curve intercepts the line indicating production at optimal illumination, I ≈ Ik, production is determined by the combined effects of temperature, nutrients, and light.

Irradiance

Irradiance at the water surface is evaluated at each model time step. Instantaneous irradiance is computed by fitting a sin function to daily total irradiance:

$$Io = \frac{\Pi}{2 \cdot FD} \cdot IT \cdot \sin\left(\frac{\Pi \cdot DSSR}{FD}\right) \qquad (9)$$

in which:

Io = irradiance at water surface (E m^{-2} d^{-1})
IT = daily total irradiance (E m^{-2})
FD = fractional daylength ($0 \leq FD \leq 1$)
DSSR = time since sunrise (d)

Io is evaluated only during the interval:

$$\frac{1 - FD}{2} \leq DSM \leq \frac{1 + FD}{2} \qquad (10)$$

in which:

DSM = time since midnight (d)

Outside the specified interval, Io is set to zero.

Irradiance declines exponentially with depth below the surface. The diffuse attenuation coefficient, Ke, is computed as a function of color and concentrations of organic and mineral solids.

Respiration

Two forms of respiration are considered in the model: photo-respiration and basal metabolism. Photo-respiration represents the energy expended by carbon fixation and is a fixed fraction of production. In the event of no production (e.g. at night), photo-respiration is zero. Basal metabolism is continuous energy expenditure to maintain basic life processes. In the model, metabolism is considered to be an exponentially increasing function of temperature (Figure 5). Total respiration is represented:

$$R = Presp \cdot G + BM \cdot e^{KTb \cdot (T - Tr)} \qquad (11)$$

in which:

Presp = photo-respiration ($0 \leq Presp \leq 1$)
BM = metabolic rate at reference temperature Tr (d^{-1})
KTb = effect of temperature on metabolism ($^oC^{-1}$)
Tr = reference temperature for metabolism (^oC)

Predation

The predation term includes the activity of zooplankton, other pelagic filter feeders including planktivorous fish, and filter-feeding benthos. Predation in the water column is modeled by assuming predators clear a specific volume of water per unit biomass:

$$PR = F \times B \times M \qquad (12)$$

in which:

F = filtration rate (m^3 g^{-1} predator C d^{-1})
M = planktivore biomass (g C m^{-3})

Detailed specification of the spatial and temporal distribution of the predator population is impossible. One approach is to assume predator biomass is proportional to algal biomass, $M = \gamma B$, in which case Equation 12 can be rewritten:

$$PR = \gamma \cdot F \cdot B^2 \qquad (13)$$

Since neither γ nor F are known precisely, the logical approach is to combine their product into a single unknown determined during the model calibration procedure. Effect of temperature on predation is represented with the same formulation as the effect of temperature on respiration. The final representation of predation is:

$$PR = Phtl \cdot B^2 \qquad (14)$$

in which:

Phtl = rate of water column planktivore predation (m^3 g^{-1} C d^{-1})

Predation by filter-feeding benthos is represented as a loss term only in model cells that intersect the bottom. Details of the benthos computations may be found in Cerco and Noel (2010).

Accounting for Algal Phosphorus

The amount of phosphorus incorporated in algal biomass is quantified through a stoichiometric ratio. Thus, total phosphorus in the model is expressed:

$$TotP = PO_4 + Apc \cdot B + DOP + LPOP + RPOP + G3OP + PIP \qquad (15)$$

in which:

TotP = total phosphorus (g P m^{-3})
PO_4 = dissolved phosphate (g P m^{-3})
Apc = algal phosphorus-to-carbon ratio (g P g^{-1} C)
DOP = dissolved organic phosphorus (g P m^{-3})
LPP = labile particulate organic phosphorus (g P m^{-3})
RPP = refractory particulate organic phosphorus (g P m^{-3})
G3OP = G3 organic phosphorus (g P m^{-3})
PIP = particulate inorganic phosphorus (g P m^{-3})

Algae take up dissolved phosphate during production and release dissolved phosphate and organic phosphorus through respiration. The fate of phosphorus released by respiration is determined by empirical distribution

coefficients. The fate of algal phosphorus recycled by predation is determined by a second set of distribution parameters.

Accounting for Algal Nitrogen

Model nitrogen state variables include ammonium, nitrate+nitrite, dissolved organic nitrogen, labile particulate organic nitrogen, refractory particulate organic nitrogen, and G3 particulate organic nitrogen. The amount of nitrogen incorporated in algal biomass is quantified through a stoichiometric ratio. Thus, total nitrogen in the model is expressed:

$$TotN = NH_4 + NO_{23} + Anc \cdot B + DON + LPON + RPON + G3ON \quad (16)$$

TotN = total nitrogen (g N m^{-3})
NH_4 = ammonium (g N m^{-3})
NO_{23} = nitrate+nitrite (g N m^{-3})
Anc = algal nitrogen-to-carbon ratio (g N g^{-1} C)
DON = dissolved organic nitrogen (g N m^{-3})
LPON = labile particulate organic nitrogen (g N m^{-3})
RPON = refractory particulate organic nitrogen (g N m^{-3})
G3ON = G3 particulate organic nitrogen (g N m^{-3})

As with phosphorus, the fate of algal nitrogen released by metabolism and predation is represented by distribution coefficients.

Algal Nitrogen Preference

Algae take up ammonium and nitrate+nitrite during production and release ammonium and organic nitrogen through respiration. Nitrate+nitrite is internally reduced to ammonium before synthesis into biomass occurs (Parsons et al. 1984). Trace concentrations of ammonium inhibit nitrate reduction so that, in the presence of multiple nitrogenous nutrients, ammonium is utilized first. The "preference" of algae for ammonium is expressed by a modification of an empirical function presented by Thomann and Fitzpatrick (1982):

$$PN = NH_4 \cdot \frac{NO_{23}}{(KHNH_4 + NH_4) \cdot (KHNH_4 + NO_{23})} + NH_4 \cdot \frac{KHNH_4}{(NH_4 + NO_{23}) \cdot (KHNH_4 + NO_{23})} \quad (17)$$

in which

PN = algal preference for ammonium uptake ($0 \leq PN \leq 1$)

$KHNH_4$ = half saturation concentration for algal ammonium uptake (g N m^{-3})

Our modification substitutes a specific half-saturation concentration for ammonium uptake, $KHNH_4$, for the original use of half-saturation concentration for nitrogen uptake, KHn. We found the modification enforces ammonium use down to lower concentrations that the original formulation.

The preference function has two limiting values (Figure 6). When nitrate+nitrite is absent, the preference for ammonium is unity. When ammonium is absent, the preference is zero. In the presence of ammonium and nitrate+nitrite, the preference depends on the abundance of both forms relative to the half-saturation constant for ammonium uptake. When ammonium and nitrate+nitrite are both abundant, the preference for ammonium approaches unity. When ammonium is scarce but nitrate+nitrite is abundant, the preference decreases in magnitude and a significant fraction of algal nitrogen requirement comes from nitrate+nitrite.

Effect of Algae on Dissolved Oxygen

Algae produce oxygen during photosynthesis and consume oxygen through respiration. The quantity produced depends on the form of nitrogen utilized for growth. More oxygen is produced, per unit of carbon fixed, when nitrate is the algal nitrogen source than when ammonium is the source. Equations describing algal uptake of carbon and nitrogen and production of dissolved oxygen (Morel 1983) are:

$$106\ CO_2 + 16\ NH_4^+ + H_2PO_4^- + 106\ H_2O \text{ - - >}$$

$$\text{protoplasm} + 106\ O_2 + 15\ H^+ \qquad (18)$$

$$106\ CO_2 + 16\ NO_3^- + H_2PO_4^- + 122\ H_2O + 17\ H^+ \text{ - - >}$$

$$\text{protoplasm} + 138\ O_2 \qquad (19)$$

When ammonium is the nitrogen source, one mole oxygen is produced per mole carbon dioxide fixed. When nitrate is the nitrogen source, 1.3 moles oxygen are produced per mole carbon dioxide fixed.

The equation that describes the effect of algae on dissolved oxygen in the model is:

$$\frac{\delta}{\delta t} DO = \left[(1.3 - 0.3 \cdot PN) \cdot P - (1 - FCD) \cdot BM\right] \cdot AOCR \cdot B \qquad (20)$$

in which:

FCD = fraction of algal metabolism recycled as dissolved organic carbon ($0 \leq FCD \leq 1$)
AOCR = dissolved oxygen-to-carbon ratio in respiration (2.67 g O_2 g^{-1} C)

The magnitude of AOCR is derived from a simple representation of the respiration process:

$$CH_2O + O_2 = CO_2 + H_2O \qquad (21)$$

The quantity (1.3 - 0.3 · PN) is the photosynthesis ratio and expresses the molar quantity of oxygen produced per mole carbon fixed. The photosynthesis ratio approaches unity as the algal preference for ammonium approaches unity.

Salinity Toxicity

Some freshwater algae, such as the cyanobacteria *microcystis*, cease production when salinity exceeds 1 to 2 ppt (Sellner et al. 1988). The potential effect of salinity on freshwater algae is represented by a mortality term in the form of a rectangular hyperbola:

$$STOX1 = STF1 \cdot \frac{S}{KHst1 + S} \qquad (22)$$

in which

STOX1 = mortality induced by salinity (d^{-1})
STF1 = maximum salinity mortality (d^{-1})
S = salinity (ppt)
KHst1 = salinity at which mortality is half maximum value (ppt)

The spring diatom bloom is limited to saline water. The limiting mechanism is not defined but appears to be related to salinity. The upstream limit of the spring bloom is defined in the model by introducing a mortality term at low salinity:

$$STOX2 = STF2 \times \frac{KHst2}{KHst2 + S} \qquad (23)$$

in which

STOX2 = mortality induced by freshwater on spring diatoms (d^{-1})
STF2 = maximum freshwater mortality on spring diatoms (d^{-1})
KHst2 = salinity at which mortality is half maximum value (ppt)

The salinity-related mortality (Figure 7) is added to the basal metabolism.

Organic Carbon

Organic carbon undergoes innumerable transformations in the water column. The model carbon cycle (Figure 8) consists of the following elements:

Phytoplankton production and excretion
Predation on phytoplankton
Dissolution of particulate carbon
Heterotrophic respiration
Settling

Algal production is the primary carbon source to the water column although carbon also enters the system through external loading. Predation on algae by zooplankton and other organisms releases particulate and dissolved organic carbon to the water column. A fraction of the particulate organic carbon undergoes first-order dissolution to dissolved organic carbon. Dissolved organic carbon produced by excretion, by predation, and by dissolution is respired at a first-order rate to inorganic carbon. Particulate organic carbon which does not undergo dissolution settles to the bottom sediments.

Organic carbon dissolution and respiration are represented as first-order processes in which the reaction rate is proportional to concentration of the reactant. An exponential function (Figure 5) relates dissolution and respiration to temperature.

Dissolved Organic Carbon

The complete representation of dissolved organic carbon sources and sinks in the model ecosystem is: (24)

$$\frac{\delta}{\delta t} DOC = FCD \cdot R \cdot B + FCDP \cdot PR + Klpoc \cdot LPOC$$

$$+ Krpoc \cdot RPOC + Kg3poc \cdot G3OC - \frac{DO}{KHodoc + DO} \cdot Kdoc \cdot DOC$$

in which:

DOC = dissolved organic carbon (g m^{-3})
LPOC = labile particulate organic carbon (g m^{-3})
RPOC = refractory particulate organic carbon (g m^{-3})
G3OC = G3 particulate organic carbon (g m^{-3})
FCD = fraction of algal respiration released as DOC ($0 < FCD < 1$)
FCDP = fraction of predation on algae released as DOC ($0 < FCDP < 1$)
Klpoc = dissolution rate of LPOC (d^{-1})
Krpoc = dissolution rate of RPOC (d^{-1})
Kg3poc = dissolution rate of G3OC (d^{-1})

Kdoc = respiration rate of DOC (d^{-1})

Particulate Organic Carbon

The complete representation of labile particulate organic carbon sources and sinks in the model ecosystem is:

$$\frac{\delta}{\delta t} LPOC = FCL \cdot R \cdot B + FCLP \cdot PR - Klpoc \cdot LPOC - Wl \cdot \frac{\delta}{\delta z} LPOC \quad (25)$$

in which:

FCL = fraction of algal respiration released as LPOC ($0 < FCL < 1$)
FCLP = fraction of predation on algae released as LPOC ($0 < FCLP < 1$)
Wl = settling velocity of labile particles (m d^{-1})

The equations for refractory and G3 particulate organic carbon are analogous.

Phosphorus

The model phosphorus cycle (Figure 9) includes the following processes:

Algal uptake and excretion
Predation
Hydrolysis of particulate organic phosphorus
Mineralization of dissolved organic phosphorus
Dissolution of particulate inorganic phosphorus
Settling and resuspension

External loads provide the ultimate source of phosphorus to the system. Dissolved phosphate is incorporated by algae during growth and released as phosphate and organic phosphorus through respiration and predation. Dissolved organic phosphorus is mineralized to phosphate. A portion of the particulate organic phosphorus hydrolyzes to dissolved organic phosphorus. The balance settles to the sediments. Dissolution of particulate inorganic phosphorus is also possible. Within the sediments, particulate phosphorus is mineralized and recycled to the water column as dissolved phosphate.

Hydrolysis and Mineralization

Within the model, hydrolysis is defined as the process by which particulate organic substances are converted to dissolved organic form. Mineralization is defined as the process by which dissolved organic substances are converted to dissolved inorganic form. Conversion of particulate organic phosphorus to phosphate proceeds through the sequence of hydrolysis and mineralization. Direct mineralization of particulate organic phosphorus does not

occur.

Mineralization of organic phosphorus is mediated by the release of nucleotidase and phosphatase enzymes by bacteria (Ammerman and Azam 1985; Chrost and Overbeck 1987) and algae (Matavulj and Flint 1987; Chrost and Overbeck 1987; Boni et al. 1989). Since the algae themselves release the enzyme and since bacterial abundance is related to algal biomass, the rate of organic phosphorus mineralization is related, in the model, to algal biomass. A most remarkable property of the enzyme process is that alkaline phosphatase activity is inversely proportional to ambient phosphate concentration (Chrost and Overbeck 1987; Boni et al. 1989). Put in different terms, when phosphate is scarce, algae stimulate production of an enzyme that mineralizes organic phosphorus to phosphate. This phenomenon is simulated by relating mineralization to the algal phosphorus nutrient limitation. Mineralization is highest when algae are strongly phosphorus limited and is least when no limitation occurs.

The expression for mineralization rate is:

$$Kdop = Kdp + \frac{KHp}{KHp + PO_4} \cdot Kdpalg \cdot B \qquad (26)$$

in which:

Kdop = mineralization rate of dissolved organic phosphorus (d^{-1})
Kdp = minimum mineralization rate (d^{-1})
KHp = half-saturation concentration for algal phosphorus uptake (g P m^{-3})
PO_4 = dissolved phosphate (g P m^{-3})
Kdpalg = constant that relates mineralization to algal biomass (m^3 g^{-1} C d^{-1})

Potential effects of algal biomass and nutrient limitation on the mineralization rate are shown in Figure 10. When nutrient concentration greatly exceeds the half-saturation concentration for algal uptake, the rate roughly equals the minimum. Algal biomass has little influence. As nutrient becomes scarce relative to the half-saturation concentration, the rate increases. The magnitude of the increase depends on algal biomass. Factor of two to three increases are feasible. Exponential functions (Figure 5) relate mineralization and hydrolysis rates to temperature.

Dissolved Phosphate

The mass-balance equation for dissolved phosphate is:

$$\frac{\delta}{\delta t} PO_4 = Kdop \cdot DOP + Kpip \cdot PIP - APC \cdot G \cdot B$$
$$+ APC \cdot \left[FPI \cdot BM \cdot B + FPIP \cdot PR\right] - Wpo_4 \cdot \frac{\delta}{\delta z} PO_4 \qquad (27)$$

in which:

PIP = particulate inorganic phosphorus (g P m^{-3})
Kpip = dissolution rate of particulate inorganic phosphorus (d^{-1})
FPI = fraction of algal metabolism released as dissolved phosphate ($0 \leq FPI \leq 1$)
FPIP = fraction of predation released as dissolved phosphate ($0 \leq FPIP \leq 1$)
Wpo_4 = settling rate of precipitated phosphate (m d^{-1})

Phosphate settling represents phosphate removal through co-precipitation with iron and manganese during the break-up of seasonal bottom-water anoxia. The settling rate is implemented for a thirty-day period in appropriate portions of the system.

Dissolved Organic Phosphorus

The mass balance equation for dissolved organic phosphorus is:

$$\frac{\delta}{\delta t} DOP = APC \cdot (BM \cdot B \cdot FPD + PR \cdot FPDP) + Klpop \cdot LPOP + Krpop \cdot RPOP + Kg3op \cdot G3OP - Kdop \cdot DOP \quad (28)$$

in which:

DOP = dissolved organic phosphorus (g P m^{-3})
LPOP = labile particulate organic phosphorus (g P m^{-3})
RPOP = refractory particulate organic phosphorus (g P m^{-3})
G3OP = G3 particulate organic phosphorus (g P m^{-3})
FPD = fraction of algal metabolism released as DOP ($0 < FPD < 1$)
FPDP = fraction of predation on algae released as DOP ($0 < FPDP < 1$)
Klpop = hydrolysis rate of LPOP (d^{-1})
Krpop = hydrolysis rate of RPOP (d^{-1})
Kg3op = hydrolysis rate of G3OP (d^{-1})
Kdop = mineralization rate of DOP (d^{-1})

Particulate Organic Phosphorus

The mass balance equation for labile particulate organic phosphorus is:

$$\frac{\delta}{\delta t} LPOP = APC \cdot (BM \cdot B \cdot FPL + PR \cdot FPLP) - Klpop \cdot LPOP - Wl \cdot \frac{\delta}{\delta z} LPOP \quad (29)$$

in which:

FPL = fraction of algal metabolism released as LPOP ($0 < FPL < 1$)
FPLP = fraction of predation on algae released as LPOP ($0 < FPLP < 1$)

The equations for refractory and G3 particulate organic phosphorus are analogous.

Particulate Inorganic Phosphorus

A large fraction of particulate phosphorus in the Chesapeake Bay system is in inorganic form (Keefe 1994). Examination of dissolved phosphate, fixed solids, and PIP observations indicates the PIP is not loosely sorbed to sediment particles as commonly represented in water quality models (references?). PIP is represented here as a distinct substance which potentially dissolves into phosphate. Otherwise, the ultimate fate of PIP is settling to bottom sediments. The mass balance equation for PIP is:

$$\frac{\partial}{\partial t} PIP = -Kpip \cdot PIP - Wspip \cdot \frac{\delta}{\delta z} PIP \qquad (30)$$

in which:

Wspip = settling rate of particulate inorganic phosphorus (m d^{-1})

Nitrogen

The model nitrogen cycle (Figure 11) includes the following processes:

Algal production and metabolism
Predation
Hydrolysis of particulate organic nitrogen
Mineralization of dissolved organic nitrogen
Settling
Nitrification

External loads provide the ultimate source of nitrogen to the system. Available nitrogen is incorporated by algae during growth and released as ammonium and organic nitrogen through respiration and predation. A portion of the particulate organic nitrogen hydrolyzes to dissolved organic nitrogen. The balance settles to the sediments. Dissolved organic nitrogen is mineralized to ammonium. In an oxygenated water column, a fraction of the ammonium is subsequently oxidized to nitrate+nitrite through the nitrification process. Particulate nitrogen which settles to the sediments is mineralized and recycled to the water column, primarily as ammonium. Nitrate+nitrite moves in both directions across the sediment-water interface, depending on relative concentrations in the water column and sediment interstices.

Nitrification

Nitrification is a process mediated by specialized groups of autotrophic bacteria that obtain energy through the oxidation of ammonium to nitrite and oxidation of nitrite to nitrate. A simplified expression for complete nitrification (Tchobanoglous and Schroeder 1987) is:

$$NH_4^+ + 2O_2 \text{ --> } NO_3^- + H_2O + 2H^+ \qquad (31)$$

The simplified stoichiometry indicates that two moles of oxygen are required to nitrify one mole of ammonium into nitrate. The simplified equation is not strictly true, however. Cell synthesis by nitrifying bacteria is accomplished by the fixation of carbon dioxide so that less than two moles of oxygen are consumed per mole ammonium utilized (Wezernak and Gannon 1968).

The kinetics of complete nitrification are modeled as a function of available ammonium, dissolved oxygen, and temperature:

$$NT = \frac{DO}{KHont + DO} \cdot \frac{NH_4}{KHnnt + NH_4} \cdot f(T) \cdot NTm \qquad (32)$$

in which:

NT = nitrification rate (g N m^{-3} d^{-1})
KHont = half-saturation constant of dissolved oxygen required for nitrification (g O_2 m^{-3})
KHnnt = half-saturation constant of NH_4 required for nitrification (g N m^{-3})
NTm = maximum nitrification rate at optimal temperature (g N m^{-3} d^{-1})

The kinetics formulation (Figure 12) incorporates the products of two Monod-like functions. The first function diminishes nitrification at low dissolved oxygen concentration. The second function expresses the influence of ammonium concentration on nitrification. When ammonium concentration is low, relative to KHnnt, nitrification is proportional to ammonium concentration. For NH4 << KHnnt, the reaction is approximately first-order. (The first-order decay constant ≈ NTm/KHnnt.) When ammonium concentration is large, relative to KHnnt, nitrification approaches a maximum rate. This formulation is based on a concept proposed by Tuffey et al. (1974). Nitrifying bacteria adhere to benthic or suspended sediments. When ammonium is scarce, vacant surfaces suitable for nitrifying bacteria exist. As ammonium concentration increases, bacterial biomass increases, vacant surfaces are occupied, and the rate of nitrification increases. The bacterial population attains maximum density when all surfaces suitable for bacteria are occupied. At this point, nitrification proceeds at a maximum rate independent of additional increase in ammonium concentration.

The optimal temperature for nitrification may be less than peak temperatures that occur in coastal waters. To allow for a decrease in nitrification at superoptimal temperature, the effect of temperature on nitrification is modeled in the Gaussian form of Equation 7.

Nitrogen Mass Balance Equations

The mass-balance equations for nitrogen state variables are written by summing all previously-described sources and sinks:

Ammonium

$$\frac{\delta}{\delta t} NH_4 = ANC \cdot \left[(BM \cdot FNI - PN \cdot P) \cdot B + PR \cdot FNIP\right] + Kdon \cdot DON - NT \quad (33)$$

in which:

FNI = fraction of algal metabolism released as NH4 ($0 \leq FNI \leq 1$)
PN = algal ammonium preference ($0 \leq PN \leq 1$)
FNIP = fraction of predation released as NH4 ($0 \leq FNIP \leq 1$)

Nitrate+Nitrite

$$\frac{\delta}{\delta t} NO_{23} = - ANC \cdot (1 - PN) \cdot P \cdot B + NT \quad (34)$$

Dissolved Organic Nitrogen

$$\frac{\delta}{\delta t} DON = ANC \cdot (BM \cdot B \cdot FND + PR \cdot FNDP) + Klpon \cdot LPON + Krpon \cdot RPON + Kg3on \cdot G3ON - Kdon \cdot DON \quad (35)$$

in which:

DON = dissolved organic nitrogen (g N m^{-3})
LPON = labile particulate organic nitrogen (g N m^{-3})
RPON = refractory particulate organic nitrogen (g N m^{-3})
G3ON = G3 particulate organic nitrogen (g N m^{-3})
FND = fraction of algal metabolism released as DON ($0 < FND < 1$)
FNDP = fraction of predation on algae released as DON ($0 < FNDP < 1$)
Klpon = hydrolysis rate of LPON (d^{-1})
Krpon = hydrolysis rate of RPON (d^{-1})
Kg3on = hydrolysis rate of G3ON (d^{-1})
Kdon = mineralization rate of DON (d^{-1})

Particulate Organic Nitrogen

The mass balance equation for labile particulate organic nitrogen is:

$$\frac{\delta}{\delta t} LPON = ANC \cdot (BM \cdot B \cdot FNL + PR \cdot FNLP) - Klpon \cdot LPON - Wl \cdot \frac{\delta}{\delta z} LPON \quad (36)$$

in which:

FNL = fraction of algal metabolism released as LPON ($0 < FNL < 1$)
FNLP = fraction of predation on algae released as LPON ($0 < FNLP < 1$)

The equations for refractory and G3 particulate organic nitrogen are analogous.

Chemical Oxygen Demand

Chemical oxygen demand is the concentration of reduced substances that are oxidized through abiotic reactions. The source of chemical oxygen demand in saline water is sulfide released from sediments. A cycle occurs in which sulfate is reduced to sulfide in the sediments and re-oxidized to sulfate in the water column. In freshwater, methane may be released to the water column by bottom sediments. Both sulfide and methane are quantified in units of oxygen demand and are treated with the same kinetics formulation:

$$\frac{\delta}{\delta t} COD = - \frac{DO}{KHocod + DO} \cdot Kcod \cdot COD \qquad (37)$$

in which:

COD = chemical oxygen demand concentration (g oxygen-equivalents m^{-3})
KHocod = half-saturation concentration of dissolved oxygen required for exertion of chemical oxygen demand (g O_2 m^{-3})
Kcod = oxidation rate of chemical oxygen demand (d^{-1})

An exponential function (Figure 5) describes the effect of temperature on exertion of chemical oxygen demand.

Dissolved Oxygen

Sources and sinks of dissolved oxygen in the water column (Figure 13) include:

Algal photosynthesis
Atmospheric reaeration
Algal respiration
Heterotrophic respiration
Nitrification
Chemical oxygen demand

Reaeration

The rate of reaeration is proportional to the dissolved oxygen deficit in model segments that form the air-water interface:

$$\frac{\delta}{\delta t} DO = \frac{Kr}{\Delta z} \cdot (DOs - DO) \qquad (38)$$

in which:

DO = dissolved oxygen concentration (g O_2 m^{-3})
Kr = reaeration coefficient (m d^{-1})
DOs = dissolved oxygen saturation concentration (g O_2 m^{-3})
Δz = model layer thickness (m)

In freeflowing streams, the reaeration coefficient depends largely on turbulence generated by bottom shear stress (O'Connor and Dobbins 1958). In lakes and coastal waters, however, wind effects may dominate the reaeration process (O'Connor 1983). The model code provides three options for the reaeration coefficient:

Calculate reaeration as a function of stream velocity and depth.
Calculate reaeration as a function of wind speed.
Specify a reaeration coefficient

The relationship to velocity and depth is based on O'Connor and Dobbins (1958). In SI units, the O'Connor-Dobbins relationship is:

$$Kr = 3.9\sqrt{u/H} \qquad (39)$$

in which:

u = stream velocity (m s^{-1})
H = depth (m)

The relationship to wind is from Hartman and Hammond (1985):

$$Kr = Arear \bullet R\nu \bullet Wms^{1.5} \qquad (40)$$

in which:

Arear = empirical constant (≈ 0.1)
Rv = ratio of kinematic viscosity of pure water at 20 ^{o}C to kinematic viscosity of water at specified temperature and salinity
Wms = wind speed measured at 10 m above water surface (m s^{-1})

Hartman and Hammond (1985) indicate Arear takes the value 0.157. In the present model, Arear is treated as a variable to allow for effects of wind sheltering, for differences in height of local wind observations, and for other factors. An empirical function (Figure 14) which fits tabulated values of Rv is:

$$R\nu = 0.54 + 0.0233 \bullet T - 0.0020 \bullet S \qquad (41)$$

in which:

S = salinity (ppt)
T = temperature (^{o}C)

Saturation dissolved oxygen concentration diminishes as temperature and salinity increase. An empirical formula that describes these effects (Genet et al. 1974) is:

$$DOs = 14.5532 - 0.38217 \cdot T + 0.0054258 \cdot T^2 - CL \cdot (1.665 \times 10^{-4} - 5.866 \times 10^{-6} \cdot T + 9.796 \times 10^{-8} \cdot T^2) \quad (42)$$

in which:

CL = chloride concentration (= salinity/1.80655)

Mass Balance Equation for Dissolved Oxygen

$$\frac{\delta}{\delta t} DO = AOCR \cdot [(1.3 - 0.3 \cdot PN) \cdot P - (1 - FCD) \cdot BM] \cdot B - AONT \cdot NT - \frac{DO}{KHodoc + DO} \cdot AOCR \cdot Kdoc \cdot DOC - \frac{DO}{KHocod + DO} \cdot Kcod \cdot COD + \frac{Kr}{H} \cdot (DOs - DO) \quad (43)$$

in which:

AOCR = oxygen-to-carbon mass ratio in production and respiration (= 2.67 g O_2 g^{-1} C)
AONT = oxygen consumed per mass ammonium nitrified (= 4.33 g O_2 g^{-1} N)

Temperature

Computation of temperature employs a conservation of internal energy equation that is analogous to the conservation of mass equation. For practical purposes, the internal energy equation can be written as a conservation of temperature equation. The only source or sink of temperature considered is exchange with the atmosphere. Atmospheric exchange is considered proportional to the temperature difference between the water surface and a theoretical equilibrium temperature (Edinger et al. 1974):

$$\frac{\delta}{\delta t} T = \frac{KT}{\rho \cdot Cp \cdot H} \cdot (Te - T) \quad (44)$$

in which:

T = water temperature (^oC)
Te = equilibrium temperature (^oC)
KT = Heat exchange coefficient (watt m^{-2} $^oC^{-1}$)
Cp = specific heat of water (4200 watt s kg^{-1} $^oC^{-1}$)
ρ = density of water (1000 kg m^{-3})

Salinity

Salinity is modeled by the conservation of mass equation with no internal sources or sinks

Parameter Values

Model parameter evaluation is a recursive process. Parameters are selected from a range of feasible values, tested in the model, and adjusted until satisfactory agreement between predicted and observed variables is obtained. Ideally, the range of feasible values is determined by observation or experiment. For some parameters, however, no observations are available. Then, the feasible range is determined by parameter values employed in similar models or by the judgment of the modeler. A review of parameter values was included in documentation of the first application of this model (Cerco and Cole 1994). Parameters from the initial study were refined in successive applications and refined again for the present model. A complete set of parameter values is provided in Table 2.

Table 1
Water Quality Model State Variables

Temperature	Salinity
Fixed Solids	Freshwater Algae
Spring Diatoms	Other (Green) Algae
Dissolved Organic Carbon	Labile Particulate Organic Carbon
Refractory Particulate Organic Carbon	G3 Particulate Organic Carbon
Ammonium	Nitrate+Nitrite
Dissolved Organic Nitrogen	Labile Particulate Organic Nitrogen
Refractory Particulate Organic Nitrogen	G3 Particulate Organic Nitrogen
Phosphate	Dissolved Organic Phosphorus
Labile Particulate Organic Phosphorus	Refractory Particulate Organic Phosphorus
G3 Particulate Organic Phosphorus	Particulate Inorganic Phosphorus
Chemical Oxygen Demand	Dissolved Oxygen

Table 2
Parameters in Kinetics Equations

Symbol	Definition	Value	Units
ANC	nitrogen-to-carbon ratio of algae	0.175 (fresh), 0.135 (spring), 0.175 (green)	g N g^{-1} C
AOCR	dissolved oxygen-to-carbon ratio in respiration	2.67	g O_2 g^{-1} C
AONT	mass dissolved oxygen consumed per mass ammonium nitrified	4.33	g O_2 g^{-1} N
APC	algal phosphorus-to-carbon ratio	0.0125 (fresh), 0.0125 (spring) 0.0125 (green)	g P g^{-1} C
BM	basal metabolic rate of algae at reference temperature Tr	0.03 (fresh), 0.01 (spring), 0.02 (green)	d^{-1}
CChl	algal carbon-to-chlorophyll ratio	45 (fresh), 75 (spring), 60 (green)	g C g^{-1} Chl
FCD	fraction of dissolved organic carbon produced by algal metabolism	0.0	$0 \leq FCD \leq 1$
FCDP	fraction of dissolved organic carbon produced by predation	0.5	$0 \leq FCDP \leq 1$
FCL	fraction of labile particulate carbon produced by algal metabolism	0.0	$0 \leq FCL \leq 1$
FCLP	fraction of labile particulate carbon produced by predation	0.3	$0 \leq FCLP \leq 1$
FCR	fraction of refractory particulate carbon produced by algal metabolism	0.0	$0 \leq FCR \leq 1$
FCRP	fraction of refractory particulate carbon produced by predation	0.15	$0 \leq FCRP \leq 1$
FCG3	fraction of G3 particulate carbon produced by algal metabolism	0.0	$0 \leq FCG3 \leq 1$
FCG3P	fraction of G3 particulate carbon produced by predation	0.05	$0 \leq FCG3P \leq 1$
FNI	fraction of inorganic nitrogen produced by algal metabolism	0.45	$0 \leq FNI \leq 1$
FNIP	fraction of inorganic nitrogen produced by predation	0.35	$0 \leq FNIP \leq 1$
FND	fraction of dissolved organic nitrogen produced by algal metabolism	0.2	$0 \leq FND \leq 1$
FNDP	fraction of dissolved organic nitrogen	0.15	$0 \leq FNDP \leq 1$

Table 2
Parameters in Kinetics Equations

Symbol	Definition	Value	Units
	produced by predation		
FNL	fraction of labile particulate nitrogen produced by algal metabolism	0.25	$0 \leq FNL \leq 1$
FNLP	fraction of labile particulate nitrogen produced by predation	0.3	$0 \leq FNLP \leq 1$
FNR	fraction of refractory particulate nitrogen produced by algal metabolism	0.07	$0 \leq FNR \leq 1$
FNRP	fraction of refractory particulate nitrogen produced by predation	0.13	$0 \leq FNRP \leq 1$
FNG3	fraction of G3 particulate nitrogen produced by algal metabolism	0.03	$0 \leq FNG3 \leq 1$
FNG3P	fraction of G3 particulate nitrogen produced by predation	0.07	$0 \leq FNG3P \leq 1$
FPD	fraction of dissolved organic phosphorus produced by algal metabolism	0.25	$0 \leq FPD \leq 1$
FPDP	fraction of dissolved organic phosphorus produced by predation	0.4	$0 \leq FPDP \leq 1$
FPI	fraction of dissolved inorganic phosphorus produced by algal metabolism	0.75	$0 \leq FPI \leq 1$
FPIP	fraction of dissolved inorganic phosphorus produced by predation	0.5	$0 \leq FPIP \leq 1$
FPL	fraction of labile particulate phosphorus produced by algal metabolism	0.0	$0 \leq FPL \leq 1$
FPLP	fraction of labile particulate phosphorus produced by predation	0.07	$0 \leq FPLP \leq 1$
FPR	fraction of refractory particulate phosphorus produced by algal metabolism	0.0	$0 \leq FPR \leq 1$
FPRP	fraction of refractory particulate phosphorus produced by predation	0.02	$0 \leq FPRP \leq 1$
FPG3	fraction of G3 particulate phosphorus produced by algal metabolism	0.0	$0 \leq FPG3 \leq 1$
FPG3P	fraction of G3 particulate phosphorus produced by predation	0.01	$0 \leq FPG3P \leq 1$
Kcod	oxidation rate of chemical oxygen demand	20 (saltwater), 0.025 (fresh)	d^{-1}
Kdoc	dissolved organic carbon respiration rate	0.037 – 0.075	d^{-1}
Kdon	dissolved organic nitrogen mineralization rate	0.022	d^{-1}
Kdp	minimum mineralization rate of dissolved organic phosphorus	0.025	d^{-1}

Table 2
Parameters in Kinetics Equations

Symbol	Definition	Value	Units
Kdpalg	constant that relates mineralization rate to algal biomass	0.4	$m^3 g^{-1} C d^{-1}$
KHn	half-saturation concentration for nitrogen uptake by algae	0.01(fresh), 0.025(spring), 0.025 (green)	g N m^{-3}
KHnh4	half-saturation concentration of ammonium in nitrogen preference formula	0.01 (fresh), 0.01 (spring), 0.025 (green)	g N m^{-3}
KHnnt	half-saturation concentration of NH_4 required for nitrification	1.0	g N m^{-3}
KHocod	half-saturation concentration of dissolved oxygen required for exertion of COD	0.1	g O_2 m^{-3}
KHodoc	half-saturation concentration of dissolved oxygen required for oxic respiration	0.1	g O_2 m^{-3}
KHont	half-saturation concentration of dissolved oxygen required for nitrification	1.0	g O_2 m^{-3}
KHp	half-saturation concentration for phosphorus uptake by algae	0.0025	g P m^{-3}
KHst	salinity at which algal mortality is half maximum value	15 (fresh), 2.0 (spring)	ppt
Klpoc	labile particulate organic carbon dissolution rate	0.15	d^{-1}
Klpon	labile particulate organic nitrogen hydrolysis rate	0.12	d^{-1}
Klpop	labile particulate organic phosphorus hydrolysis rate	0.12	d^{-1}
Kpip	particulate inorganic phosphorus dissolution rate	0.0	d^{-1}
Krdo	Reaeration coefficient	1.5	m d^{-1}
Krpoc	refractory particulate organic carbon dissolution rate	0.006	d^{-1}
Krpon	refractory particulate organic nitrogen hydrolysis rate	0.005	d^{-1}
Krpop	refractory particulate organic phosphorus hydrolysis rate	0.005	d^{-1}
Kg3p	g3 particulate organic carbon hydrolysis rate	0.0	d^{-1}
Kg3n	g3 particulate organic nitrogen hydrolysis rate	0.0	d^{-1}
Kg3p	g3 particulate organic phosphorus hydrolysis rate	0.0	d^{-1}

Table 2
Parameters in Kinetics Equations

Symbol	Definition	Value	Units
KTb	effect of temperature on basal metabolism of algae	0.032	$^oC^{-1}$
KTcod	effect of temperature on exertion of chemical oxygen demand	0.041	d^{-1}
KTg1	effect of temperature below Tm on growth of algae	0.005 (fresh), 0.0018 (spring), 0.0035 (green)	$^oC^{-2}$
KTg2	effect of temperature above Tm on growth of algae	0.004 (fresh), 0.006 (spring), 0.0 (green)	$^oC^{-2}$
KThdr	effect of temperature on hydrolysis rates	0.069	$^oC^{-1}$
KTmnl	effect of temperature on mineralization rates	0.069	$^oC^{-1}$
KTnt1	effect of temperature below Tmnt on nitrification	0.003	$^oC^{-2}$
KTnt2	effect of temperature above Tmnt on nitrification	0.003	$^oC^{-2}$
KTpr	effect of temperature on predation	0.032	$^oC^{-1}$
NTm	maximum nitrification rate at optimal temperature	0.062 to 0.125	g N m^{-3} d^{-1}
Phtl	predation rate on algae	0.05 (fresh), 0.1 (spring), 0.4 (green)	m^3 g^{-1} C d^{-1}
Pm^B	maximum photosynthetic rate	200 (fresh), 300 (spring), 450 (green)	g C g^{-1} Chl d^{-1}
Presp	photo-respiration fraction	0.25	$0 \leq Presp \leq 1$
STF	salinity toxicity factor	0.3 (fresh), 0.1 (spring)	d^{-1}
Topt	optimal temperature for growth of algae	29 (fresh), 16 (spring), 25 (green)	^oC
Tmnt	optimal temperature for nitrification	30	^oC
Tr	reference temperature for metabolism	20	^oC
Trcod	reference temperature for COD oxidation	23	^oC
Trhdr	reference temperature for hydrolysis	20	^oC
Trmnl	reference temperature for mineralization	20	^oC
Trpr	reference temperature for predation	20	^oC
Wa	algal settling rate	0.0 (fresh), 0.5 (spring), 0.1 to 0.5 (green)	m d^{-1}

Table 2
Parameters in Kinetics Equations

Symbol	Definition	Value	Units
Wl	settling velocity of labile particles	1.0	m d^{-1}
Wr	settling velocity of refractory particles	1.0	m d^{-1}
Wg3	Settling velocity of G3 particles	1.0	m d^{-1}
Wpip	Settling velocity of particulate inorganic phosphorus	0.5	m d^{-1}
Wspo4	settling velocity for precipitated phosphate	1.0	m d^{-1}
α	initial slope of production vs. irradiance relationship	3.15 (fresh), 8.0 (spring), 10.0 (green)	g C g^{-1} Chl $(E\ m^{-2})^{-1}$

References

Ammerman, J., and Azam, F. (1985). "Bacterial 5'-nucleodase in aquatic ecosystems: a novel mechanism of phosphorus regeneration," *Science*, 227, 1338-1340.

Boni, L., Carpene, E., Wynne, D., and Reti, M. (1989). "Alkaline phosphatase activity in *Protogonyaulax Tamarensis*," *Journal of plankton research*, 11, 879-885.

Bunch, B., Cerco, C., Dortch, M., Johnson, B., and Kim, K. (2000). "Hydrodynamic and water quality model study of San Juan Bay and Estuary," ERDC TR-00-1, U.S. Army Engineer Research and Development Center, Vicksburg MS.

Cerco, C., and Cole, T. (1994). "Three-dimensional eutrophication model of Chesapeake Bay," Technical Report EL-94-4, US Army Engineer Waterways Experiment Station, Vicksburg, MS.

Cerco, C., Bunch, B., Cialone, M., and Wang, H. (1994). "Hydrodynamic and eutrophication model study of Indian River and Rehoboth Bay, Delaware," Technical Report EL-94-5, US Army Engineer Waterways Experiment Station, Vicksburg, MS.

Cerco, C., and Bunch, B. (1997). "Passaic River tunnel diversion model study, Report 5, water quality modeling," Technical Report HL-96-2, US Army Engineer Waterways Experiment Station, Vicksburg, MS.

Cerco, C., Johnson, B., and Wang, H. (2002). "Tributary refinements to the Chesapeake Bay model," ERDC TR-02-4, US Army Engineer Research and Development Center, Vicksburg, MS.

Cerco, C., and Noel, M. (2004). "The 2002 Chesapeake Bay eutrophication model," EPA 903-R-04-004, Chesapeake Bay Program Office, US Environmental Protection Agency, Annapolis MD. (available at http://www.chesapeakebay.net/modsc.htm)

Cerco, C., Kim, S.-C. and Noel, M. (2010). "The 2010 Chesapeake Bay eutrophication model," Chesapeake Bay Program Office, US Environmental Protection Agency, Annapolis MD. (available at http://www.chesapeakebay.net/publications/title/the_2010_chesapeake_bay_eutrophication_model1)

Cerco, C., and Noel, M. (2010). "Monitoring, modeling, and management impacts of bivalve filter feeders in the oligohaline and tidal fresh regions of the Chesapeake Bay system," *Ecological Modeling* 221, 1054-1064.

Chrost, R., and Overbeck, J. (1987). "Kinetics of alkaline phosphatase activity and

phosphorus availability for phytoplankton and bacterioplankton in Lake Plubsee (north German eutrophic lake)," *Microbial Ecology*, 13, 229-248.

DiToro, D., and Fitzpatrick, J. (1993). "Chesapeake Bay sediment flux model," Contract Report EL-93-2, US Army Corps of Engineers Waterways Experiment Station, Vicksburg MS.

Edinger, J., Brady, D., and Geyer, J. (1974). "Heat exchange and transport in the environment," Report 14, Department of Geography and Environmental Engineering, Johns Hopkins University, Baltimore, MD.

Genet, L., Smith, D., and Sonnen, M. (1974). "Computer program documentation for the Dynamic Estuary Model," US Environmental Protection Agency, Systems Development Branch, Washington, DC.

Hartman, B., and Hammond, D. (1985). "Gas exchange in San Francisco Bay," *Hydrobiologia* 129, 59-68.

HydroQual (2000). "Development of a suspension feeding and deposit feeding benthos model for Chesapeake Bay," Project USCE0410, prepared for US Army Engineer Research and Development Center, Vicksburg MS.

Jassby, A., and Platt, T. (1976). "Mathematical formulation of the relationship between photosynthesis and light for phytoplankton," *Limnology and Oceanography* 21, 540-547.

Keefe, C. (1994). "The contribution of inorganic compounds to the particulate carbon, nitrogen, and phosphorus in suspended matter and surface sediments of Chesapeake Bay," *Estuaries* 17,122-130.

Leonard, B. (1979). "A stable and accurate convection modelling procedure based on quadratic upstream interpolation," *Computer Methods in Applied Mechanics and Engineering*, 19, 59-98.

Matavulj, M., and Flint, K. (1987). "A model for acid and alkaline phosphatase activity in a small pond," *Microbial Ecology*, 13, 141-158.

Monod, J. (1949). "The growth of bacterial cultures," *Annual Review of Microbiology* 3, 371-394.

Morel, F. (1983). *Principles of Aquatic Chemistry*, John Wiley and Sons, New York, NY, 150.

O'Connor, D., and Dobbins, W. (1958). "Mechanisms of reaeration in natural streams," *Transactions of the American Society of Civil Engineers*, 123, 641-666.

O'Connor, D. (1983). "Wind effects on gas-liquid transfer coefficients," *Journal of the Environmental Engineering Division*, 190, 731-752.

Parsons, T., Takahashi, M., and Hargrave, B. (1984). *Biological oceanographic processes*. 3rd ed., Pergamon Press, Oxford.

Sellner, K., Lacoutre, R., and Parrish, C. (1988). "Effects of increasing salinity on a Cyanobacteria bloom in the Potomac River Estuary," *Journal of Plankton Research,* 10, 49-61.

Stumm, W., and Morgan, J. (1981). *Aquatic chemistry*. 2nd ed., Wiley-Interscience, New York.

Thomann, R., and Fitzpatrick, J. (1982). "Calibration and verification of a mathematical model of the eutrophication of the Potomac Estuary," HydroQual Inc., Mahwah, NJ.

Tchobanoglous, G., and Schroeder, E. (1987). *Water quality,* Addison Wesley, Reading, MA.

Tuffey, T., Hunter, J., and Matulewich, V. (1974). "Zones of nitrification", *Water Resources Bulletin*, 10, 555-564.

Wezernak, C., and Gannon, J. (1968). "Evaluation of nitrification in streams," *Journal of the Sanitary Engineering Division*, 94(SA5), 883-895.

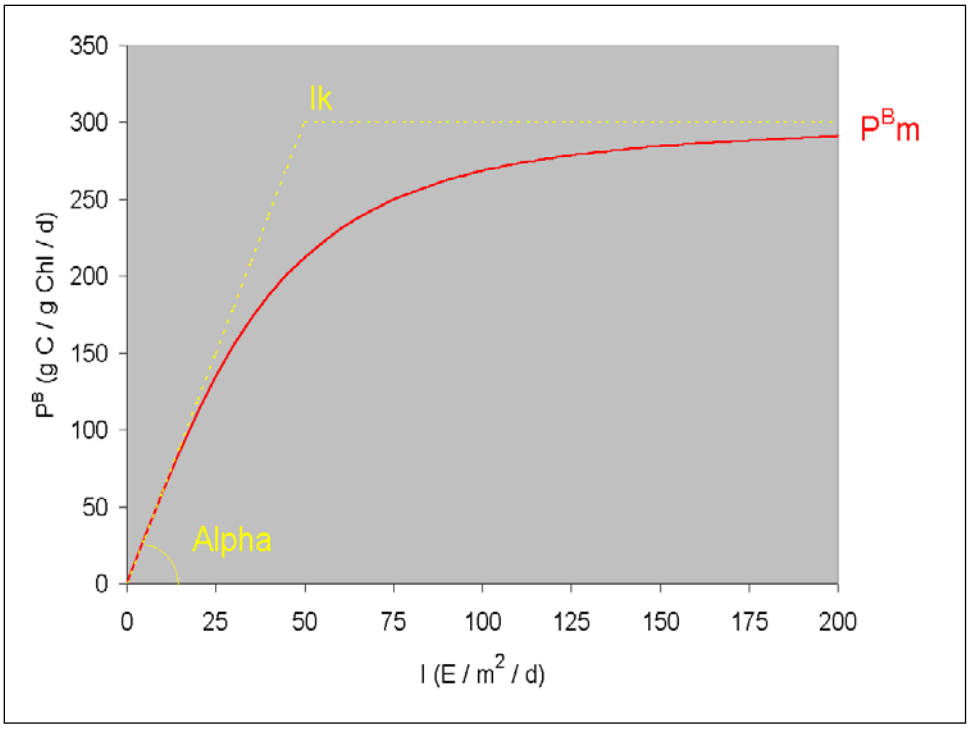

Figure 1. Production versus irradiance curve.

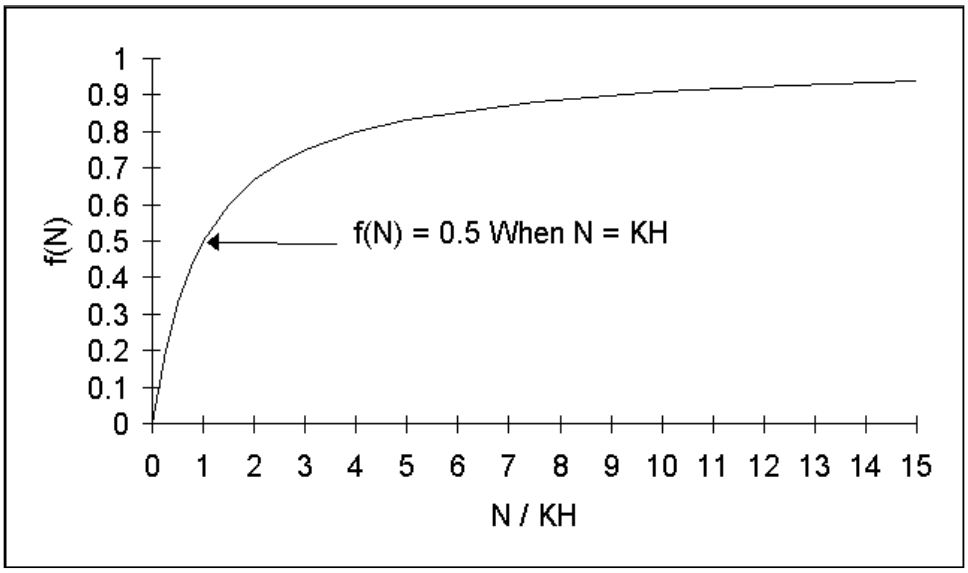

Figure 2. Monod formulation for nutrient-limited growth.

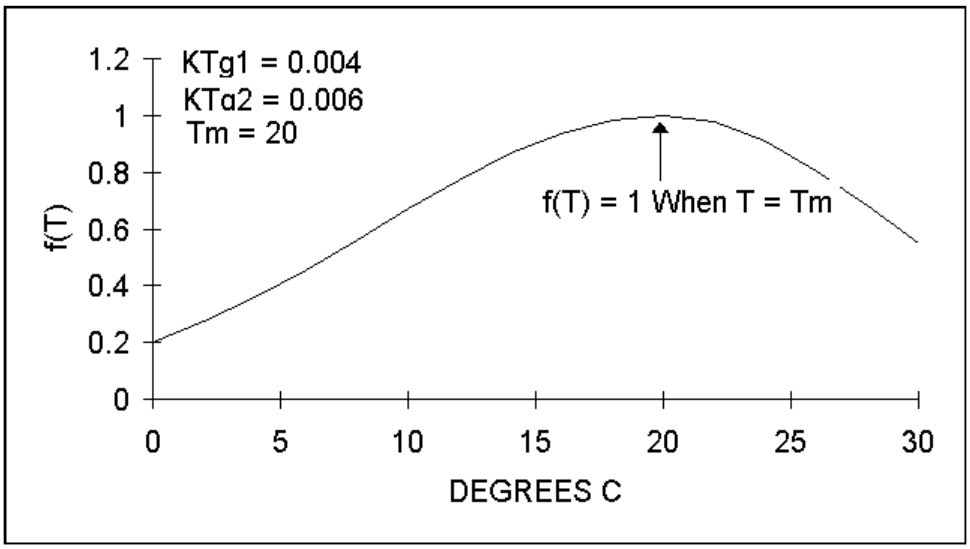

Figure 3. Relation of algal production to temperature.

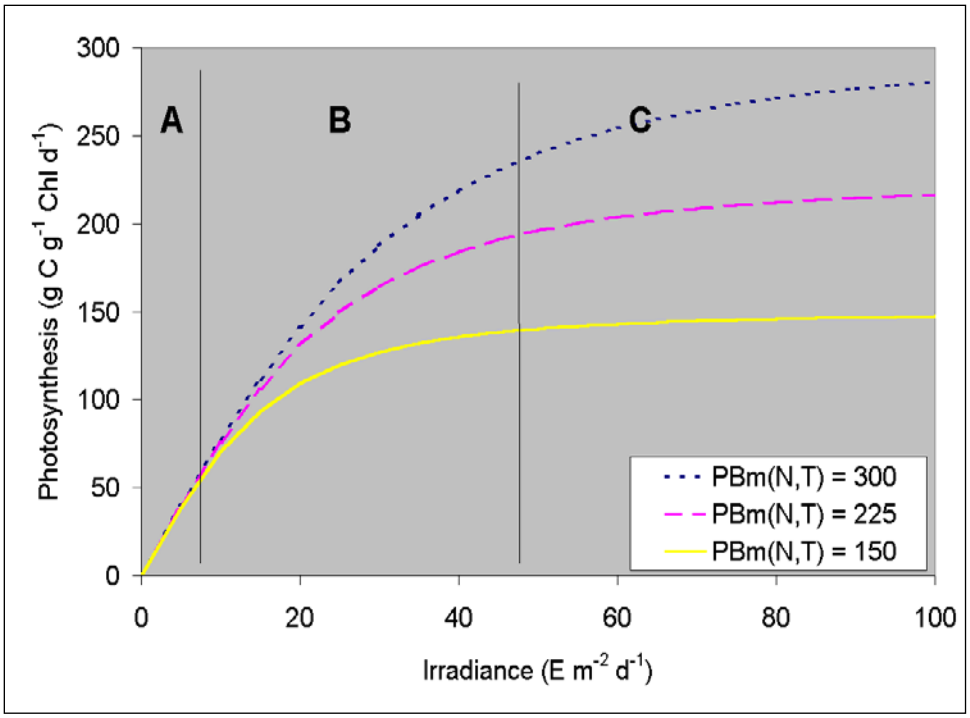

Figure 4. Effects of light and nutrients on production versus irradiance curve, determined for α = 8 (g C g^{-1} Chl (E m^{-2})$^{-1}$).

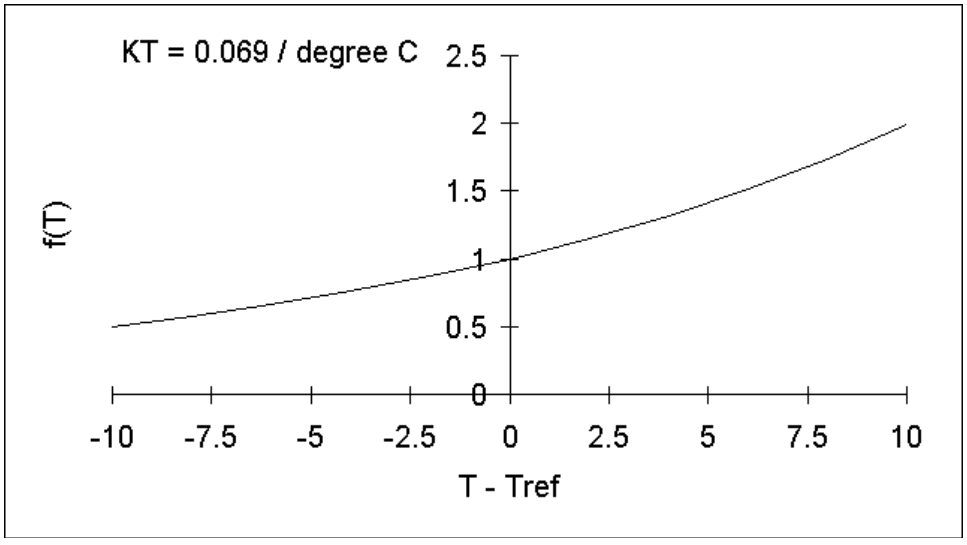

Figure 5. Exponential temperature relationship employed for metabolism and other processes

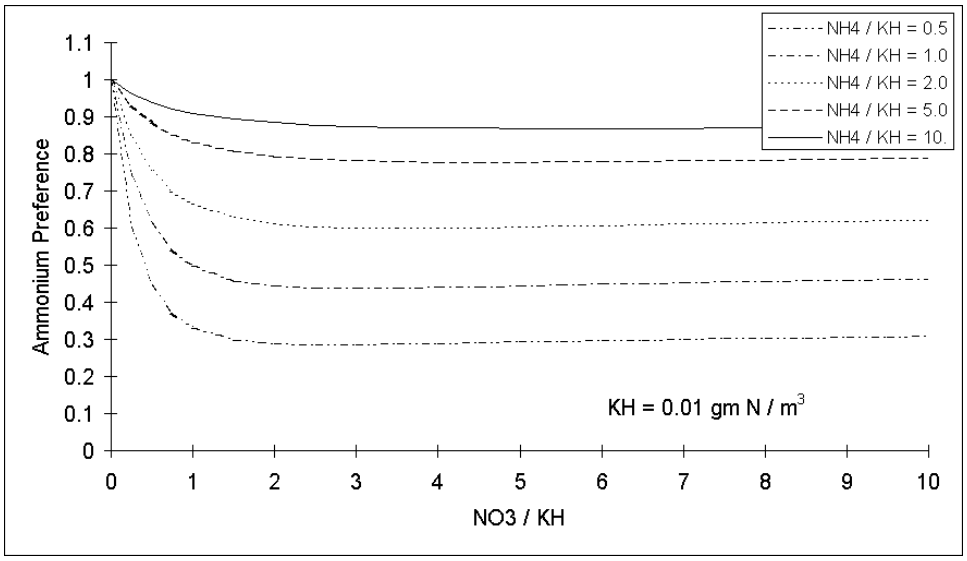

Figure 6. Algal ammonium preference

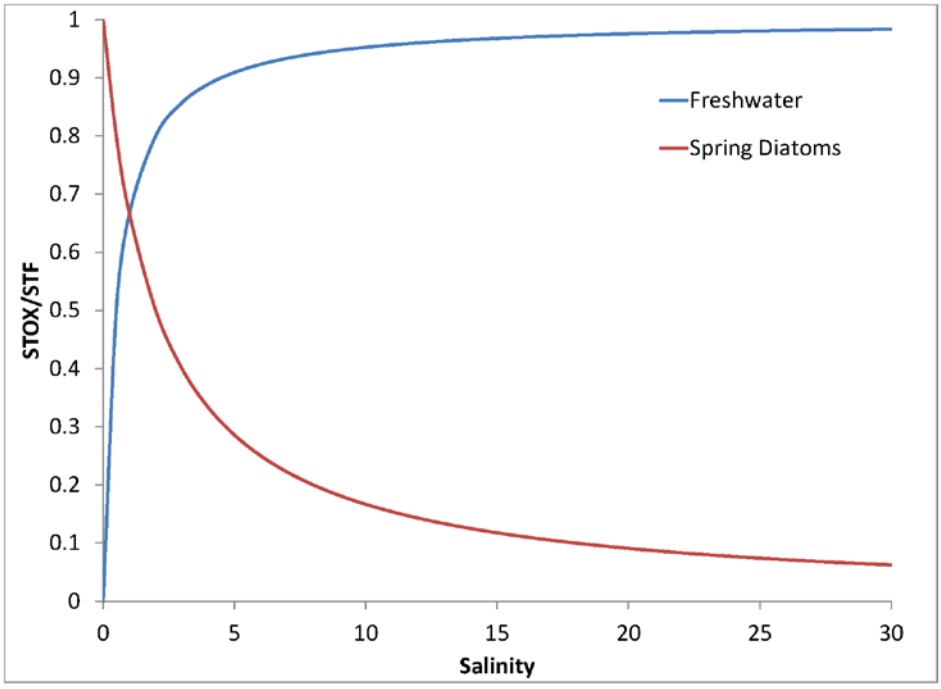

Figure 7. Salinity toxicity relationship.

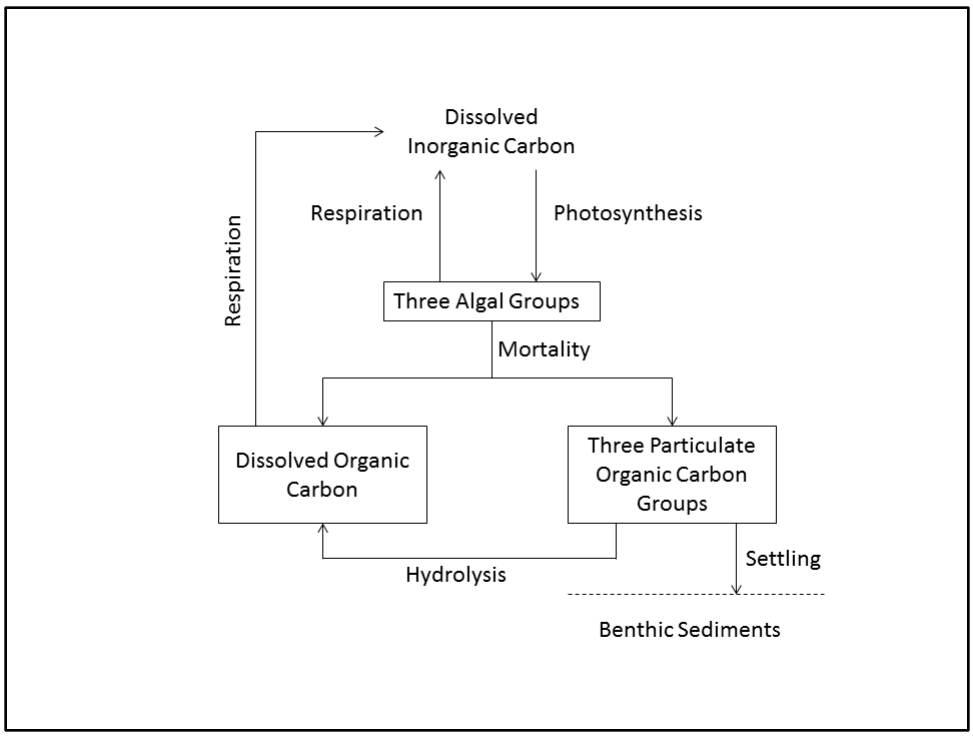

Figure 8. Model carbon cycle.

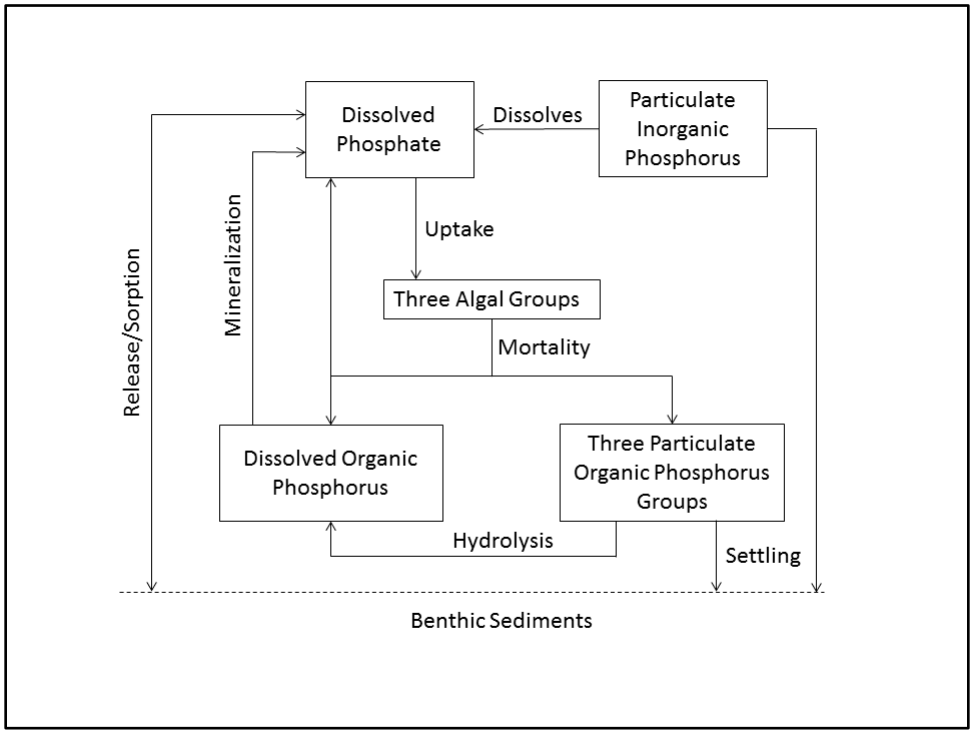

Figure 9. Model phosphorus cycle.

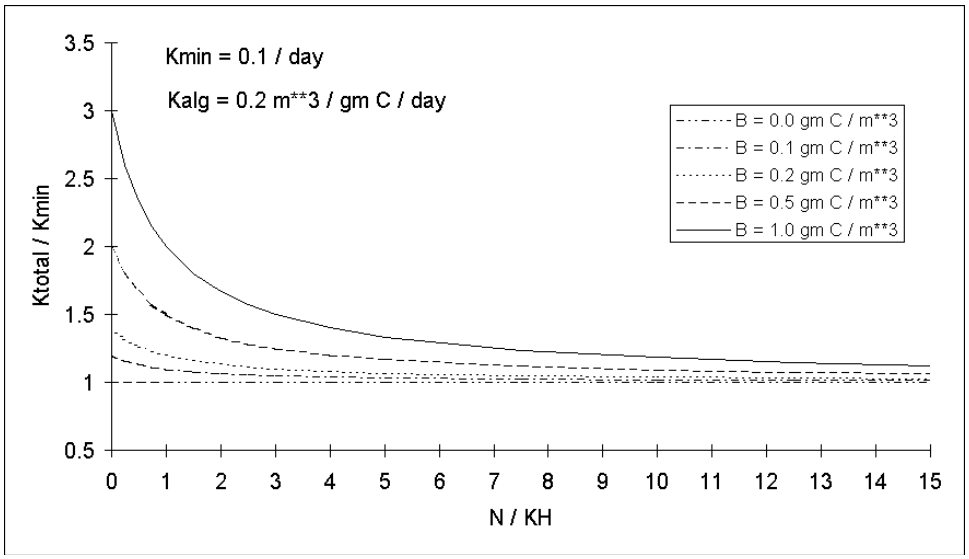

Figure 10. Effect of algal biomass and nutrient concentration on phosphorus mineralization.

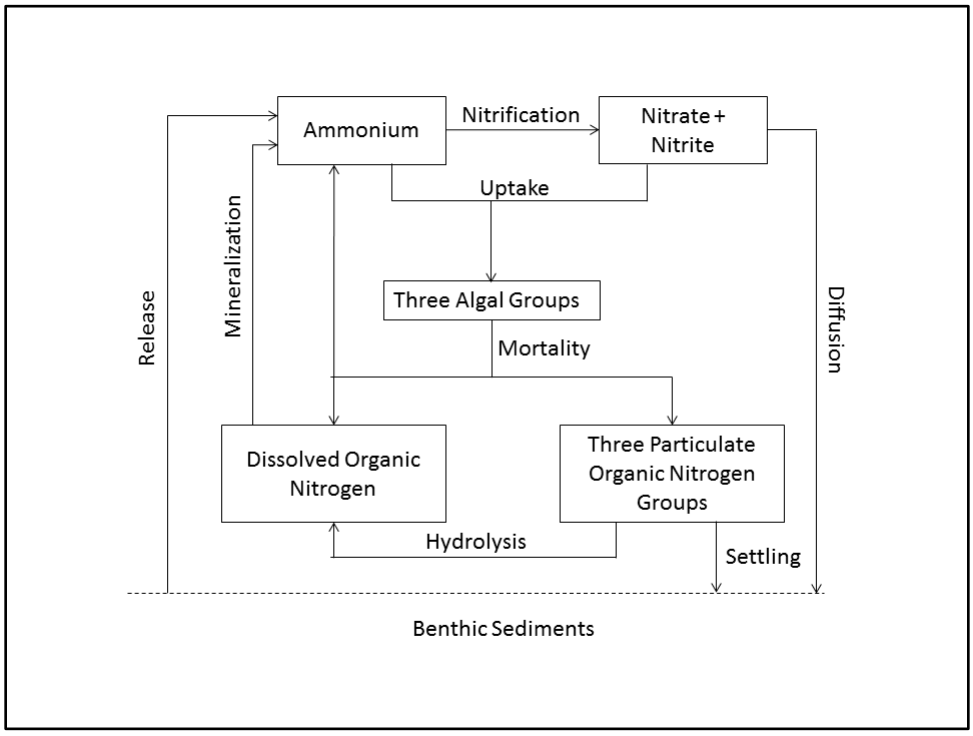

Figure 11. Model nitrogen cycle.

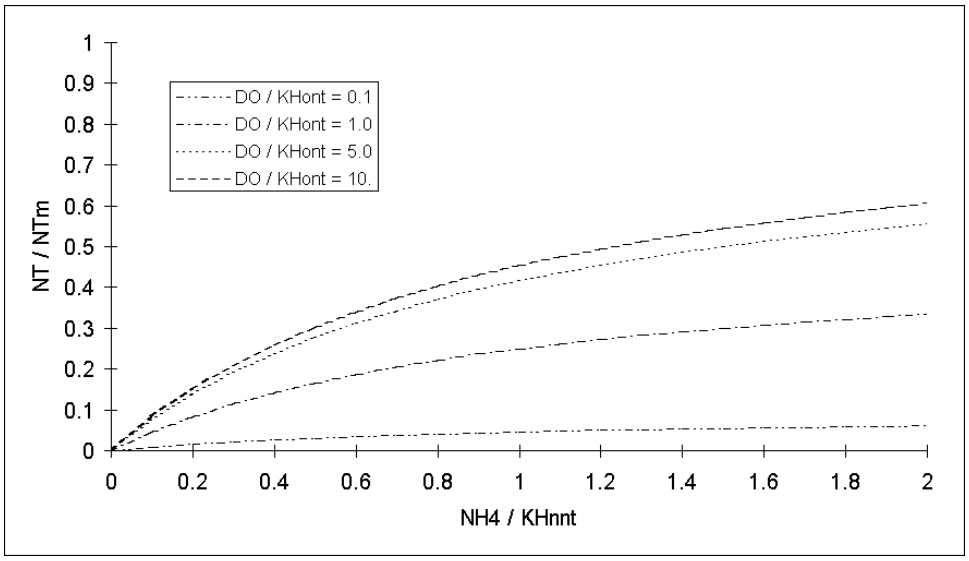

Figure 12. Effect of dissolved oxygen and ammonium concentration on nitrification rate.

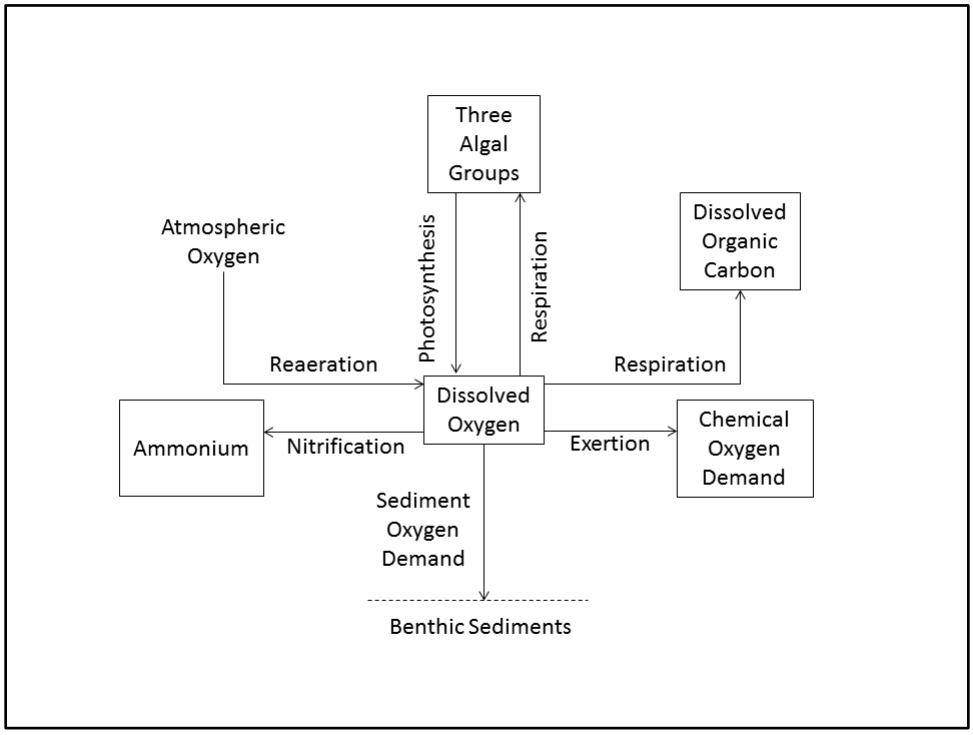

Figure 13. Dissolved oxygen sources and sinks.

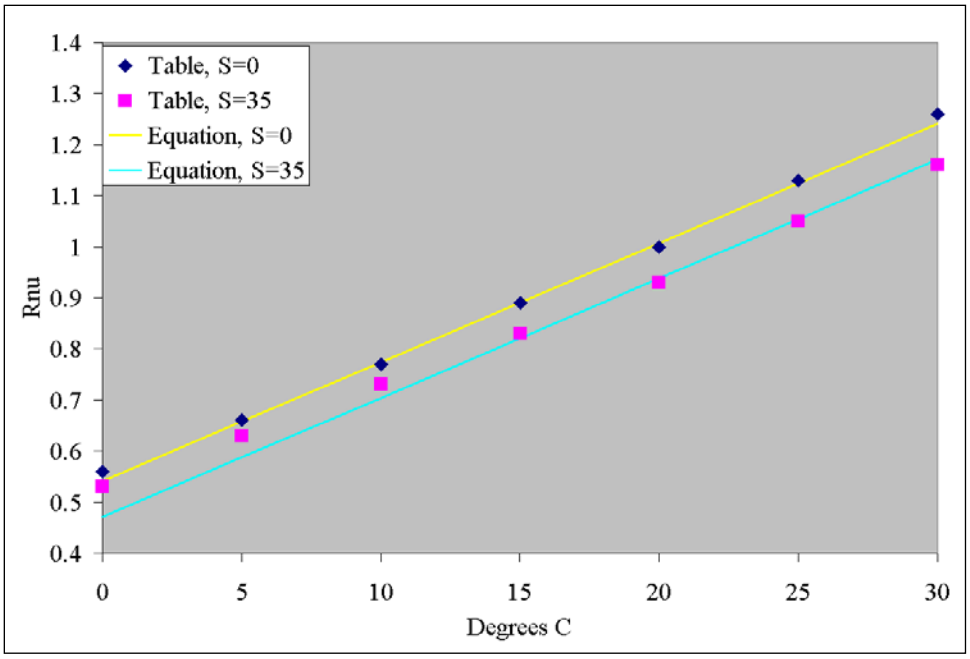

Figure 14. Computed and tabulated values of Rv.

3 Light Attenuation

Introduction

Light attenuation is computed using a "partial attenuation model" in which light attenuation is considered as the sum of the contribution from individual components. The components include water itself, colored organic matter, and suspended particles. The selection of components depends on available observations. The contribution from each component depends on local conditions.

Methods

Observations of light attenuation (Ke) and of contributors to attenuation were obtained from the Chesapeake Bay Program on-line data base (http://www.chesapeakebay.net/data/downloads/cbp_water_quality_database_1984_present). Observations were obtained for the years 2000 – 2010 from the Tidal Water Quality Monitoring Program and the Shallow Water Monitoring Program. Contributors included particulate organic carbon (POC), dissolved organic carbon (DOC), volatile suspended solids (VSS), total suspended solids (TSS), salinity (SALT), and chlorophyll 'a' (CHL). DOC and SALT were included as potential indicators of color while the other contributors represented various fractions of suspended solids. Negative values and outliers were removed from the data base, leaving nearly 18,000 observations of KE and contributing factors.

Stepwise regression was employed to evaluate additive models which included various combinations of contributing factors. Superior results (R^2 = 0.623) were obtained for a simple model which related KE to TSS and SALT:

$$Ke = a1 + a2 \cdot TSS + a3 \cdot SALT \qquad (1)$$

in which:

Ke = coefficient of diffuse light attenuation (m^{-1})
a1 = background attenuation (m^{-1})
a2 = attenuation by total suspended solids ($m^2\ g^{-1}$)
a3 = relationship between attenuation and salinity ($m^2\ kg^{-1}$)
TSS = total suspended solids concentration ($g\ m^{-3}$)
SALT = salinity ($kg\ m^{-3}$)

CHL was an additional significant ($p < 0.0001$) contributor to attenuation but the marginal improvement in R^2 was small, 0.012, so CHL was neglected in the model.

After the model was established, residuals were examined by monitoring station. Background attenuation (parameter a1) was adjusted in regions of the Bay which were judged to have significant, consistent, residuals. Additional adjustments to parameter a1 were performed in a few regions based on model-data comparisons following operation of the water quality model (WQM).

Results

Parameter values obtained from regression were: a1 = 1.647 m^{-1}; a2 = 0.0557 m^2 g^{-1}; a3 = -0.0624 m^2 kg^{-1}. The negative value for a3 implies that freshwater is more highly-colored than ocean water. Attenuation due to color diminishes as the fraction of ocean water at the sample location increases. Examination of residuals indicated:

- Negative residuals (observed attenuation less than modeled) near the James, Rappahannock, Potomac and Susquehanna fall lines.
- Negative residuals in the lower Potomac and St. Marys River.
- Positive residuals (observed attenuation greater than modeled) in the York and Mattaponi rivers.
- Positive residuals in the lower James and Elizabeth Rivers.

Adjustments to background attenuation are presented in Table 1 for Chesapeake Bay Program Segments as shown in Figure 1.

Additional Model Considerations

Observed TSS in the attenuation relationship is the sum of organic and inorganic particulate matter. Multiple WQM state variables must be summed to obtain TSS for use in the relationship. Concentration of inorganic solids is obtained from the WQM as the sum of the fine clay, clay, silt, and sand state variables. Observed organic (volatile) solids correspond to model POC state variables. For idealized organic matter, represented as CH_2O, organic solids concentration would be 2.5 times POC concentration. In reality, this ratio can vary. The appropriate ratio for Chesapeake Bay was obtained by Type II regression (Laws and Archie, 1981) of observed VSS on observed POC. The result indicated organic solids = 2.9 * POC ($R^2 = 0.889$). Model POC is the sum of the three algal groups and three particulate organic carbon variables.

The negative relationship between Ke and SALT can result in negative values for Ke under conditions of high salinity coupled with low TSS. To avoid negative values, a minimum Ke value of 0.15 m^{-1} is imposed.

Comparison of Two Optical Models

The partial attenuation model (PAM) described here replaces an advanced optical model (AOM) employed in the 2010 model study (Cerco et al. 2010). Following parameterization of the PAM and implementation in the WQM, a model run was made for comparison of results with the previous optical

model. Computations of Ke were compared using the absolute mean difference statistic developed for the initial Chesapeake Bay model (Cerco and Cole 1994) and utilized thereafter to examine model performance:

$$AMD = \frac{\sum|P - O|}{N} \quad (4)$$

in which:

AMD = absolute mean difference
O = observation
P = prediction
N = number of observations

The absolute mean difference is a measure of the characteristic difference between individual observations and computations. An absolute mean difference of zero indicates the model perfectly reproduces each observation.

Statistics were determined using the model-data pairs employed in the model validation time series plots and grouped into systems. Results indicate the AOM and PAM deliver comparable performance in the mainstem Bay (Figure 2). For most other regions of the system, AMD is lower for the PAM than the AOM. Only in the Potomac River are results from the AOM superior to the PAM. These results should not be interpreted that PAMs are superior to AOMs. AOMs such as the one employed in the 2010 study are based on rigorous physics and are preferred in applications which emphasize optical properties of surface waters. The less rigorous PAM described here is suitable, however, to describe light attenuation in a study such as this one and is advantageous in terms of computational requirements and data requirements.

References

Cerco, C.F. and Cole, T. M. (1994). "Three-dimensional eutrophication model of Chesapeake Bay," Technical Report EL-94-4, U.S. Army Engineer Waterways Experiment Station, Vicksburg MS.

Cerco, C., Kim, S.-C. and Noel, M. (2010). "The 2010 Chesapeake Bay eutrophication model," Chesapeake Bay Program Office, US Environmental Protection Agency, Annapolis MD. (available at http://www.chesapeakebay.net/publications/title/the_2010_chesapeake_bay_eutrophication_model1)

Laws, E., and Archie, J. (1981). "Appropriate use of regression analysis in marine biology," *Marine Biology* 65, 13-16.

Table 1
Adjustments to Background Attenuation

CBPS	Adjustment	CBPS	Adjustment
CB1	-0.4	SBEMH	+0.6
CB2	-0.3	WBEMH	+0.6
CB3	-0.3	LAFMH	+0.6
CB4	-0.3	POTOH	-0.4
CB5	-0.3	YRKMH	+0.5
BOHOH	+0.7	POTTF	-0.4
CHSTF	+0.7	ANATF	-0.4
CHOOH	+0.6	MATTF	-0.4
PAXMH	-0.5	PISTF	-0.4
POTMH	-0.4	MPNOH	+0.5
EBEMH	+0.6	MPNTF	+0.5
ELIPH	+0.6	BSHOH	+0.5

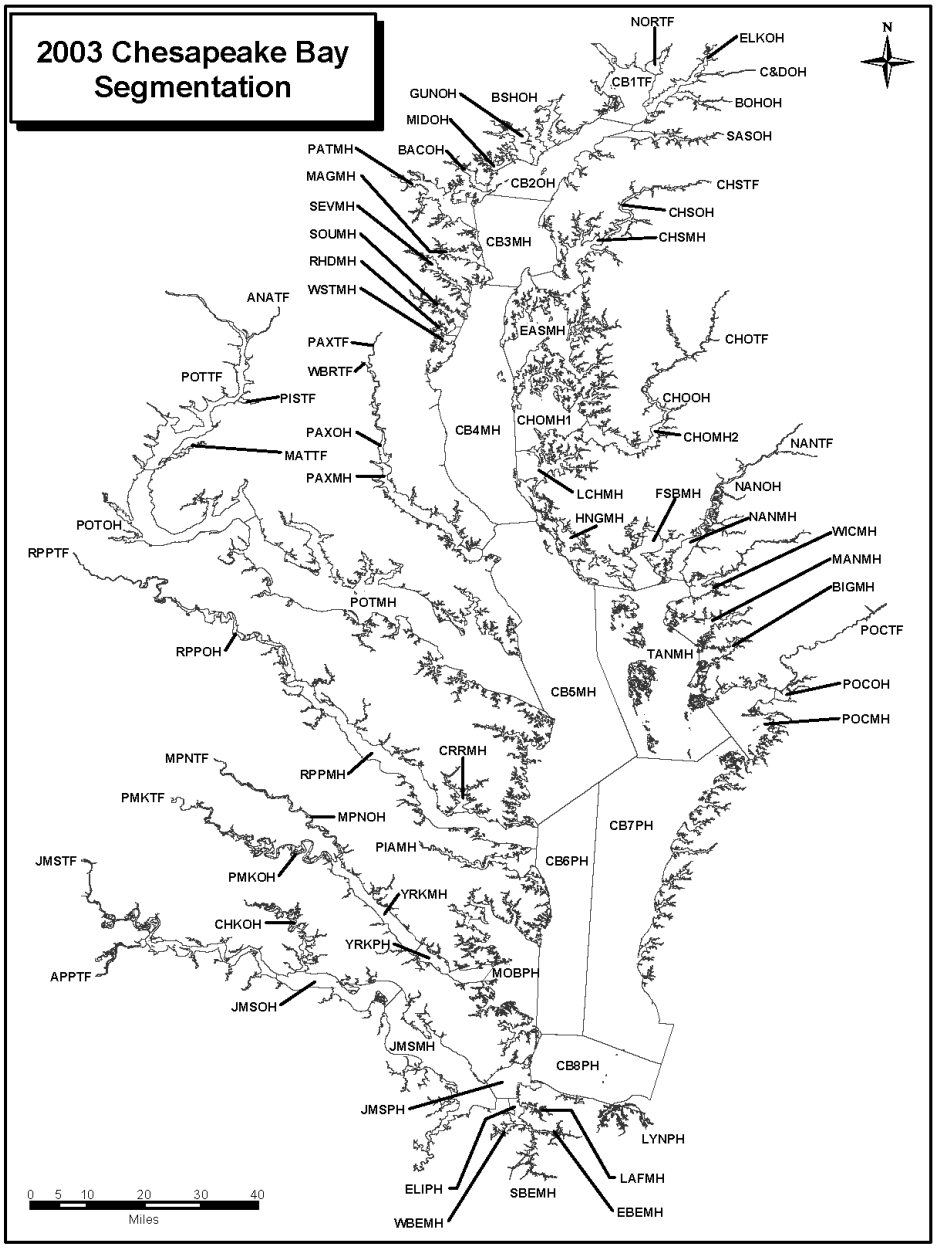

Figure 1. Chesapeake Bay Program Segments. Background attenuation was adjusted on segment-wide basis for segments listed in Table 1.

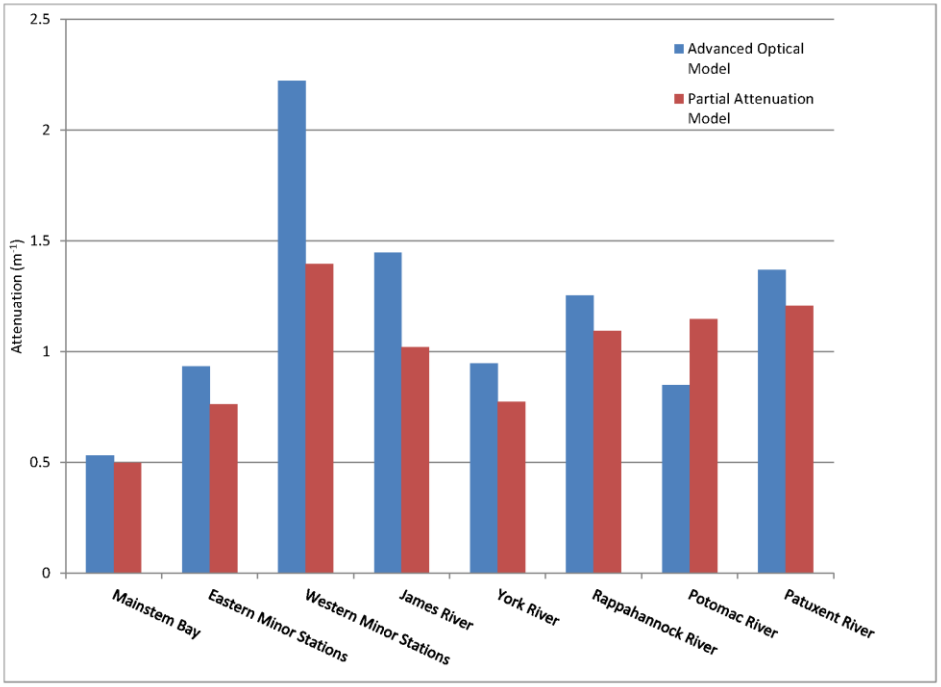

Figure 2. Light attenuation absolute mean difference statistic for the partial attenuation model vs. the advanced optical model.

4 Wetlands Module

Introduction

A decades long, abundant literature describes tidal wetlands processes and interactions between tidal wetlands and open waters of the Chesapeake Bay system. Wetlands processes relevant to management include: nitrogen removal through denitrification (Neubauer et al. 2005; Hopfensperer et al. 2009; Seldomridge and Prestegaard 2014); nitrogen removal through burial (Morse et al. 2004; Neubauer et al. 2005; Boynton et al. 2008; Palinkas and Cornwell 2012); phosphorus removal through burial (Morse et al. 2004; Boynton et al. 2008; Palinkas and Cornwell 2012); production and burial of organic carbon (Flemer et al. 1978; Neubauer et al. 2000; Neubauer et al. 2002; Morse et al. 2004); burial of organic and inorganic solids (Stevenson et al. 1985; Ward et al. 1998; Morse et al. 2004; Palinkas et al. 2013); and dissolved oxygen consumption through respiration (Neubauer et al. 2000; Neubauer et al. 2002; Neubauer and Anderson 2003). In recognition of wetland effects, protocols have been developed to provide nutrient and sediment mass reduction credits for shoreline management projects that include restoration of vegetation (Drescher and Stack 2015). Wetlands loss, associated with sea-level rise and diminishing sediment inputs, has been noted in the Bay for decades (Stevenson et al. 1985; Ward et al. 1998; Kearney et al. 2002). Concern over potential wetlands loss is increasing in parallel with concern over sea-level rise associated with climate change (Glick et al. 2008).

The effect of wetlands respiration on adjacent open water was included in the 2010 Chesapeake Bay model (Cerco et al. 2010). In view of the load-reduction credits recommended for wetlands restoration and the potential ecosystem effects of wetlands loss, a more detailed wetlands module has been incorporated into the 2015 Chesapeake Bay model. The module focuses on wetlands functions which have management implications: nutrient removal, solids removal, and respiration.

Formulations

Formulation of a detailed model of wetlands biogeochemical processes is a formidable prospect in view of the process complexity and the variety of wetlands in the Chesapeake Bay system. We focus here on basic relationships which describe the desired functions. The relationships incorporate rate-limiting functions which provide "feedback" between the rate of material removal by wetlands and the amount of material available in the adjacent open water column.

Potential effects of wetlands location and type are accommodated by local variations in parameter assignment.

Denitrification

The effect of wetland denitrification on adjacent open water is represented through a nitrate-removal algorithm. Nitrate removal is not exactly equivalent to denitrification (Neubauer et al. 2005; Seldomridge 2014) but the removal process is readily inferred and easily parameterized through nitrate observations in the water column. The relationship is:

$$V \cdot \frac{dC}{dT} = Transport + Kinetics - MTC \cdot f(T) \cdot C \cdot Aw \qquad (1)$$

in which:

V = volume of water-quality model cell adjacent to wetlands (m^3)
C = nitrate concentration (g m^{-3})
MTC = mass-transfer coefficient (m d^{-1})
f(T) = temperature effect
Aw = area of wetland adjacent to water-quality model cell (m^2)

The temperature effect is an exponential relationship in which denitrification doubles for a 10 ^{o}C temperature increase.

Particle Settling

Settling of all particles, organic and inorganic is represented by the same formulation:

$$V \cdot \frac{dC}{dT} = Transport + Kinetics - WSw \cdot C \cdot Aw \qquad (2)$$

in which:

C = particle concentration (g m^{-3})
WSw = wetland settling velocity (m d^{-1})

Differences in settling rates for different particle types are accommodated by varying parameter WSw.

Respiration

Net dissolved oxygen uptake is represented:

$$V \cdot \frac{dDO}{dT} = Transport + Kinetics - f(DO) \cdot f(T) \cdot WOC \cdot Aw \qquad (3)$$

in which:

DO = dissolved oxygen concentration (g m^{-3})
f(DO) = limiting factor: DO/(Kh + DO)

Kh = dissolved oxygen concentration at which uptake is halved (g m^{-3})
WOC = wetlands oxygen consumption (g m^{-2} d^{-1})

Process Observations

Observations of relevant wetlands processes are concentrated in several "hot spots" around the Bay system (Figure 1). These hotspots include reaches in the York (MPNON, PMKOH) and Patuxent Rivers (PAXOH), and in the vicinity of the Nanticoke River (NANOH, NANMH, FSBMH, WICMH). Additional observations useful for parameter evaluation and for comparison with the model are found in the Potomac (POTTF), Bush (BSHOH), and Chester Rivers (CHSMH). The observations were collected for varying purposes and represent a wide variety of methods, reporting units, and time frames. Reports from multiple studies (Table 1) were assembled, converted to relevant units, and summarized for use in the wetlands module (Table 2).

Wetlands Areas

Tidal wetlands areas were obtained from an application of the SLAMM (Sea Level Affecting Marshes Model). The SLAMM application (Glick et al. 2008) projected wetlands areas in the Chesapeake and Delaware Bay regions as a function of sea-level rise associated with climate change. GIS files of wetlands areas adjoining Chesapeake Bay were provided by Dr. Lora Harris of the University of Maryland Center for Environmental Science. The Chesapeake Bay portion of the SLAMM application was extracted previously as part of a study of nitrogen removal by Chesapeake Bay tidal wetlands (Bryan 2014). Wetlands areas from SLAMM for the year 1996 were employed in our model. Chesapeake Bay tidal wetlands totaled 130,000 hectares. More than 90% was classified as salt or brackish marsh with the remainder tidal freshwater (Figure 2). The SLAMM areas were compared to projections from a 1996 National Wetlands Inventory (NWI) provided by the Chesapeake Bay Program. Good agreement was noted between the SLAMM area and the sum of NWI "emergent" wetlands, 125,000 hectares.

GIS projections of tidal wetlands were combined with projections of the Bay watershed and of the model grid (Figure 3). Next, contiguous wetlands were divided into a "fishnet" of sub-segments (Figure 4). Sub-segment areas were assigned to the nearest model surface cell (Figure 5), taking care not to cross local "HUC 10" watershed boundaries (Figure 6). The final product was a table of tidal wetlands area associated with surface cells on the model grid. Roughly 2,300 of the total 11,000 surface cells adjoin tidal wetlands.

The tidal wetlands area is roughly 11% of the open-water area of the bay system, as represented on the model grid. For some regions, the area of adjacent tidal wetlands equals or exceeds the open-water area (Figures 7, 8). These regions are expected to demonstrate the greatest influence of tidal wetlands on water-quality constituents.

Initial Model Results

The observed removal rates are often quantified by methods, such as analysis of sediment profiles, which provide rates averaged over lengthy periods. Some studies also describe rates at small spatial scales not represented in the model. The various methodologies, time scales, and spatial scales restrict the nature of model-data comparisons. The comparisons we provide here are of long-term average model rates versus the range of rates observed in each of the regions with observations (Figure 1). Comparisons for burial of carbon, nitrogen, phosphorus, and fixed solids are shown in Figures 9-12, based on an initial parameter set presented in Table 3. An initial judgment is that the model wetlands are burying less material, on average, then depicted in the range of observations. One inference from this judgement is that the initial wetlands settling rates should be increased. An alternate explanation is that the observed burial rates for carbon, nitrogen and phosphorus are not comprised exclusively of particulate material removed from the water column, as represented in the module. Burial may include carbon fixed by wetlands vegetation and dissolved nutrients converted by vegetation to particulate organic form. Modeled wetlands nitrate uptake is less than the range of observations (Figure 13) suggesting need for revision of the initial nitrate mass-transfer coefficient. Parameter assignment and judgments of model performance will both require revision following revision to watershed loads and examination of water quality model calibration status.

The Water Quality Goals Implementation Team has provided values for nutrient reduction credits associated with vegetation restoration (Drescher and Stack 2015). The values, 0.026 g N m^{-2} d^{-1} and 0.016 g P m^{-2} d^{-1}, are based on an extensive literature survey which includes studies outside the limited geographic range considered here. The model nitrogen removal rates, which combine denitrification and burial, are representative of the recommended credits (Figure 14). Model phosphorus removal, equivalent to burial, is much less than the recommended credit (Figure 11). Model phosphorus removal can be increased through an increase in the wetlands settling velocity but the recommended credit is outside the range of the observed burial rates considered herein.

A uniform wetlands oxygen consumption rate of 0.5 g m^{-2} d^{-1} was implemented in the module. The implemented rate is reduced, on average, by local dissolved oxygen availability and seasonal temperature variation (Figure 15). The model rate is less than limited reported rates (Table 2) although larger instantaneous rates are expected from the model based on local temperature and dissolved oxygen conditions.

Preliminary sensitivity runs demonstrate the ability of the wetlands module to improve water quality model performance. Nitrate computations in a 40-km reach of the York River are improved when wetlands nitrate uptake is represented in the model (Figure 16). Dissolved oxygen sags in the Patuxent and York River are explained by wetlands respiration (Figure 17) and total nitrogen computations in the Nanticoke River are improved when wetlands nitrogen removal is considered (Figure 18).

The wetlands module is still under development. Major changes in the formulations are not expected but comparisons to observations will be revised

following implementation of final watershed model loads and additional calibration of the water quality model and the wetlands module.

References

Cerco, C., Kim, S.-C. and Noel, M. (2010). "The 2010 Chesapeake Bay eutrophication model," Chesapeake Bay Program Office, US Environmental Protection Agency, Annapolis MD. (available at http://www.chesapeakebay.net/publications/title/the_2010_chesapeake_bay_eutrophication_model1)

Bryan, J. (2014). "Effects of sea level rise on tidal marshes," Thesis submitted to the faculty of the graduate school of the University of Maryland, College Park, in partial fulfillment of the requirements for the degree of Master of Science.

Boynton, W., Hagy, J., Cornwell, J., Kemp, W., Greene, S., Owens, M., Baker, J., and Larsen, R. (2008). "Nutrient budgets and management actions in the Patuxent River estuary," *Estuaries and Coasts*, 31, 623-651.

Drescher, S., and Stack, B. (2015). "Recommendations of the expert panel to define removal rates for shoreline management projects," Chesapeake Bay Partnership. (available at http://www.chesapeakebay.net/documents/Shoreline_Management_Protocols_Final_Approved_07132015-WQGIT-approved.pdf)

Flemer, D., Heinle, D., Keefe, C., and Hamilton, D. (1978). "Standing crops of marsh vegetation of two tributaries of Chesapeake Bay," *Estuaries*, 1(3), 157-163

Glick, P., Clough, J., and Nunley, B. (2008). "Sea-level rise and coastal habitats in the Chesapeake Bay region," National Wildlife Federation. (available at https://www.nwf.org/~/media/PDFs/Global-Warming/Reports/SeaLevelRiseandCoastalHabitats_ChesapeakeRegion.ashx)

Hopfensperer, K., Kaushal, S., Findlay, S., and Cornwell, J. (2009). "Influence of plant communities on denitrification in a tidal freshwater marsh of the Potomac River, United States," *Journal of Environmental Quality*, 38, 618-626

Kearney, M., Rogers, J., Townshend, E., Rizzo, E., Stutzer, D., Stevenson, J., and Sundborg, K. (2002). "Landsat Imagery Shows Decline of Coastal Marshes in Chesapeake and Delaware Bays," *Eos* 83(16), 173, 177-178.

Morse, J., Megonigal, J., and Waldbridge, M. (2004). "Sediment nutrient accumulation and nutrient availability in two tidal freshwater marshes along the Mattaponi River, Virginia, US," *Biogeochemistry*, 69, 175-206

Neubauer, S., Miller, W., and Anderson, I. (2000). "Carbon cycling in a tidal freshwater marsh ecosystem: a carbon gas flux study," *Marine Ecology Progress Series*, 199, 13-30.

Neubauer, S., Anderson, I., Constantine, J., and Kuel, S. (2002). "Sediment deposition and accretion in a Mid-Atlantic (U.S.) tidal freshwater marsh," *Estuarine, Coastal and Shelf Science*, 54, 713-727.

Neubauer, S., and Anderson, I. (2003). "Transport of dissolved inorganic carbon from a tidal freshwater marsh to the York River estuary," Limnology and Oceanography, 4891), 299-307

Neubauer, S., Anderson, I., and Neikirk, B. (2005). "Nitrogen cycling and ecosystem exchanges in a Virginia tidal freshwater marsh," *Estuaries*, 28(6), 909-922.

Palinkas, C., and Cornwell, J. (2012). "A preliminary sediment budget for the Corsica River (MD): Improved estimates of nitrogen burial and implications for restoration," *Estuaries and Coasts*, 35, 546-558.

Palinkas, C., Engelhardt, K., and Cadol, D. (2013). "Evaluating physical and biological influences on sedimentation in a tidal fresh marsh with 7Be," *Estuarine, Coastal and Shelf Science*, 129, 152-161

Seldomridge, E., and Prestegaard, K. (2014). "Geochemical, temperature, and hydrologic transport limitations on nitrate retention in tidal freshwater wetlands, Patuxent River, Maryland," *Wetlands*, 34, 641-651.

Stevenson, J., Kearney, M., and Pendleton, E. (1985). "Sedimentation and erosion in a Chesapeake Bay brackish marsh system," *Marine Geology*, 67, 213-235.

Ward, L., Kearney, M., and Stevenson, J. (1998). "Variations in sedimentary environments and accretionary patterns in estuarine marshes undergoing rapid submergence, Chesapeake Bay," *Marine Geology*, 151, 111-134.

Table 1
Studies Contributing to Process Data Base

Authors	Year	Citation
Boynton, W., Hagy, J., Cornwell, J., Kemp, W., Greene, S., Owens, M., Baker, J., and Larsen, R.	2008	Estuaries and Coasts, 31, 623-651
Flemer, D., Heinle, D., Keefe, C., and Hamilton, D.	1978	Estuaries, 1(3), 157-163
Hopfensperer, K., Kaushal, S., Findlay, S., and Cornwell, J.	2009	Journal of Environmental Quality, 38, 618-626
Merrill, J., and Cornwell, J.	2002	Weinstein, W., and Kreeger, D., eds., EBSCO Publishing
Morse, J., Megonigal, J., and Waldbridge, M.	2004	Biogeochemistry, 69, 175-206
Neubauer, S., Anderson, I., and Neikirk, B.	2005	Estuaries, 28(6), 909-922
Neubauer, S., Miller, W., and Anderson, I.	2000	Marine Ecology Progress Series, 199, 13-30
Newbauer, S., and Anderson, I	2003	Limnology and Oceanography, 4891, 299-307
Newbauer, S., Anderson, I., Constantine, J., and Kuel, S	2002	Estuarine, Coastal and Shelf Science, 54, 713-727
Palinkas, C., and Cornwell, J.	2012	Estuaries and Coasts, 35, 546-558
Palinkas, C., Engelhardt, K., and Cadol, D.	2013	Estuarine, Coastal and Shelf Science, 129, 152-161
Seldomridge, E., and Prestegaard, K.	2014	Wetlands, 34, 641-651
Stevenson, J., Kearney, M., and Pendleton, E.	1985	Marine Geology, 67, 213-235
Ward, L., Kearney, M., and Stevenson, J.	1998	Marine Geology, 151, 111-134

Table 2
Summary of Wetlands Process Observations for Use in Model Parameterization and Validation.

CBPS	C deposition, g m^{-2} d^{-1}	N deposition, g m^{-2} d^{-1}	P deposition, g m^{-2} d^{-1}	denitrification, g N m^{-2} d^{-1}	solids deposition, g m^{-2} d^{-1}	respiration, g DO m^{-2} d^{-1}
BSHOH		0.008 to 0.032	0.001 to 0.006			
CHSMH		0.02 to 0.064	0.01 to 0.019		3.6	
FSBMH	0.16 to 0.33				0.3	
MPNOH	0.24 to 2.77	0.019 to 0.238	0.004 to 0.085		1.43 to 42.0	
MPNTF						
NANMH	0.033 to 0.126				1.61 to 8.12	
NANOH	0.033 to 0.126				1.61 to 8.12	
PAXOH		0.008	0.002		5.75	
PAXTF		0.033 to 0.064	0.01	0.108 to 0.197	5.75	
PMKOH	0.61	0.05		0.04		1.12 to 2.77
POTTF	1.44			0.043 to 0.06	5.88	
WICMH	0.033 to 0.126	0.037	2.74 e-5 to 0.004		1.61 to 8.12	
CHOMH		0.053 to 0.074	4.9 e-4 to 0.005			
WQGIT			0.0016	0.026		

Table 3
Wetlands Module Parameters

Parm	Definition	Value	Units
WSl	settling velocity of labile organic particles	0.05	m d^{-1}
WSr	settling velocity of refractory organic particles	0.05	m d^{-1}
WSg3	settling velocity of G3 organic particles	0.05	m d^{-1}
WSb1	settling velocity of Group 1 phytoplankton	0.005	m d^{-1}
WSb2	settling velocity of Group 2 phytoplankton	0.005	m d^{-1}
WSb3	settling velocity of Group 3 phytoplankton	0.005	m d^{-1}
WSpip	settling velocity of particulate inorganic phosphorus	0.01	m d^{-1}
WSfclay	settling velocity of fine clay	0.05	m d^{-1}
WSclay	settling velocity of clay	0.13	m d^{-1}
WSsilt	settling velocity of silt	0.432	m d^{-1}
WOC	wetlands oxygen consumption at 20 ^{o}C	0.5	g DO m^{-2} d^{-1}
Kh	DO concentration at which wetlands consumption is halved	1	g m^{-3}
MTC	nitrate mass-transfer coefficient	0.05	m d^{-1}

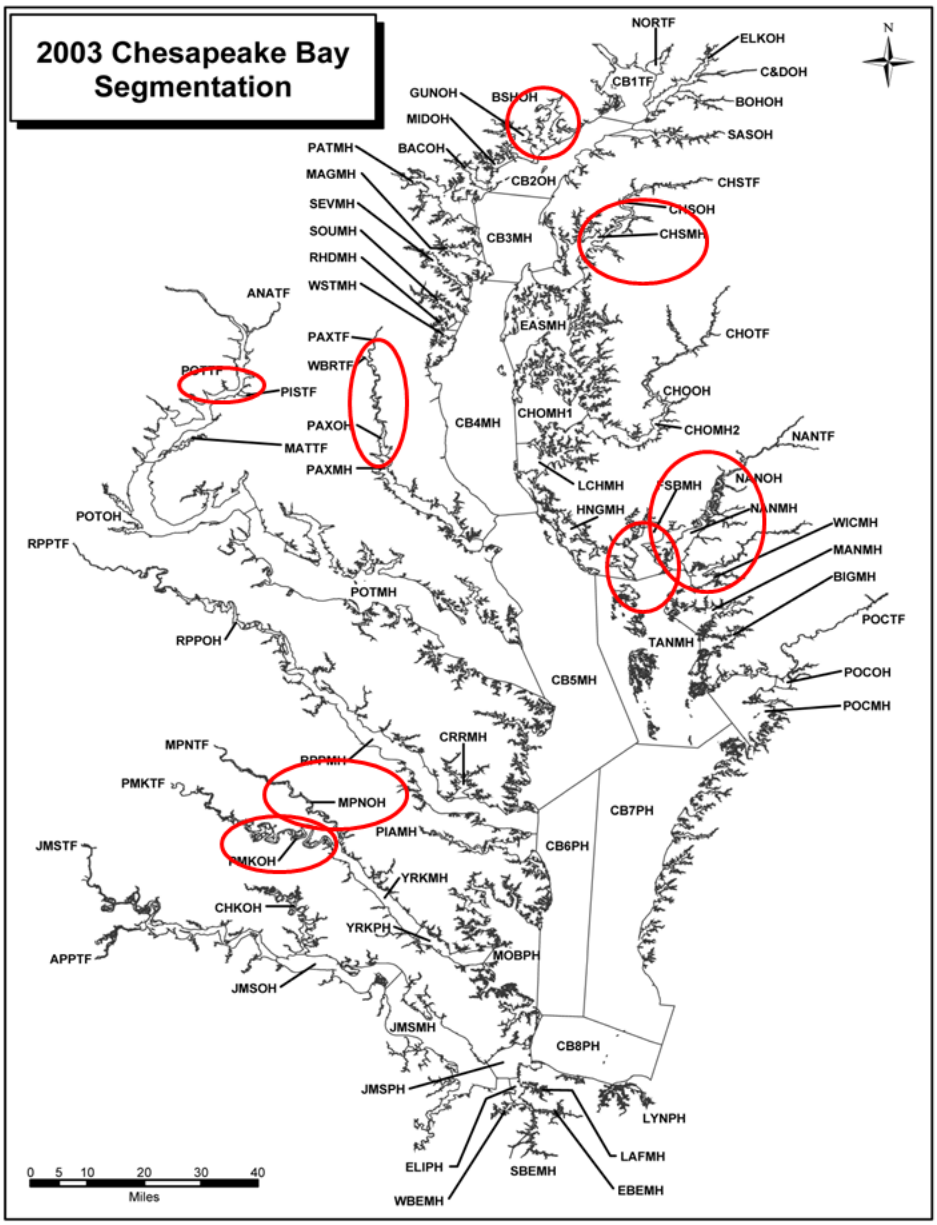

Figure 1. Regions with wetlands observations used to parameterize the wetlands module of the water quality model.

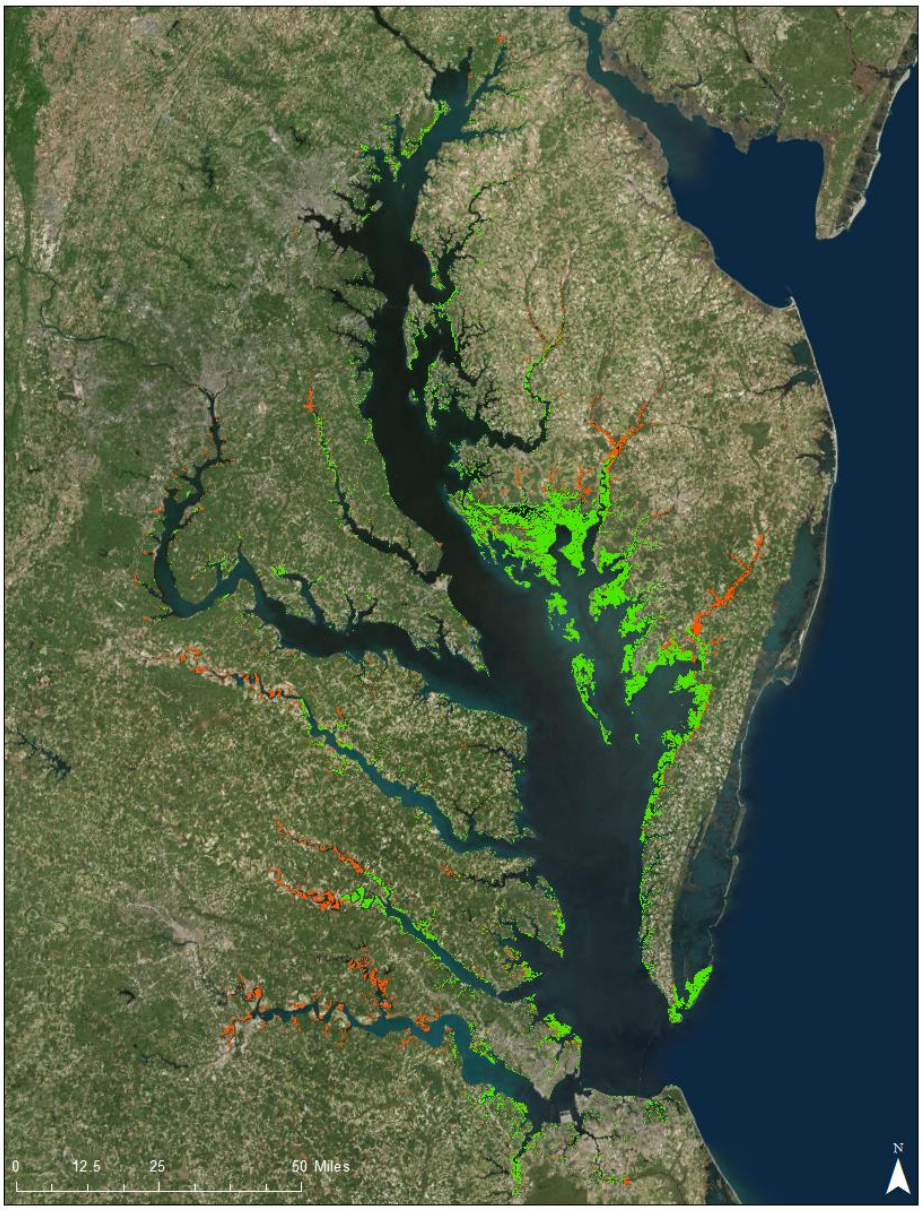

Figure 2. Chesapeake Bay tidal wetlands. Salt and brackish wetlands are shown in green, freshwater wetlands are shown in red.

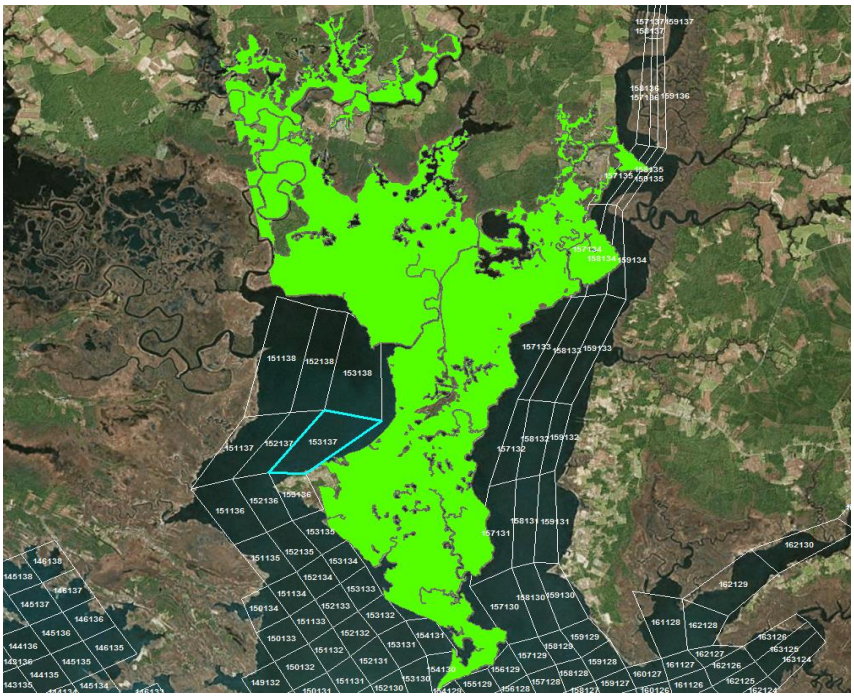

Figure 3. Example of wetlands area combined with model grid and Bay watershed.

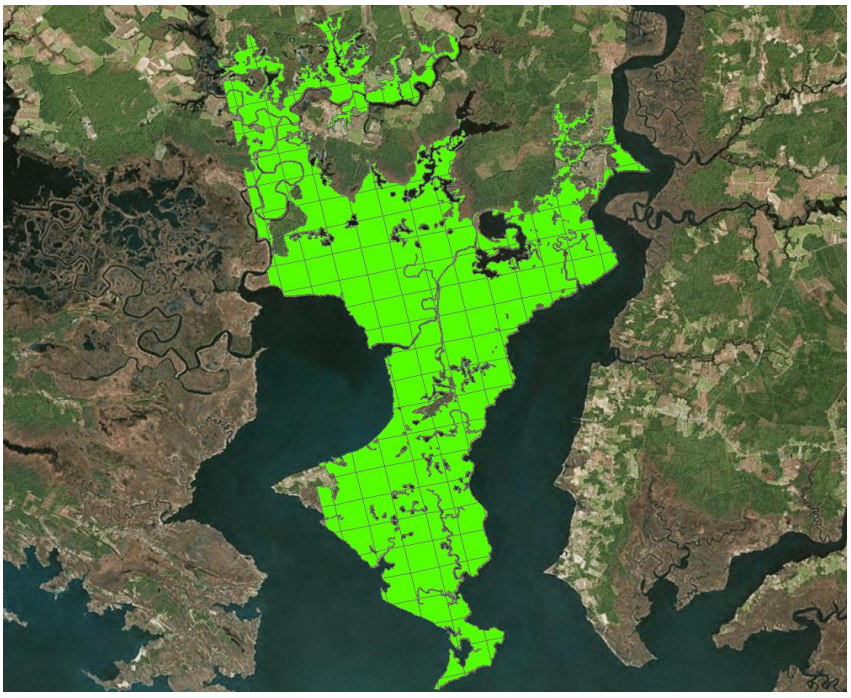

Figure 4. Example of "fishnet" superimposed on wetlands area.

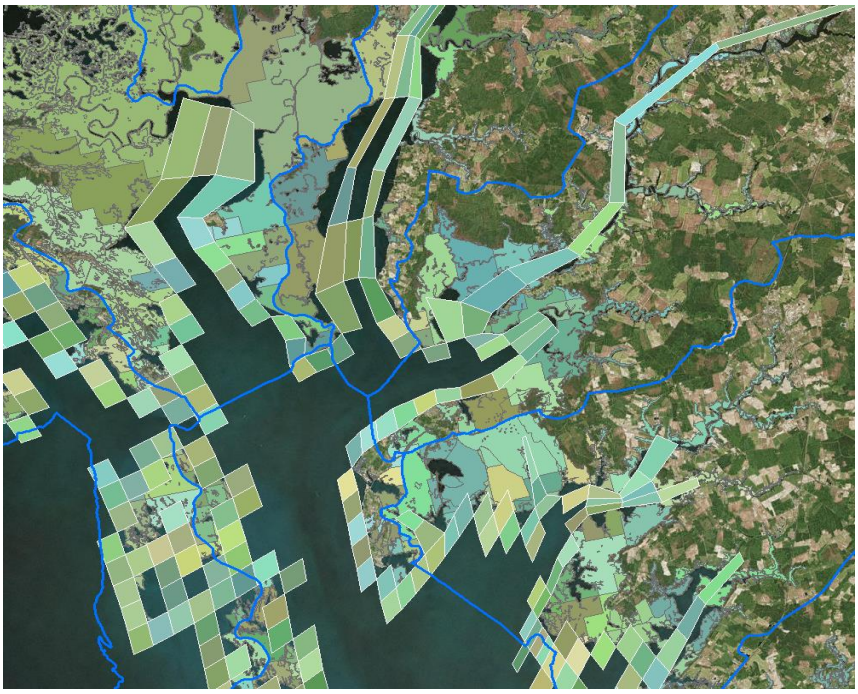

Figure 5. Example of wetlands area mapped to model cells. Wetlands squares from the fishnet are shown in the same color as the cells to which they are mapped.

Figure 6. Example of HUC 10 local watershed boundaries superimposed on map of Bay watershed. Mapping of wetlands to model cells was restricted to not cross local watershed boundaries.

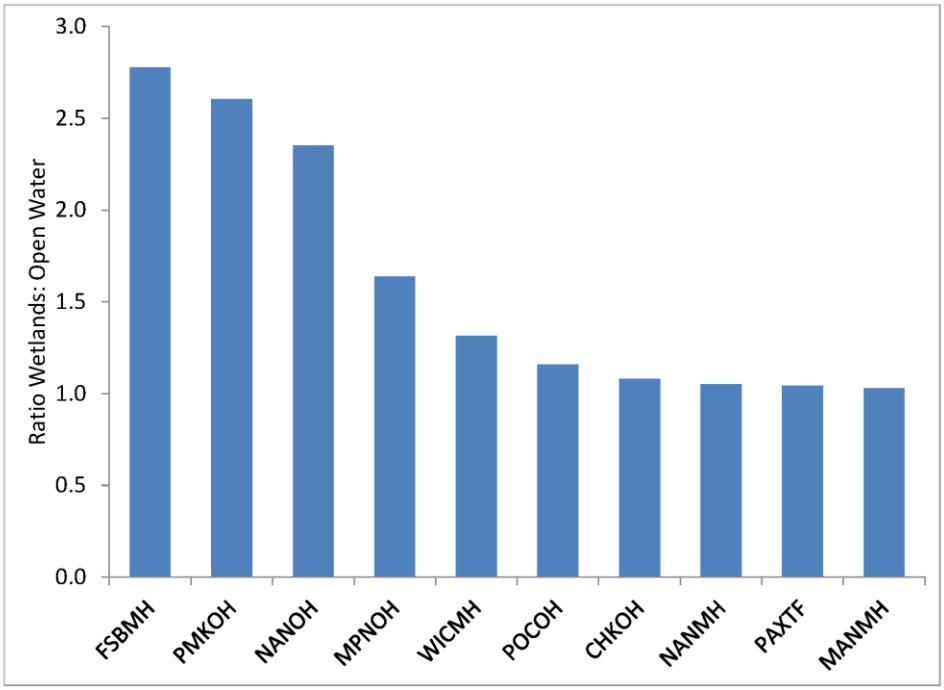

Figure 7. Ten regions of the Bay with the greatest ratio of tidal wetlands to open-water area. Open-water areas are as represented on the model grid.

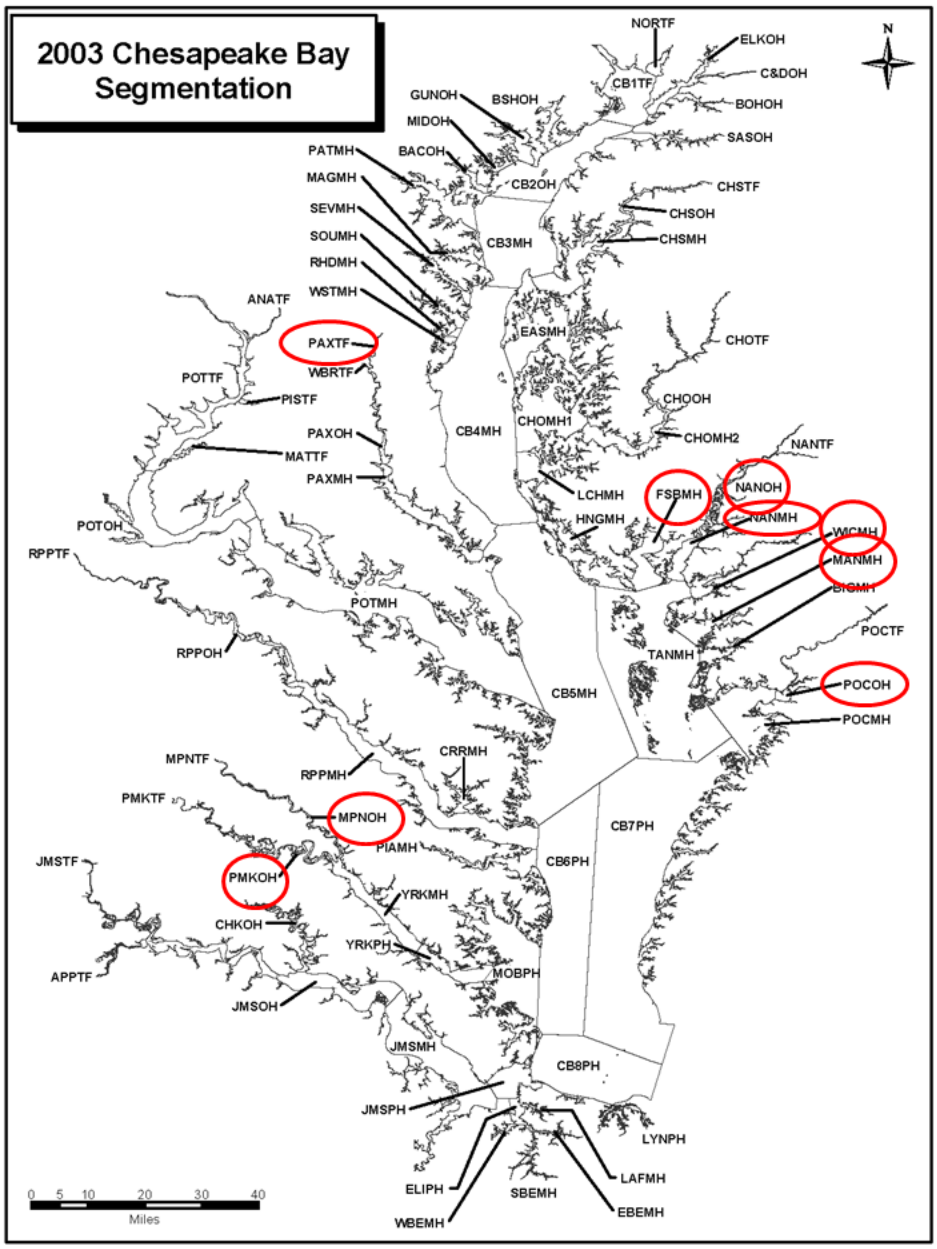

Figure 8. Locations of ten regions with greatest ratio of tidal wetlands area to open-water area.

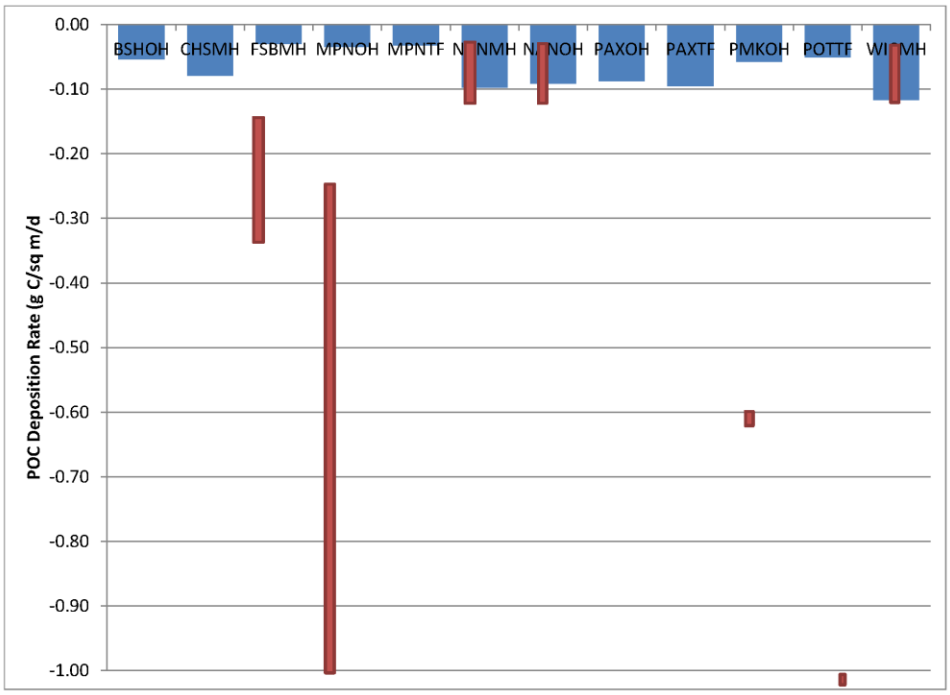

Figure 9. Comparison of computed daily-average wetlands carbon burial (blue bars) with range of reported rates (red bars).

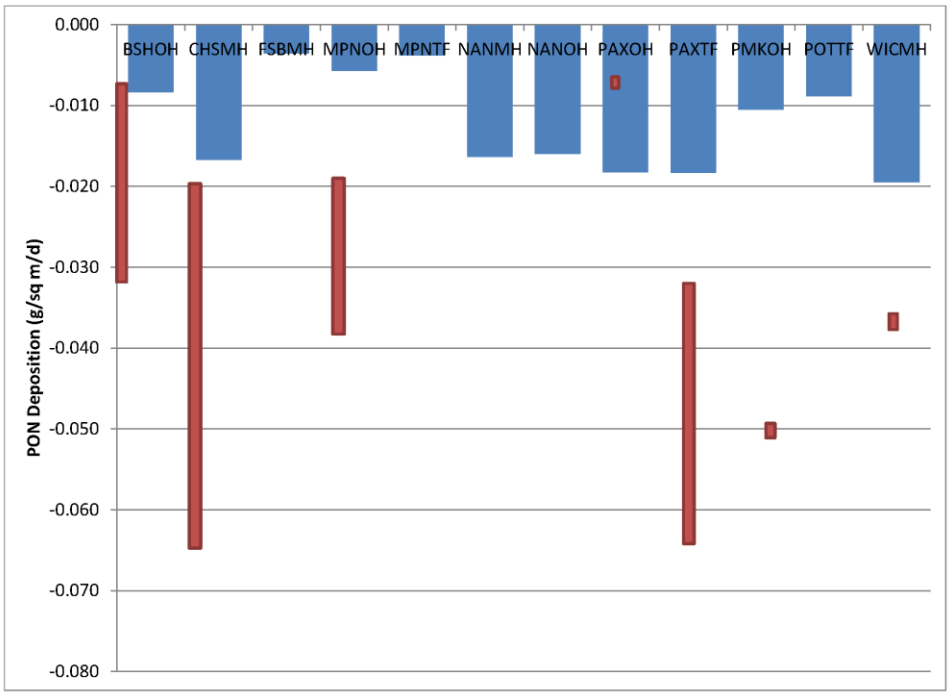

Figure 10. Comparison of computed daily-average wetlands nitrogen burial (blue bars) with range of reported rates (red bars).

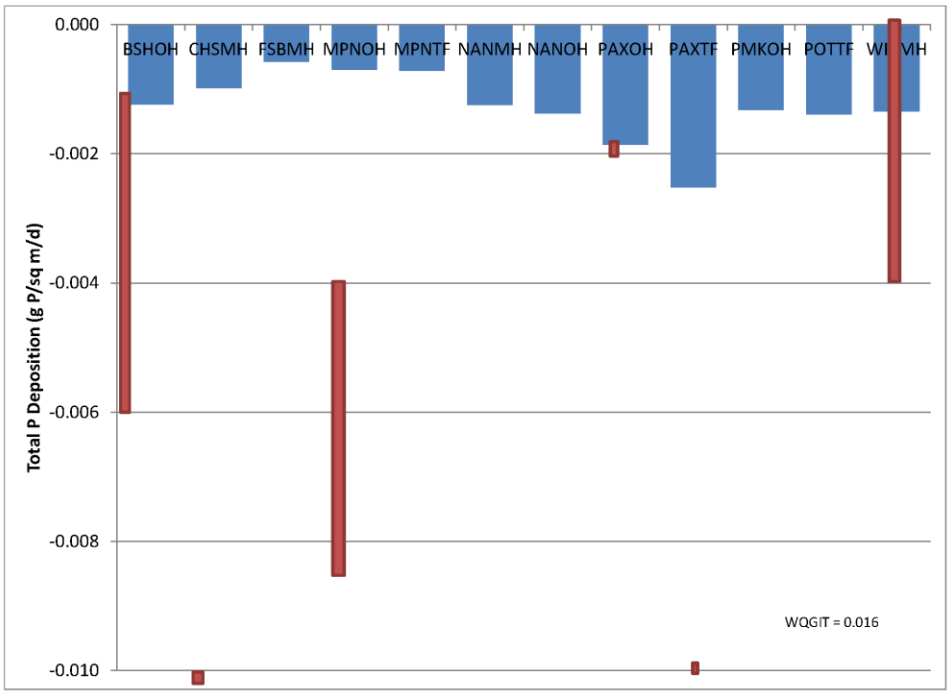

Figure 11. Comparison of computed daily-average wetlands phosphorus burial (blue bars) with range of reported rates (red bars).

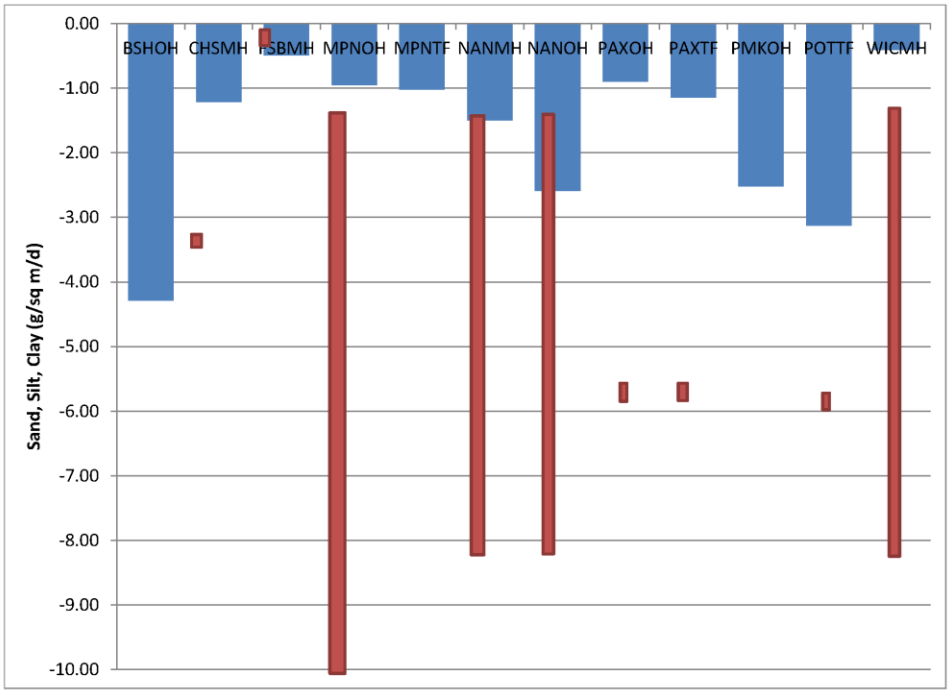

Figure 12 Comparison of computed daily-average wetlands fixed solids burial (blue bars) with range of reported rates (red bars).

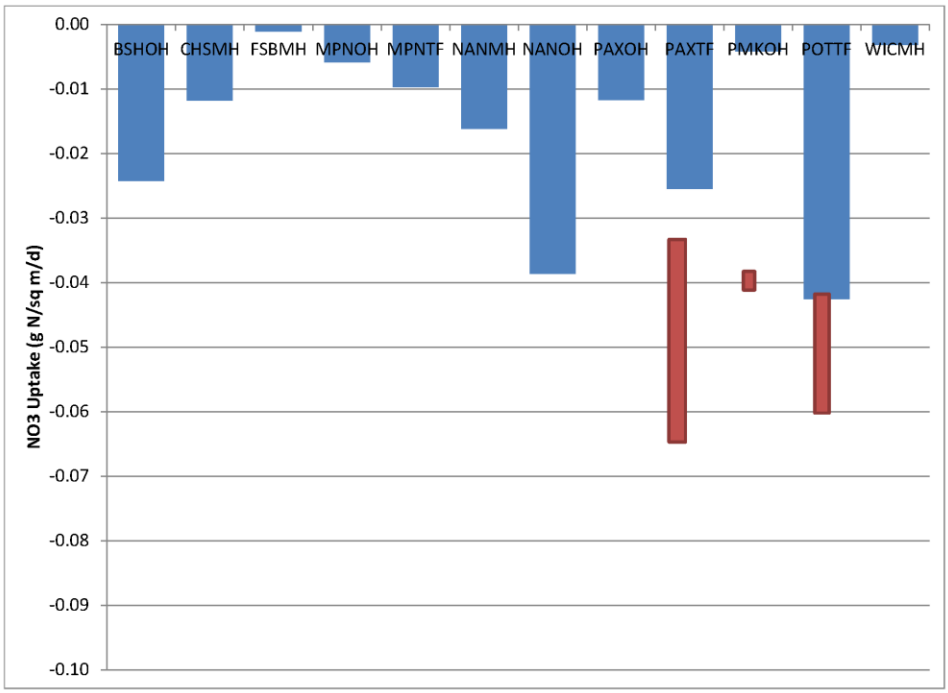

Figure 13. Comparison of computed daily-average wetlands nitrate removal (blue bars) with range of reported rates (red bars).

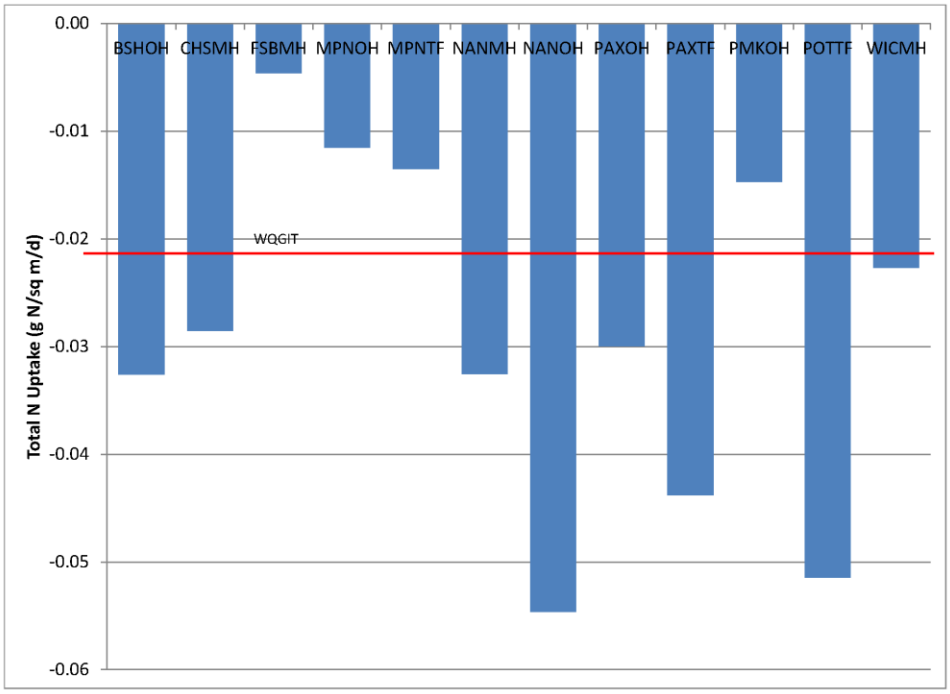

Figure 14. Comparison of computed daily-average wetlands nitrogen removal (blue bars) with recommended rate (red line).

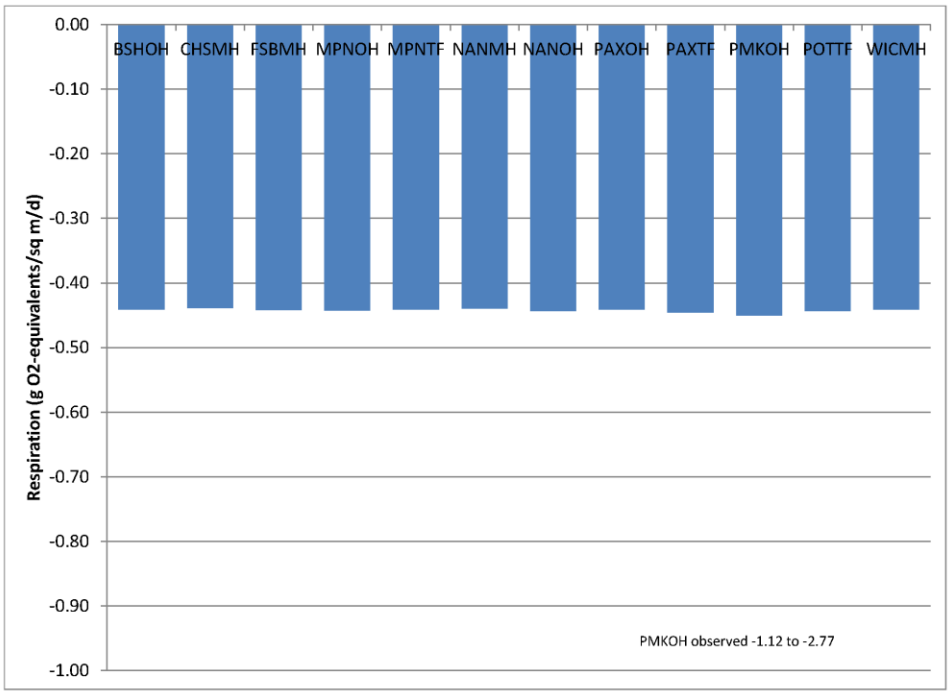

Figure 15. Model daily-average wetlands oxygen demand (blue bars).

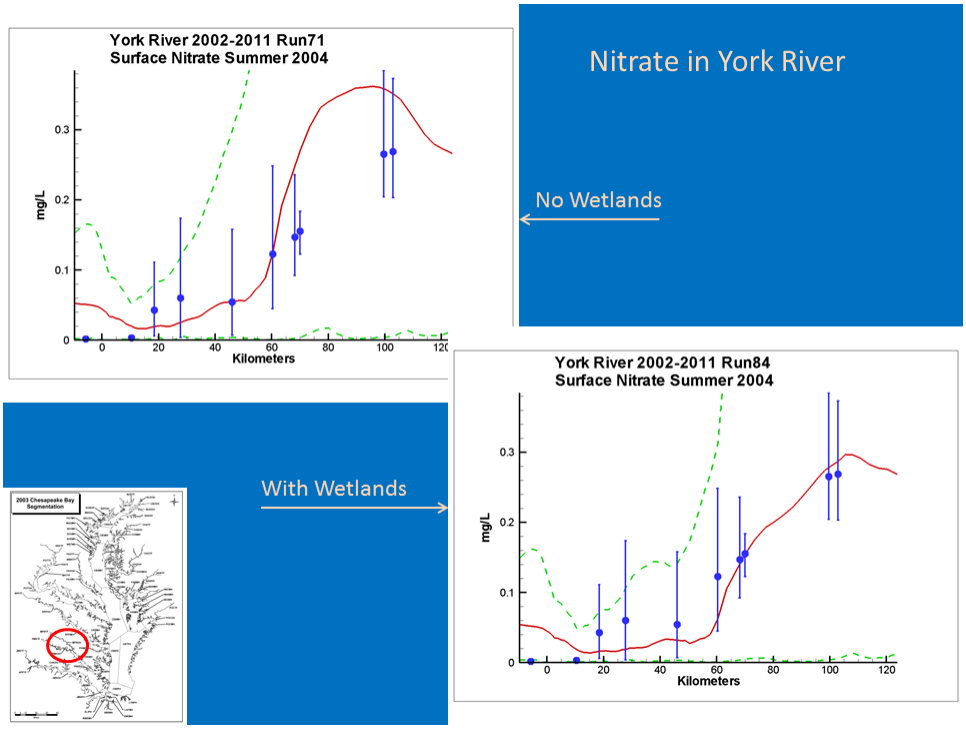

Figure 16. Sensitivity of York River model nitrate concentration to wetlands removal. Comparison shown for summer 2004.

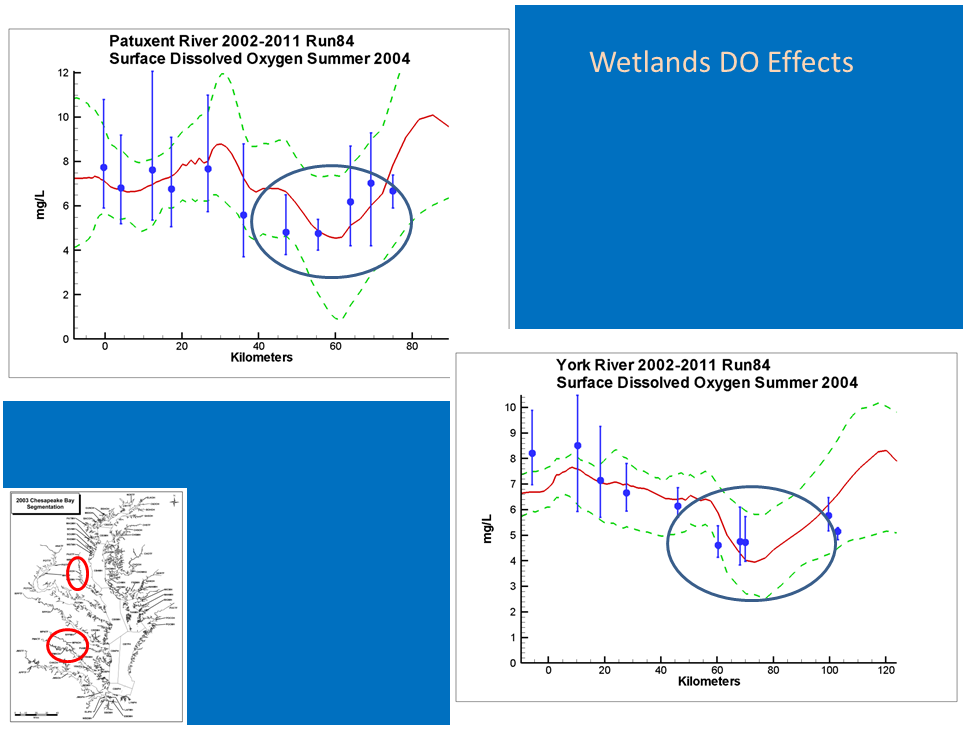

Figure 17. Effect of wetlands oxygen uptake on dissolved oxygen computations in the Patuxent and York Rivers. Results shown for summer 2004.

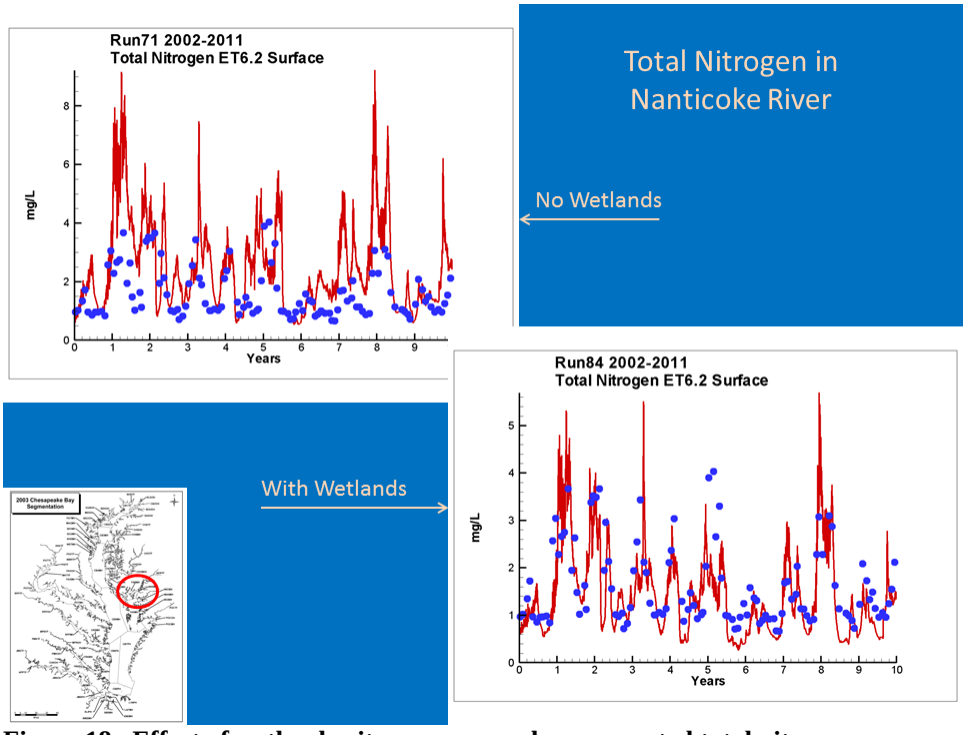

Figure 18. Effect of wetlands nitrogen removal on computed total nitrogen concentration in the Nanticoke River. Ten year time series 2002 – 2011.

5 Shoreline Erosion

Introduction

The 2002 study (Cerco and Noel 2004) identified solids loads from shoreline erosion as a major source of suspended solids to the bay and tributaries. The data base for quantification of loads (USACE 1990) was sparse, however, and the loads were input to the model on a spatially and temporally uniform basis. For the 2010 study (Cerco et al. 2010), we determined to complete the best possible quantification of bank loads. These revised loads were based on contemporary information and reflected spatial variability caused by local shoreline characteristics and the presence of shoreline structures. The resulting estimates were multi-decadal averages based on shoreline recession determined from aerial surveys and hydrographic maps.

The significant potential contribution of shoreline erosion to Chesapeake Bay total phosphorus was noted in the earliest phase of the Chesapeake Bay model (Cerco and Cole, 1993). Carbon, nitrogen, and phosphorus from shoreline erosion were included in the 2002 model version (Cerco and Noel 2004). These loads were omitted, however, from the 2010 model version (Cerco et al. 2010) used to guide the determination of the Total Maximum Daily Load (TMDL). The loads were omitted because no guidance existed as to how to incorporate them in the TMDL development. In addition, there was no authoritative source for specification of shoreline carbon and nutrient loads.

More recently, an expert panel (Drescher and Stack 2015) provided protocols to define pollutant load reductions associated with shoreline management practices. One protocol provides an annual mass sediment reduction credit for qualifying shoreline management practices that prevent tidal shoreline erosion that would otherwise be delivered to nearshore/downstream waters. The panel report recognizes potential nutrient reduction credits associated with erosion management practices but withholds recommendations pending more information on nutrient availability/reactivity. In view of the recognized contribution of shoreline erosion to the Bay nutrient budget and the pending consideration of these nutrients in TMDL development, nutrient loads from shoreline erosion are restored to this model version. Loads and availability are described below.

Methods for Determining Solids Loads

Primary references for the determination of shoreline erosion loads are a report by Hennesee et al. (2006) and a PowerPoint presentation (Halka and Hopkins 2006). Methods for determining solids loads, gleaned from these reports, are summarized below.

Quantifying solids loads from bank erosion requires two fundamental calculations. First, calculate the volume of sediment lost from erosion. Then, convert sediment volume into sediment mass. The volume is determined:

$$V = L \cdot W \cdot H \quad (1)$$

in which:

V = volume of annual sediment loss from shore erosion ($m^3\ yr^{-1}$)
L = shoreline length (m)
W = rate of shoreline retreat ($m\ yr^{-1}$)
H = bank height or marsh elevation (m)

Volume is converted to mass via:

$$Mtotal = Bd \cdot V \quad (2)$$

in which:

Mtotal = total mass of annual sediment (sand, silt, and clay) loss from bank erosion ($kg\ yr^{-1}$)
Bd = dry bulk density of eroding bank ($kg\ m^{-3}$)

Approximately 250,000 shoreline-normal transects were available for the Maryland shoreline alone to determine the rate of shoreline retreat. Available Maryland shorelines spanned the period from approximately 1850 to1990. For the model calculations the two most recent shorelines in each analyzed reach or section were utilized. For most areas, the two most recent shorelines dated from *circa* 1940 and *circa* 1990, though intervals shorter and longer than 50 years occurred. Shoreline characteristics, notably the presence of protective structures, were reported in surveys conducted by Virginia Institute of Marine Science. Still, complete information for the system-wide characterization of shorelines was missing. When necessary, missing information (recession rate, presence of structures, bulk density) was filled in based on information from adjacent shoreline reaches or on regional average characteristics. Other key assumptions included:

- Erosion of fastland from unprotected shorelines represents 65% of the total load; nearshore erosion represents 35% (Figure 1).
- No sediment is eroded, from fastland or nearshore, along accreting shorelines.
- No sediment is delivered to the bay from fastland protected by structures. However, the nearshore in regions protected by structures erodes at the same rate as nearby unprotected reaches.

- The average dry bulk density of banks is 1.38 g cm^{-3} and of marshes 0.62 g cm^{-3}.
- On average, silts and clays constitute 56% of sediment eroded from banks and 44% of sediment eroded from marshes.
- Organic matter is delivered only from marsh erosion and constitutes 34% of this material.
- Bulk density and composition of nearshore sediments are the same as adjacent fastland.

Summary

Results indicate the bay shoreline above the Potomac River junction produces the largest sediment mass per unit shoreline length (Figure 2). Reaches with high erosion are also found in the Potomac River, the Rappahannock River, and the James River. Although the Virginia shoreline is longer than Maryland and less protected (Table 1), the largest sediment loads originate in the Maryland portion of the bay system. Both the total loading and the loading per unit shoreline length are higher in Maryland than in Virginia.

Mapping Shoreline Loads to the WQSTM

The shoreline erosion study resulted in decadal-average mass erosion rates per unit shoreline length throughout the bay system. For some regions, with complete information, the rates were available on the spatial scale of shoreline structures. For other regions, necessary information was lacking (Figures 3, 4) and uniform erosion rates were employed for kilometers of shoreline length. The CBP GIS team merged three key pieces of information: mass erosion rates, shoreline length, and CBEMP computational grid. Shoreline length was assigned to each cell adjoining the shore (2,928 cells) and the mass loading to each cell was computed. This information was supplied to the CBEMP team in the original categories employed by the developers: coarse material, fine material, and organic material. The modelers converted the loads to model units, kg d^{-1}, and mapped the loads into WQSTM state variables: fine clay, clay, silt, and sand.

Shoreline Nutrient Loads

The nutrient content attributed to eroded sediments was provided by the CBP: 0.29 mg N g^{-1} solids and 0.205 mg P g^{-1} solids. Using these values, the total nitrogen and total phosphorus shoreline erosion loads to the Bay are readily computed (Table 2). Comparison to other watershed loads indicates the contribution of shoreline erosion to the Bay nitrogen budget is minor, less than 1% of the total watershed load. Total phosphorus loading from shoreline erosion is comparable in magnitude to alternate sources and comprises 11% of the decadal average total load.

Little guidance exists for partitioning the total nutrients into model state variables. The nitrogen content of sediments must be mapped into labile, refractory and G3 organic particles. Sediment phosphorus must be mapped into particulate inorganic form as well as the three organic classes. Initial model sensitivity runs indicated the model could not withstand an 11% increase in

available phosphorus without deviating greatly from observed conditions. These model experiments suggested the shoreline nutrient loads must be largely non-reactive. A second interpretation of the model experiments might be that previous estimates of the reactivity of loads from alternate sources over-estimated the reactivity of these loads so that additional reactive material from shoreline erosion could not be accommodated. Likely both interpretations contain grains of truth.

Subsequent model experiments were performed that kept the total reactive nutrient load constant. Reactive loads from alternate sources were reduced to compensate for newly-introduced reactive loads from shoreline erosion. The final fractionation of shoreline erosion loads was:

- 50% of total phosphorus is in particulate inorganic form.
- 20% of total nitrogen and 10% of total phosphorus is in refractory particulate organic form.
- 80% of total nitrogen and 40% of total phosphorus is in G3 particulate organic form.

Acknowledgements

Jeff Halka, of the Maryland Department of Natural Resources – Maryland Geological Survey, led the team which computed loads from bank and marsh erosion. Kate Hopkins, of the University of Maryland and EPA Chesapeake Bay Program, performed the GIS operations. Scott Hardaway, of the Virginia Institute of Marine Science, provided invaluable assistance in computing shoreline erosion loads in the Virginia portion of the bay.

References

Cerco, C., and Cole, T. (1993). "Three-dimensional eutrophication model of Chesapeake Bay," *Journal of Environmental Engineering*, 119(6), 1006-1025.

Cerco, C., and Noel, M. (2004). "The 2002 Chesapeake Bay eutrophication model," EPA 903-R-04-004, Chesapeake Bay Program Office, US Environmental Protection Agency, Annapolis MD. (available at http://www.chesapeakebay.net/modsc.htm)

Cerco, C., Kim, S.-C. and Noel, M. (2010). "The 2010 Chesapeake Bay eutrophication model," Chesapeake Bay Program Office, US Environmental Protection Agency, Annapolis MD. (available at http://www.chesapeakebay.net/publications/title/the_2010_chesapeake_bay_eutrophication_model1)

Drescher, S., and Stack, B. (2015). "Recommendations of the expert panel to define removal rates for shoreline management projects," Chesapeake Bay Partnership. (available at http://www.chesapeakebay.net/documents/Shoreline_Management_Protocols_Final_Approved_07132015-WQGIT-approved.pdf)

Hennessee, L., Offerman, K., and Halka, J. (2006). "Suspended sediment load contributed by shore erosion in Chesapeake Bay, Maryland," Coastal and Estuarine Geology File Report No. 06-03, Maryland Geological Survey, Baltimore MD.

Halka, J., and Hopkins, K. (2006). "Final WQM shoreline report," PowerPoint presentation to Chesapeake Bay Program Modeling and Research Subcommittee, Annapolis MD. (available from Jeff Halka, Maryland Geological Survey, JHalka@dnr.state.md.us)

Hardaway, S., Thomas, G., Glover, J., Smithson, J., Berman, M., and Kenne, A. (1992). "Bank erosion study," SRAMSOE 391, Virginia Institute of Marine Science, Gloucester Pt. VA.

United States Army Corps of Engineers. (1990). "Chesapeake Bay shoreline erosion study," Feasibility Report October 1990, Baltimore District, Corps of Engineers, Baltimore MD.

Table 1
Summary of Shoreline Erosion Loads to Chesapeake Bay (from Halka and Hopkins 2006)

	Maryland	**Virginia**
Total Length, m	2,912,000	4,060,000
Unprotected Length, m	1,993,000	3,276,000
Percent Protected	32	19
Loading, metric ton yr^{-1} Fines Coarse Organic	2,425,000 1,331,000 1,018,000 76,000	1,500,000 506,000 994,000 -
Loading, kg m^{-1} d^{-1} Fines Coarse Organic	2.28 1.25 0.96 0.07	1.01 0.34 0.67 -

Table 2 Nonpoint Source Load Summary 1991-2000[1]			
Metric ton d^{-1}	**Total Nitrogen**	**Total Phosphorus**	**Total Suspended Solids**
Susquehanna	191.2	7.32	3761
Potomac	49.2	3.47	2141
James	12.2	1.47	1570
Other Tributaries	12.6	1.31	961
Below-Fall-Line	106.2	5.14	1832
Shoreline Erosion	3.3	2.33	11375

[1]Watershed loads are from the Phase 6 Beta 4 version of the Watershed Model.

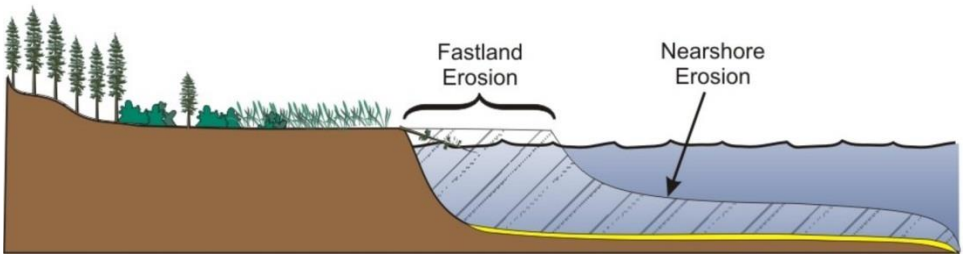

Figure 1. Fastland versus nearshore erosion (From Hennessee et al. 2006).

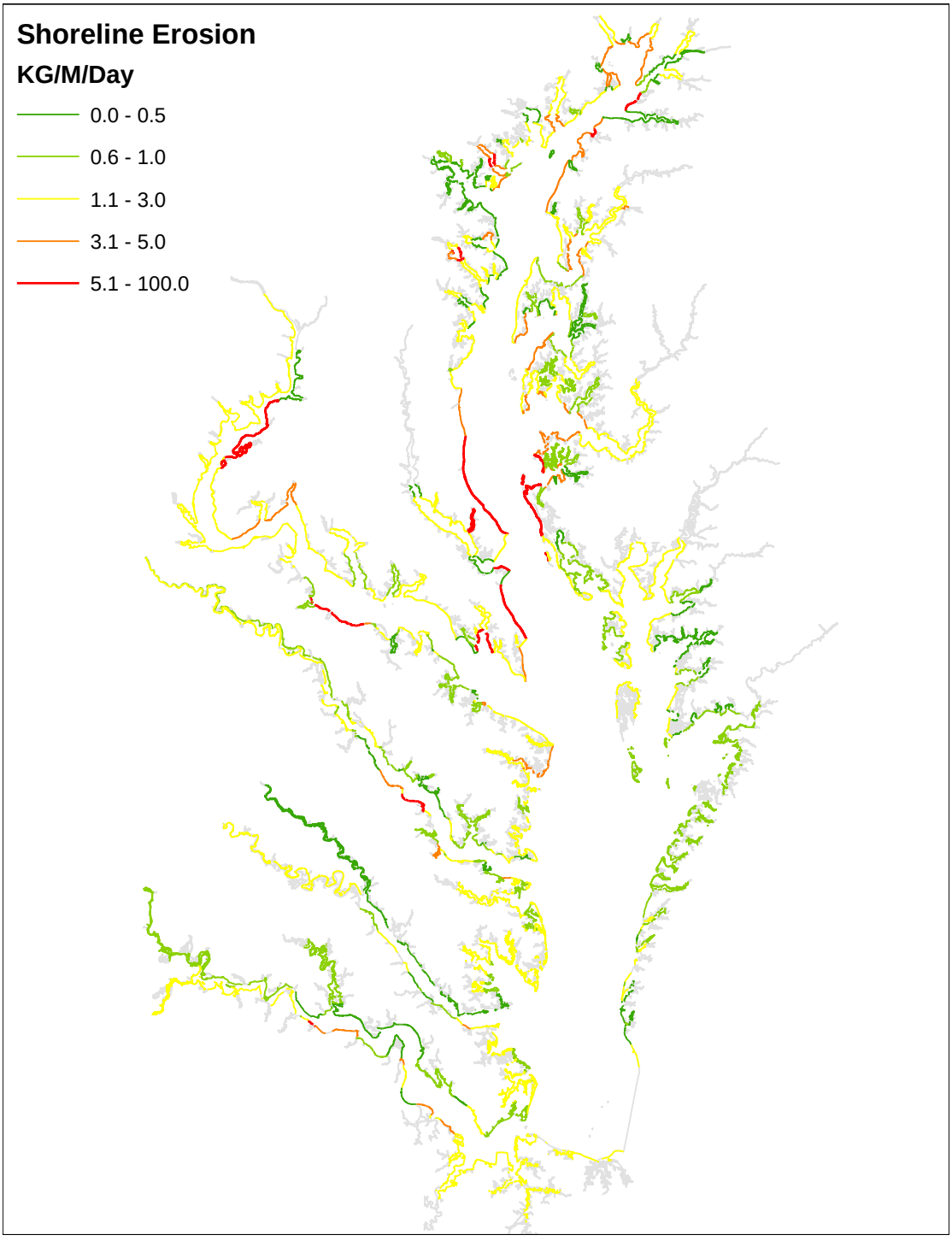

Figure 2. Long-term average shoreline erosion in the Chesapeake Bay system (From Halka and Hopkins 2006).

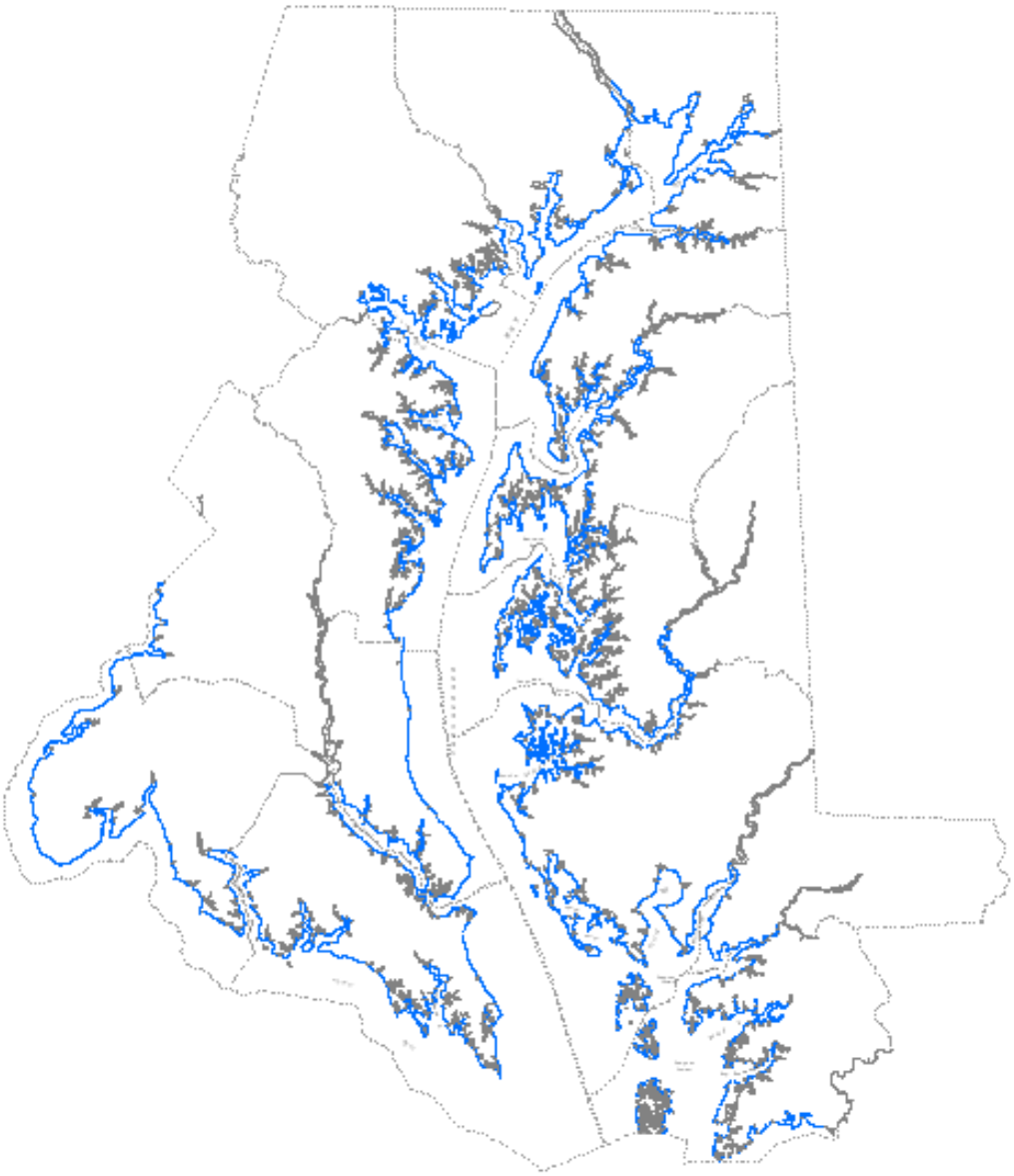

Figure 3. Extent of Maryland shoreline data. No small creeks or upper headwaters. 30% of Maryland shoreline surveyed. (From Halka and Hopkins 2006).

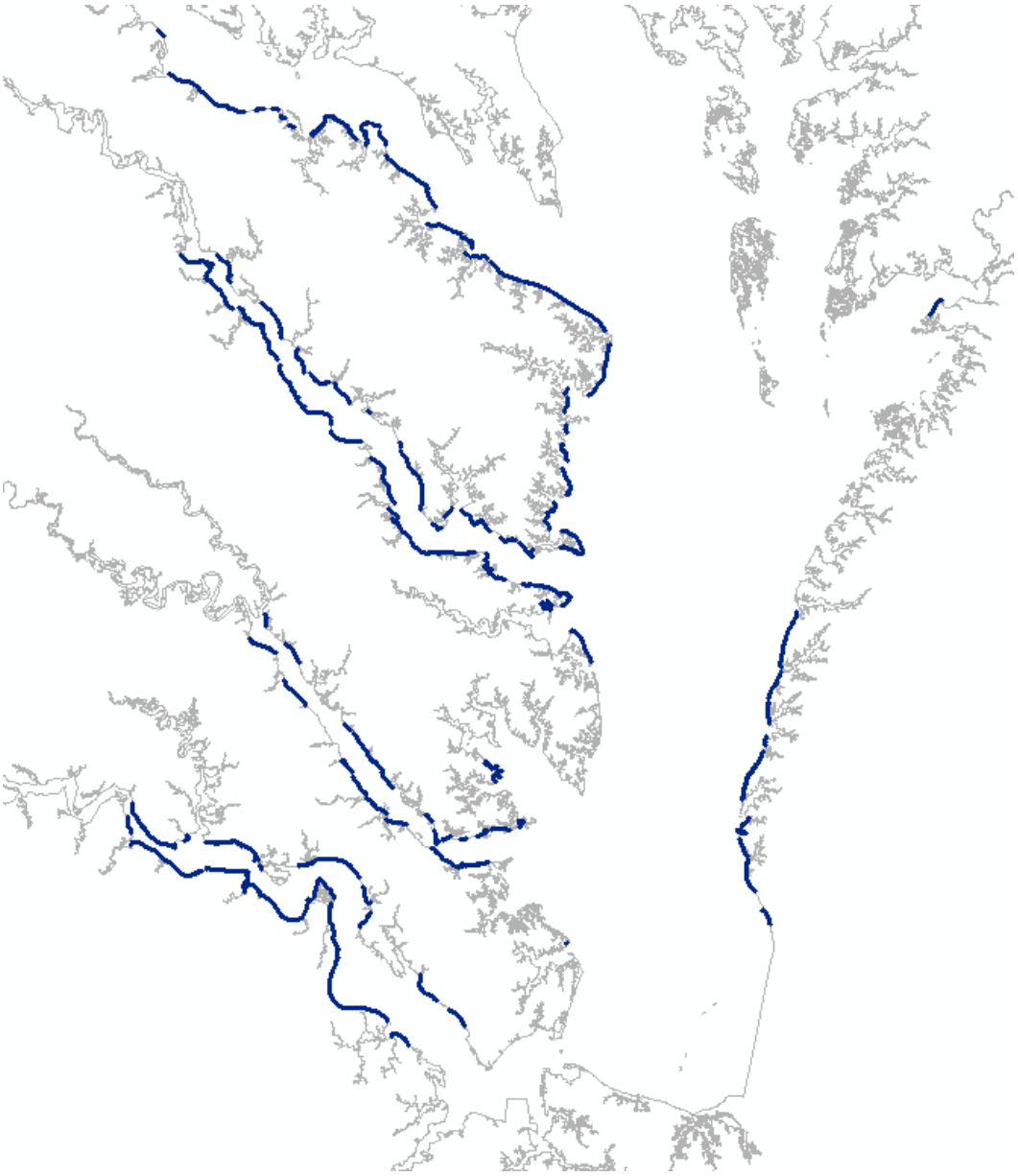

Figure 4. Virginia erosion data available from 1992 Bank Erosion Study (Hardaway et al. 1992). Study incomplete, ends at Westmoreland County on the Potomac. Headwaters of the Potomac, Rappahannock, York and James Rivers missing (Figure from Halka and Hopkins 2006).

6 Linking in the Loads

Introduction

Loads input to the Chesapeake Bay model come from a variety of sources and are reported in multiple forms. The loads must be linked or mapped into specific WQM state variables. The linkage process has evolved as the WQM has evolved and as the sources of loads have changed. The current linkage process combines methods developed for this phase of the study along with methods inherited from earlier phases. The methods employed to link to loads from the watershed, from point sources, and from direct atmospheric deposition are described below.

Watershed Loads

Watershed loads are provided by Phase 6 Beta 4 version of the Chesapeake Bay Program Watershed Model (WSM). The loads presently in use included an adjustment in total nitrogen and total phosphorus to improve agreement with annual loads computed by the WRTDS statistical method (Hirsch et al. 2010). The WSM output is provided in annual files in which daily loads and flows are routed to WQM surface cells around the perimeter of the Bay and tributaries. Several WSM state variables have direct equivalents in the WQM while others require conversion to WQM state variables (Table 1). Two differences in the models require attention. The first is the conversion of the general WSM organic nitrogen and organic phosphorus state variables to the detailed suite of WQM variables. The second is provision of watershed organic carbon loads in the absence of a WSM state variable corresponding to the WQM organic carbon variable suite. The linkage process allows for individual specification of the parameters involved in the linkage at seven river inputs: Susquehanna, Patuxent, Potomac, Rappahannock, York, James, and Choptank. The remaining distributed loads are converted with one more available parameter set.

Organic Nitrogen

The steps required to map WSM organic nitrogen into WQM variables (Figure 1) are as follows:

- Remove the amount of nitrogen associated with phytoplankton loads.
- Split organic nitrogen into particulate and dissolved forms.
- Split particulate organic nitrogen into three reactive classes.

Phytoplankton nitrogen is represented implicitly in the WQM. That is, the nitrogen is represented as a fraction of phytoplankton carbon (see Chapter 2 Kinetics). The present version of the WQM employs WSM chlorophyll to compute phytoplankton entering tributaries from the watershed. In order to load the WQM with precisely the quantity of nitrogen provided by the WSM, the implicit nitrogen load incorporated in phytoplankton is removed from the explicit organic nitrogen load provided by the WSM.

The split of organic nitrogen into particulate and dissolved organic form is difficult to describe definitively. Some uncertainty results from the multiple data bases and analyses available to inform the splits. Earlier analyses (Cerco and Cole 1994, Cerco and Noel 2004) detected an influence of river flow. For this phase of the study, we examined particulate and dissolved organic nitrogen at the first tidal monitoring station downstream of each river inflow. Our assumption was that the observations at these stations are representative of the material entering from the watershed. This method ensured consistency between the methodologies used to determine the splits and the data used to calibrate and validate the WQM. Little or no influence of flow was evident in this data base (Figures 2, 3). Splits (Table 2) were determined from the median fractions of particulate and dissolved organic nitrogen at each location.

Splits of particulate organic nitrogen into reactive classes were obtained from an ongoing study of the Conowingo Reservoir (Qian Zhang, personal comunication). The study estimated the splits through a mass balance analysis of solids entering and leaving the reservoir and of sediment-water nutrient fluxes within the reservoir. For the Susquehanna River, the reactive splits are influenced by flow above 6,500 $m^3\ s^{-1}$. The relationships used to determine the reactive classes are of the form:

$$Fg1 = FLPON{-}\propto 1 \cdot (Q - 6500) \quad (1)$$
$$Fg2 = FRPON{-}\propto 2 \cdot (Q - 6500) \quad (2)$$
$$Fg3 - 1 - Fg1 - Fg2 \quad (3)$$

in which:

Fg1 = labile fraction of particulate organic nitrogen ($0 < Fg1 < 1$)
Fg2 = refractory fraction of particulate organic nitrogen ($0 < Fg2 < 1$)
Fg3 = G3 fraction of particulate organic nitrogen ($0 < Fg3 < 1$)
$\alpha 1$ = Effect of flow > 6,500 $m^3\ s^{-1}$ on Fg1 ($s\ m^{-3}$)
$\alpha 2$ = Effect of flow > 6,500 $m^3\ s^{-1}$ on Fg2 ($s\ m^{-3}$)
Q = Flow at Conowingo outfall ($m^3\ s^{-1}$)

The parameters $\alpha 1$ and $\alpha 2$ (Table 3) have non-zero values only when flow exceeds 6,500 $m^3\ s^{-1}$. In the absence of information, the values of FLPON and FRPON determined for the Susquehanna are transferred to the other river inputs without flow effects.

Organic and Particulate Inorganic Phosphorus

The routing of WSM organic phosphorus into WQM state variables is similar to organic nitrogen. The presence of particulate inorganic phosphorus (PIP) requires an additional step, however. Both the WSM and the WQM include PIP state variables but their nature differs in the two models. PIP in the WSM is loosely sorbed to sediment particles. The amount sorbed is determined by a linear partition coefficient. Exchange is possible between dissolved and particulate form. In the WQM, PIP is an independent form of phosphorus which is inert in the water column. In view of the differences in these two PIP variables, WSM PIP is first combined with organic phosphorus. The combination is then mapped into WQM variables (Figure 4). The steps necessary to route WSM organic phosphorus and PIP into WQM state variables are:

- Combine WSM organic phosphorus and particulate inorganic phosphorus.
- Remove the amount of phosphorus associated with phytoplankton loads.
- Split the combination into particulate and dissolved forms.
- Split particulate phosphorus into organic and inorganic forms.
- Split particulate organic phosphorus into three reactive classes.

The reasoning behind the removal of algal phosphorus is analogous to removal of algal nitrogen. Likewise, the splits between dissolved and particulate phosphorus are determined for individual river inflows based on median fractions observed immediately below the river inputs (Table 2). Observations collected at the river inputs indicate PIP represents a consistent faction of particulate phosphorus (Figures 5, 6). Fractions based on observations (Table 2) were used to split particulate phosphorus into organic and inorganic forms at each river inflow location. Particulate organic phosphorus was split into reactive classes with relationships analogous to Equations 1-3. Parameters appropriate to phosphorus (Table 3) were obtained from the same study which provided the nitrogen parameters.

Organic Carbon

The WSM has no state variable corresponding to the WQM organic carbon suite. Watershed organic carbon loads are derived by ratio to organic nitrogen. The ratios (Table 2) were derived from observations at the river inputs and are adapted here from the 2010 TMDL model (Cerco et al. 2010). The distribution of watershed organic carbon into WQM state variables is analogous to the process for organic nitrogen. First, organic carbon is split into dissolved and particulate forms. Then the particulate organic carbon is routed into three reaction classes. The splits between particulate and dissolved form are the same as for organic nitrogen. Routing of particulate organic carbon into reaction classes is conducted via relationships analogous to Equations 1-3. Parameters appropriate to carbon (Table 3) are obtained from the same study which provided the nitrogen parameters.

Point-Source Loads

The WQM considers loads from municipal and industrial sources located along the tidal shoreline of the Bay and tributaries. Loads from point sources above the fall lines of major tributaries are incorporated into the watershed loads. Point-source loads are provided by the CBP in a format similar to watershed loads. The loads are provided in annual files which contain monthly loads routed to WQM surface cells. Constituents in the files are similar to outputs from the WSM (Table 1). Routing of point-source loads into WQM state variables follows a process similar to the routing of WSM loads. Point-source loads of organic nitrogen and phosphorus must be routed to the detailed suite of WQM state variables. No point-source carbon loads are provided so the carbon loads must be derived from available information.

The data available to guide mapping of point-source loads into WQM state variables is sparse. The values employed here (Table 4) are adopted from the 2002 model version (Cerco and Noel 2004). Those values were based on sampling of Virginia point sources and on preliminary experiments to determine reactivity.

Atmospheric Loads

The WQM incorporates atmospheric nitrogen and phosphorus loads to the water surface. Loads to the land surface are included in the watershed loads. Atmospheric loads were obtained from two sources. For 1991-2000, loads from the 2010 TMDL study (Cerco et al. 2010) were utilized. These loads were provided by the CBP in annual files which contained daily loads to WQM surface cells. Loads included ammonium, nitrate, organic nitrogen, phosphate, and organic phosphorus. For the 2010 study, we assumed the organic loads were exclusively refractory particles. For the present study, organic nitrogen loads were considered 76% refractory and the remainder G3. Organic phosphorus loads were considered 64.8% refractory and the remainder G3.

At the commencement of this study phase, detailed spatial and temporal information on atmospheric loads was unavailable for 2002-2011. Projections of total annual nitrogen and phosphorus loads were employed. The annual loads were converted to daily rates and distributed spatially in proportion to WQM cell surface area. Total nitrogen and phosphorus were allocated to ammonium, nitrate, organic nitrogen, phosphate, and organic phosphorus according to proportions derived from the 1991-2000 loads. The organic nutrients were subsequently split into refractory and G3 particles utilizing the same splits as for 1991-2000. We expect that both of these atmospheric load sources will be replaced with a complete set based on updated information and technology.

References

Cerco, C.F. and Cole, T. M. (1994). “Three-dimensional eutrophication model of Chesapeake Bay,” Technical Report EL-94-4, U.S. Army Engineer Waterways Experiment Station, Vicksburg MS.

Cerco, C., and Noel, M. (2004). “The 2002 Chesapeake Bay eutrophication model,” EPA 903-R-04-004, Chesapeake Bay Program Office, US

Environmental Protection Agency, Annapolis MD. (available at http://www.chesapeakebay.net/modsc.htm)

Cerco, C., Kim, S.-C. and Noel, M. (2010). "The 2010 Chesapeake Bay eutrophication model," Chesapeake Bay Program Office, US Environmental Protection Agency, Annapolis MD. (available at http://www.chesapeakebay.net/publications/title/the_2010_chesapeake_bay_eutrophication_model1)

Hirsch, R., Moyer, D., and Archfield, S. (2010). "Weighted regressions on time, discharge, and season (WRTDS), with an application to Chesapeake Bay river inputs," *Journal of the American Water Resources Association*, 46(5), 857-880.

Table 1
Consituents in Watershed and Water Quality Models

WSM Variable	Maps to	WQM Variable
Ammonium	------>	Ammonium
Nitrate	------>	Nitrate
Organic Nitrogen	------>	Dissolved Organic Nitrogen, Labile Particulate Organic Nitrogen, Refractory Particulate Organic Nitrogen, G3 Particulate Organic Nitrogen
Dissolved Phosphate	------>	Phosphate
Organic Phosphorus plus Particulate Inorganic Phosphorus	------>	Dissolved Organic Phosphorus, Particulate Inorganic Phosphorus, Labile Particulate Organic Phosphorus, Refractory Particulate Organic Phosphorus, G3 Particulate Organic Phosphorus

Table 2
Routing WSM Organics into WQM State Variables

River	Fraction Particulate, Nitrogen and Carbon	Fraction Particulate, Phosphorus	Faction Particulate Inorganic Phosphorus	Carbon to Nitrogen Ratio
Susquehanna	0.4	0.65	0.58	8
Patuxent	0.26	0.692	0.6	6
Potomac	0.26	0.65	0.47	8
Rappahannock	0.36	0.772	0.6	8
York	0.21	0.516	0.6	8
James	0.21	0.61	0.6	8
Choptank	0.33	0.645	0.7	8
Other	0.3	0.65	0.6	8

Table 3
Calculation of Reactive Fractions of Watershed Particles

Parameter	Nitrogen	Phosphorus	Carbon
Fraction Labile	0.15	0.3	0.15
Fraction Refractory	0.45	0.4	0.35
$\alpha 1$	7.49×10^{-6}	1.091×10^{-5}	7.64×10^{-6}
$\alpha 2$	1.638×10^{-5}	9.49×10^{-6}	1.33×10^{-5}

Table 4
Routing Point-Source Loads into WQM Variables

	Fraction Dissolved	Faction Labile Particles	Fraction Refractory Particles	Fraction G3 Particles
Organic N	0.5	0.15	0.28	0.07
Organic P	0.4	0.07	0.42	0.11
Organic C	0.8	0.15	0.04	0.01
C:N ratio = 10				

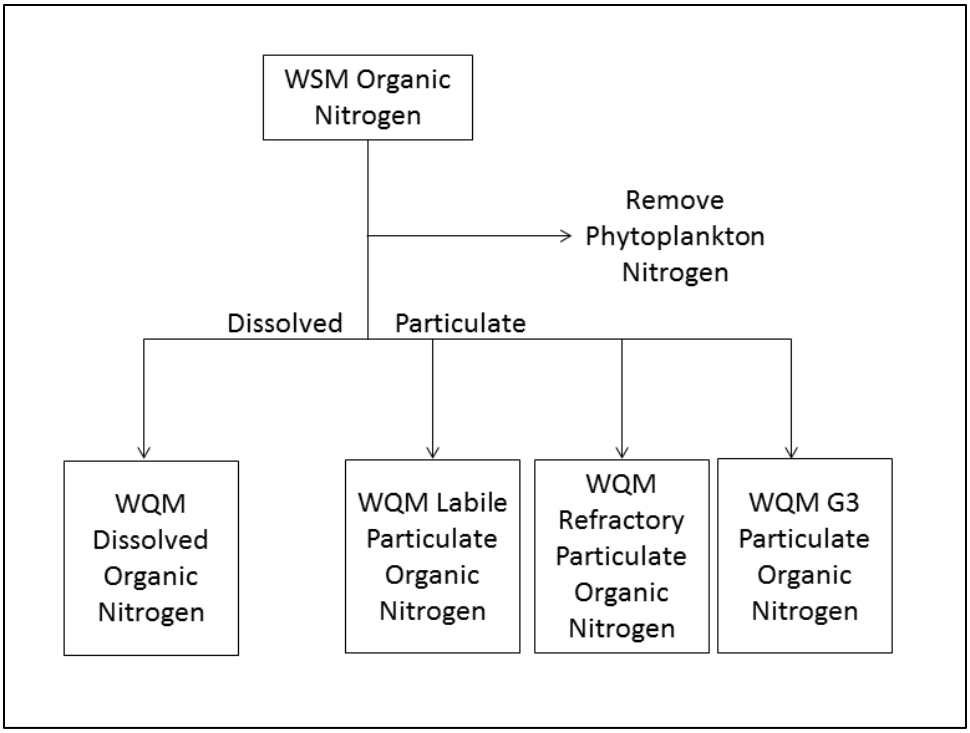

Figure 1. Routing watershed model organic nitrogen into water quality model state variables.

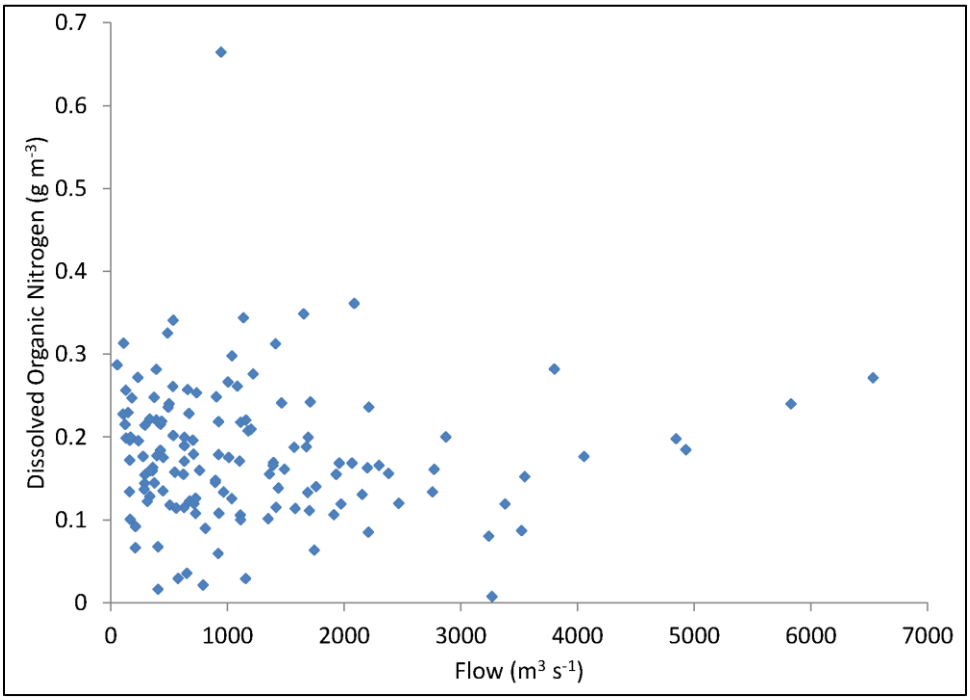

Figure 2. Dissolved organic nitrogen concentration at Station CB1.1, below Susquehanna River inflow. Note absence of relationship to flow.

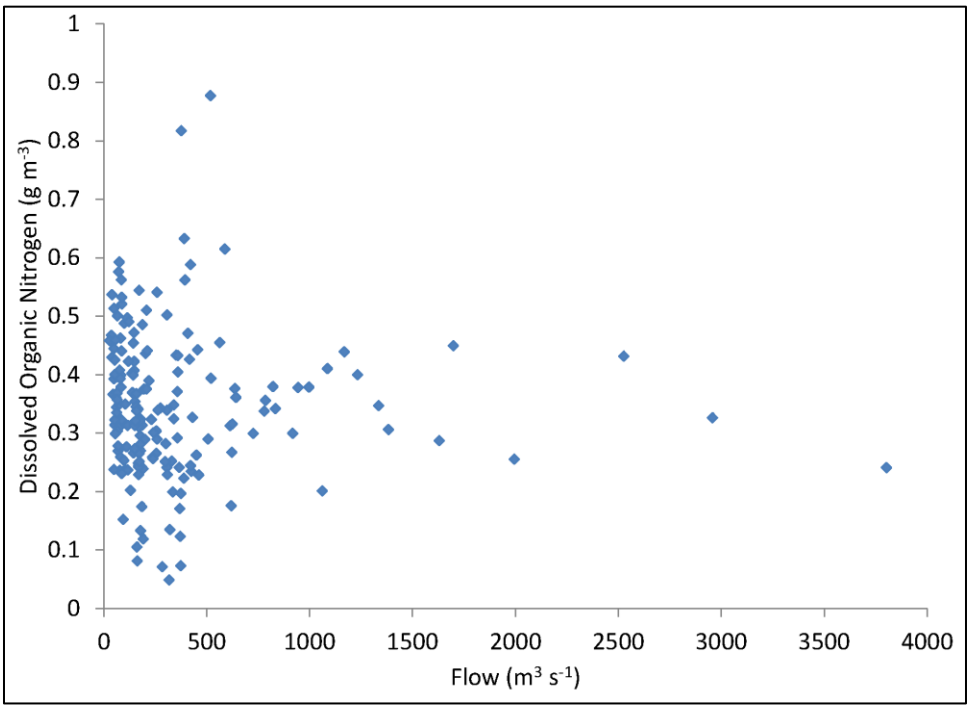

Figure 2. Dissolved organic nitrogen concentration at Station TF2.1, below Potomac River inflow. Note absence of relationship to flow.

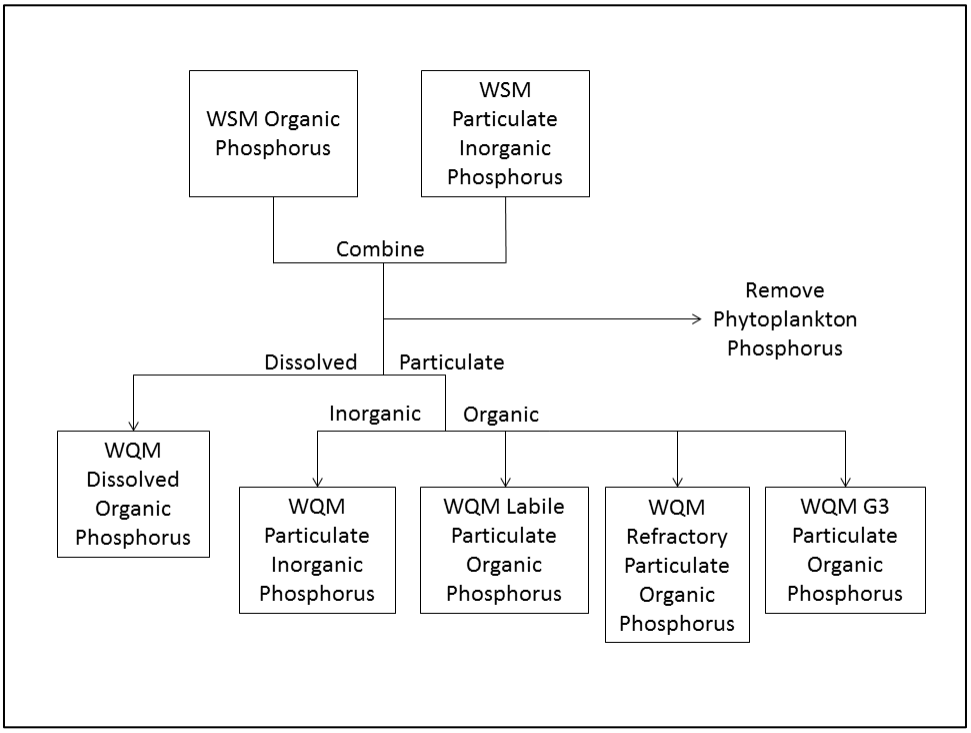

Figure 4. Routing watershed model organic and particulate inorganic phosphorus into water quality model state variables.

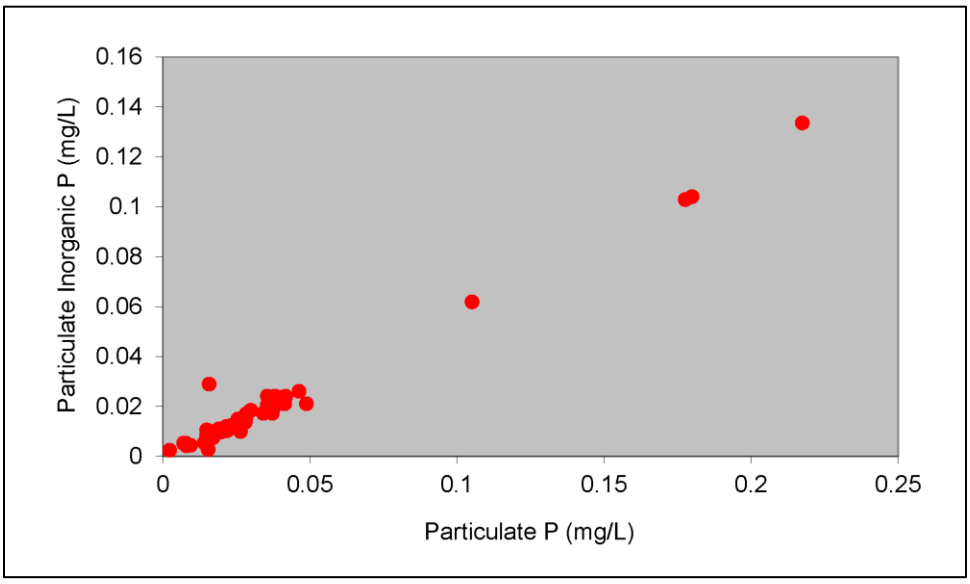

Figure 5. Particulate inorganic phosphorus vs. particulate phosphorus at Susquehanna River fall line. PIP is a consistent fraction of PP.

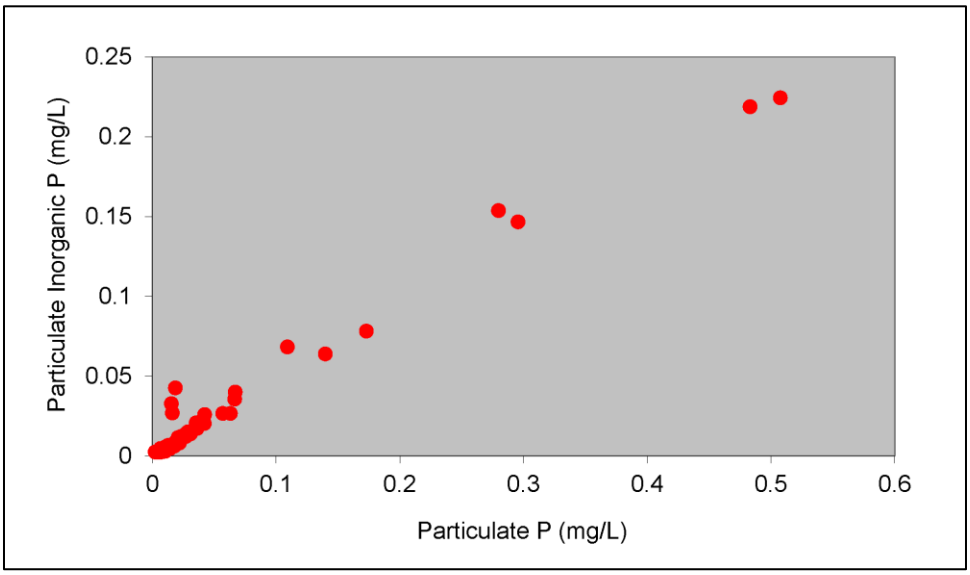

Figure 6. Particulate inorganic phosphorus vs. particulate phosphorus at Potomac River fall line. PIP is a consistent fraction of PP.

7 Statistical Summary of Calibration

Introduction

The calibration of the model involves the comparison of hundreds of thousands of observations with model results in various formats. Comparisons include conventional water quality data, process-oriented data, and living-resources observations. These graphical comparisons produce thousands of plots which are challenging to assimilate in their entirety. Evaluation of model performance requires statistical and/or graphical summaries of results. We present summaries here for major water quality constituents in the mainstem bay and tributaries. Additional graphical comparisons are available in an appendix to this report.

Methods

We employ summary statistics that were developed as part of our initial Chesapeake Bay model study (Cerco and Cole 1994). Use of a consistent set of statistics facilitates comparisons with earlier model versions and with applications to other systems. Statistics computed are mean difference, absolute mean difference, and relative difference:

$$MD = \frac{\sum(P - O)}{N} \quad (1)$$

$$AMD = \frac{\sum|P - O|}{N} \quad (2)$$

$$RD = \frac{\sum|P - O|}{\sum O} \quad (3)$$

in which:

MD = mean difference
AMD = absolute mean difference
RD = relative difference
O = observation
P = prediction
N = number of observations

The mean difference describes whether the model over-estimates (MD > 0) or under-estimates (MD < 0) the observations, on average. The mean difference can attain its ideal value, zero, while discrepancies exist between individual observations and computations. The absolute mean difference is a measure of the characteristic difference between individual observations and computations. An absolute mean difference of zero indicates the model perfectly reproduces each observation. Relative difference is the absolute mean difference normalized by the mean of the observations.

Current Model Statistics

Watershed loads for the current application are from the Phase 6 Beta 4 version of the Chesapeake Bay Program Watershed Model (WSM). Prior to use in the water quality model, results from the WSM were adjusted to provide agreement with annual loads computed by the WRTDS statistical method (Hirsch et al. 2010). The WSM loads in use at present are scheduled for replacement with a final set of Phase 6 loads. Following implementation of the final loads, final parameter adjustment of the WQM will be conducted. The set of interim results presented here provides insight into the present status of the model and into the nature of the statistics as well. The contents of the chapter will be updated following delivery of the final loads. The format of the presentation is expected to be consistent with the material below.

Quantitative statistics are determined using the same model-data pairs as in the time series plots. The stations and number of pairs depend on the system or station grouping (Table 1). In most cases, for stations classed as TF, ET, and WT, surface samples only are considered. Surface and bottom samples are considered for most RET and EE stations. Surface, mid-depth, and bottom samples are considered for most CB and LE stations. Statistics are calculated for three distinct applications. The first is the current calibration to the years 1991-2000 (Table 2). The second is a current validation to the years 2002-2011 (Table 3). This application is a classic validation in that model parameter adjustment is restricted to the 1991-2000 application. The 2002-2011 application provides validation of the parameters since the model is not “tuned” to match observations collected in this period. The third statistical summary (Table 4) is from the 1991-2000 model application used to guide development of the 2010 Total Maximum Daily Load (Cerco et al. 2010). Watershed loads for this application were from Phase 5.3.2 of the WSM.

Performance statistics from a single model run alone provide little insight. Comparisons with alternate runs provide grounds for interpreting the model behavior and the effects of various developments. The three sets of statistics presented here allow for two significant comparisons. The first is between the 1991-2000 calibration and the validation to more recent data from 2002-2011. The second significant comparison is between the current calibration to 1991-2000 and the 2010 calibration to the same data. The stated goal of the sponsor is that the current calibration should be “as good or better” than the previous calibration.

Model salinity is determined solely by transport processes. The structure of the CH3D hydrodynamic model is unchanged from the version which provided hydrodynamics for the 2010 TMDL determination (Kim 2013). New hydrodynamic runs were completed for 1991-2000, however, based on revised freshwater runoff from the updated WSM. Completely new CH3D runs were also conducted to extend the application period through 2011. An additional factor which influences transport is specification in the current WQM of a minimum vertical diffusivity: 2.2×10^{-5} m^2 d^{-1}. The minimum was determined empirically to improve computations of bottom-water dissolved oxygen (Figure 1).

The salinity MD statistic oscillates among the tributaries and WQM applications but shows no consistent differences or trend. The AMD statistic (Figure 2) shows a prevailing deterioration of ≈ 0.5 ppt in the salinity computation between the 2010 TMDL model version and the current version. We suspect the non-uniform changes in the MD statistic are the result of revised watershed runoff. Salinity may increase or decrease and performance may improve or deteriorate depending on the nature of the revised runoff. The almost universal deterioration in the AMD statistic suggests a universal change in some forcing function or model parameter and may represent the impact of the newly-imposed minimum vertical diffusivity. In view of the premier role of dissolved oxygen computations in the model, a small deterioration in salinity computations is acceptable.

The stand-out in the chlorophyll MD summary is a consistent under-prediction of chlorophyll in the minor western tributaries. On the average, chlorophyll in these reaches is 10 mg m^{-3} less than observed for any calibration state, application period, or watershed model version (Figure 3). These western minor tributaries also exhibit greater AMD in chlorophyll computation than in any other reaches (Figure 4). In the 2010 report, we attributed the chlorophyll shortfall in minor western tributaries to a deficiency in phosphorus loading. The average total phosphorus in these tributaries for 2002-2011 (Figure 5) is nearly perfect, however, while the chlorophyll MD statistic shows no improvement over alternate periods or WSM versions. Close examination of model results still suggests a phosphorus deficiency (Figure 6). The impact at specific stations for limited periods may be lost in the summary statistics.

The total phosphorus MD statistic indicates consistency among watershed model versions and within tributaries (Figure 5). Tributaries which were, on average, high or low in total phosphorus in the 2010 TMDL model version remain so in the current version. For the most part, tributary MD in the 1991-2000 application retains the same tendency, positive or negative, in the 2002-2011 application. Total phosphorus AMD is distinctly lower for the 2002-2011 simulation that for 1991-2000, however (Figure 7). Since the WQM parameter set is consistent between the two current simulations periods, the AMD statistic may indicate the phosphorus loads are more accurate for the more recent interval.

The total nitrogen MD statistic indicates total nitrogen has increased by 0.2 g m^{-3} or more in the 1991-2000 simulation based on Phase 6 Beta 4 loads compared to Phase 5.3.2 loads (Figure 8). The MD for nitrate, however, a

significant component of the total nitrogen load, often decreases with Phase 6 Beta 4 loads (Figure 9) suggesting the newer set of loads incorporates a significant increase in organic nitrogen. The total nitrogen AMD statistic indicates universal deterioration in WQM performance with the newer loads (Figure 10). The AMD for 2002-2011 is consistently lower than for 1991-2000, however, perhaps indicating the loads for the later period are improved over the earlier years.

Consistent differences in the dissolved oxygen MD statistic are difficult to discern between the same periods based on different loads or between different periods based on a single WSM version (Figure 11). One noticeable effect is that dissolved oxygen, which was high in several western tributaries (Rappahannock, Potomac, Patuxent) for the 2010 TMDL model, is higher still in the newer model. The AMD statistic for these tributaries is little changed, however (Figure 12). System-wide, the AMD statistic for the newer model is equivalent to or less that the statistic for the 2010 TMDL model. At present, the dissolved oxygen results are as good or better than the previous model. More detailed examination, following implementation of the final loads, is required for final determination. The dissolved oxygen graphical summaries include surface and sub-surface samples throughout the year. Examination of bottom water during critical periods is especially desirable.

The sediment transport parameters are unchanged between the 2010 TMDL model and the present model. No consistent difference exists in WQM results, as evidenced by the AMD statistic (Figure 13), between the two model versions. As with nitrogen and phosphorus, WQM results for the later period, 2002-2011 are often superior to the 1991-2000 period. The AMD statistic for light attenuation, however, is consistently superior for the newer model, based on a partial attenuation relationship, relative to the 2010 TMDL model, based on the advanced optical model (Figure 14). These results support the decision to revert to the simpler relationship for light attenuation.

References

Cerco, C.F. and Cole, T. M. (1994). “Three-dimensional eutrophication model of Chesapeake Bay,” Technical Report EL-94-4, U.S. Army Engineer Waterways Experiment Station, Vicksburg MS.

Cerco, C., Kim, S.-C. and Noel, M. (2010). “The 2010 Chesapeake Bay eutrophication model,” Chesapeake Bay Program Office, US Environmental Protection Agency, Annapolis MD. (available at http://www.chesapeakebay.net/publications/title/the_2010_chesapeake_bay_eutrophication_model1)

Hirsch, R., Moyer, D., and Archfield, S. (2010). “Weighted regressions on time, discharge, and season (WRTDS), with an application to Chesapeake Bay river inputs,” *Journal of the American Water Resources Association*, 46(5), 857-880.

Kim, S-C. (2013). “Evaluation of a three-dimensional hydrodynamic model applied to Chesapeake Bay through long-term simulation of transport processes,” *Journal of the American Water Resources Association*, 49(5), 1078-1090.

Table 1
Stations and Observations in 1991-2000 Statistical Summary

Grouping	Stations	Salinity Obs.	Chlorophyll Obs.	Total Nitrogen Obs.	Total Phosphorus Obs.	Dissolved Oxygen Obs.	Total Susp. Solids Obs.
Chesapeake Bay	CB1.1, CB2.2, CB3.3C, CB4.2, CB5.2, CB6.1, CB7.3, CB7.4, CB7.4N, CB8.1E, EE3.1, EE3.2	5811	5695	5657	5738	5803	5757
James River	TF5.5, RET5.2, LE5.3	823	831	465	812	829	802
York River	TF4.2, RET4.3, LE4.2, WE4.2	1153	1134	754	1114	1155	1138
Rappahannock River	TF3.3, RET3.2, LE3.2	844	822	472	820	841	831
Potomac River	TF2.1, RET2.4, LE2.2	1097	1068	1036	1083	1097	1094
Patuxent River	TF1.7, RET1.1, LE1.3	1190	1166	1188	1188	1190	1183
Eastern Shore Tributaries	EE1.1, EE2.1, ET1.1, ET3.2, ET4.2, ET5.2, ET6.2, ET9.1	1886	1832	1762	1848	1886	1866
Western Shore Tributaries	WT1.1, WT2.1, WT5.1, WT8.1	904	870	838	888	904	898

Table 2
Statistical Summary of Current Calibration 1991-2000

Salinity	Bay	Eastern Shore Tribs	Western Shore Tribs	James	York	Rappahannock	Potomac	Patuxent
MD, ppt	0.35	-0.06	-1.60	-0.23	-0.03	0.15	1.03	0.33
AMD, ppt	1.92	1.37	1.81	1.33	1.77	1.69	1.55	1.46
RD, %	10.8	13.1	26.7	14.9	12.1	15.2	17.3	14.4
Chlorophyll	**Bay**	**Eastern Shore Tribs**	**Western Shore Tribs**	**James**	**York**	**Rappahannock**	**Potomac**	**Patuxent**
MD, µg m^{-3}	0.68	-0.04	-10.36	-1.78	-1.40	0.05	3.24	0.54
AMD, µg m^{-3}	4.15	7.47	14.35	7.68	5.40	5.87	9.79	7.43
RD, %	57.6	65.6	65.7	65.4	57.3	60.7	83.5	60.2
Total Nitrogen	**Bay**	**Eastern Shore Tribs**	**Western Shore Tribs**	**James**	**York**	**Rappahannock**	**Potomac**	**Patuxent**
MD, g m^{-3}	0.13	0.46	0.29	0.32	0.18	0.55	0.20	0.49
AMD, g m^{-3}	0.23	0.59	0.55	0.40	0.27	0.57	0.41	0.51
RD, %	33.1	63.8	42.9	54.0	44.2	90.4	31.6	61.7
Total Phosphorus	**Bay**	**Eastern Shore Tribs**	**Western Shore Tribs**	**James**	**York**	**Rappahannock**	**Potomac**	**Patuxent**
MD, g m^{-3}	0.004	0.012	-0.009	-0.002	-0.028	0.028	-0.002	-0.005
AMD, g m^{-3}	0.017	0.033	0.037	0.049	0.036	0.045	0.037	0.035
RD, %	42.2	63.6	49.3	47.2	47.3	73.1	51.6	47.5
Total Susp. Solids	**Bay**	**Eastern Shore Tribs**	**Western Shore Tribs**	**James**	**York**	**Rappahannock**	**Potomac**	**Patuxent**
MD, g m^{-3}	2.21	-6.82	1.89	-11.89	-11.31	-3.59	-3.25	-2.85
AMD, g m^{-3}	12.88	11.16	16.14	25.64	18.41	12.78	14.61	11.17
RD, %	71.0	60.3	97.5	62.7	61.3	59.0	63.0	63.7
Light Attenuation	**Bay**	**Eastern Shore Tribs**	**Western Shore Tribs**	**James**	**York**	**Rappahannock**	**Potomac**	**Patuxent**
MD, m^{-1}	0.17	-0.06	0.17	-0.17	-0.20	-0.06	0.13	-0.98
AMD, m^{-1}	0.43	0.73	1.63	0.95	0.73	0.90	0.79	1.16
RD, %	39.4	38.6	61.6	31.3	32.8	37.1	37.4	46.9
Dissolved Oxygen	**Bay**	**Eastern Shore Tribs**	**Western Shore Tribs**	**James**	**York**	**Rappahannock**	**Potomac**	**Patuxent**
MD, g m^{-3}	-0.21	-0.45	-0.21	0.56	0.94	0.65	0.92	1.08
AMD, g m^{-3}	1.02	1.45	1.27	0.96	1.27	1.11	1.55	1.51
RD, %	13.4	16.8	13.8	11.2	16.6	13.8	21.6	19.5

Table 3
Statistical Summary of Current Model Verification 2002-2011

Salinity	Bay	Eastern Shore Tribs	Western Shore Tribs	James	York	Rappahannock	Potomac	Patuxent
MD, ppt	-0.13	-0.65	-2.06	-0.97	-0.88	-0.34	0.26	-0.18
AMD, ppt	1.68	1.10	2.11	1.41	1.70	1.34	1.11	1.26
RD, %	9.8	11.2	34.9	15.1	11.3	12.0	11.9	12.9
Chlorophyll	**Bay**	**Eastern Shore Tribs**	**Western Shore Tribs**	**James**	**York**	**Rappahannock**	**Potomac**	**Patuxent**
MD, µg m^{-3}	-0.55	-3.50	-12.76	-1.66	-2.51	-1.69	1.99	-3.38
AMD, µg m^{-3}	3.93	7.76	15.15	6.03	5.01	5.51	9.24	8.65
RD, %	49.8	54.2	63.3	56.3	49.2	49.5	76.8	55.9
Total Nitrogen	**Bay**	**Eastern Shore Tribs**	**Western Shore Tribs**	**James**	**York**	**Rappahannock**	**Potomac**	**Patuxent**
MD, g m^{-3}	0.09	0.24	0.17	0.23	0.11	0.33	0.17	0.35
AMD, g m^{-3}	0.20	0.45	0.45	0.29	0.21	0.35	0.27	0.37
RD, %	30.1	44.5	35.7	40.0	33.8	51.3	24.4	45.3
Total Phosphorus	**Bay**	**Eastern Shore Tribs**	**Western Shore Tribs**	**James**	**York**	**Rappahannock**	**Potomac**	**Patuxent**
MD, g m^{-3}	0.001	0.013	-0.001	0.004	-0.024	0.024	0.013	-0.013
AMD, g m^{-3}	0.013	0.025	0.028	0.039	0.032	0.036	0.028	0.030
RD, %	34.6	57.9	46.9	48.0	44.9	63.5	51.3	40.6
Total Susp. Solids	**Bay**	**Eastern Shore Tribs**	**Western Shore Tribs**	**James**	**York**	**Rappahannock**	**Potomac**	**Patuxent**
MD, g m^{-3}	7.13	-0.16	5.13	-4.22	-11.08	-4.05	6.80	-2.49
AMD, g m^{-3}	11.91	9.06	13.15	25.00	18.53	10.61	12.33	11.40
RD, %	89.0	74.6	113.1	71.2	64.7	50.7	89.7	69.7
Light Attenuation	**Bay**	**Eastern Shore Tribs**	**Western Shore Tribs**	**James**	**York**	**Rappahannock**	**Potomac**	**Patuxent**
MD, m^{-1}	0.27	0.19	0.30	0.10	-0.12	-0.25	0.18	-1.18
AMD, m^{-1}	0.48	0.48	1.11	1.26	0.80	0.90	0.51	1.32
RD, %	47.7	29.2	49.8	38.6	38.2	32.3	38.3	43.4
Dissolved Oxygen	**Bay**	**Eastern Shore Tribs**	**Western Shore Tribs**	**James**	**York**	**Rappahannock**	**Potomac**	**Patuxent**
MD, g m^{-3}	-0.05	-0.32	0.32	0.74	0.86	0.65	1.01	1.10
AMD, g m^{-3}	0.99	1.28	1.23	1.09	1.28	1.13	1.59	1.57
RD, %	12.9	14.5	13.7	12.4	16.1	13.9	22.6	20.4

Table 4
Statistical Summary of 2010 TMDL Model 1991-2000

Salinity	Bay	Eastern Shore Tribs	Western Shore Tribs	James	York	Rappahannock	Potomac	Patuxent
MD, ppt	0.04	0.25	-0.73	-1.07	-0.62	-0.24	0.78	0.50
AMD, ppt	1.84	1.15	1.31	1.51	1.40	1.38	1.26	1.20
RD, %	10.3	11.0	19.3	16.8	9.6	12.4	14.1	11.8
Chlorophyll	**Bay**	**Eastern Shore Tribs**	**Western Shore Tribs**	**James**	**York**	**Rappahannock**	**Potomac**	**Patuxent**
MD, µg m^{-3}	-0.15	-0.10	-9.64	-0.72	-1.73	2.34	4.21	2.70
AMD, µg m^{-3}	3.89	7.79	14.39	7.13	5.25	6.94	11.33	9.56
RD, %	54.0	68.4	65.9	60.8	55.7	71.7	96.6	77.5
Total Nitrogen	**Bay**	**Eastern Shore Tribs**	**Western Shore Tribs**	**James**	**York**	**Rappahannock**	**Potomac**	**Patuxent**
MD, g m^{-3}	-0.07	-0.07	-0.10	0.10	-0.06	0.08	-0.08	-0.03
AMD, g m^{-3}	0.16	0.37	0.35	0.23	0.17	0.17	0.33	0.19
RD, %	23.4	40.2	27.6	31.2	28.3	27.1	25.7	22.9
Total Phosphorus	**Bay**	**Eastern Shore Tribs**	**Western Shore Tribs**	**James**	**York**	**Rappahannock**	**Potomac**	**Patuxent**
MD, g m^{-3}	0.006	0.013	-0.013	-0.008	-0.019	0.026	0.006	-0.004
AMD, g m^{-3}	0.017	0.040	0.036	0.046	0.030	0.045	0.033	0.035
RD, %	41.7	75.8	48.0	44.3	39.1	73.2	45.5	47.0
Total Susp. Solids	**Bay**	**Eastern Shore Tribs**	**Western Shore Tribs**	**James**	**York**	**Rappahannock**	**Potomac**	**Patuxent**
MD, g m^{-3}	4.13	-4.92	-1.56	-7.92	-11.02	3.72	-0.29	-2.74
AMD, g m^{-3}	13.55	11.69	14.70	27.42	18.30	16.47	14.95	11.45
RD, %	74.6	63.2	88.8	67.0	61.0	76.0	64.4	65.3
Light Attenuation	**Bay**	**Eastern Shore Tribs**	**Western Shore Tribs**	**James**	**York**	**Rappahannock**	**Potomac**	**Patuxent**
MD, m^{-1}	0.31	0.01	-0.06	0.30	-0.27	0.21	-0.02	-0.82
AMD, m^{-1}	0.53	0.93	2.22	1.45	0.95	1.26	0.85	1.37
RD, %	48.4	49.5	84.0	47.8	42.5	51.8	40.1	55.5
Dissolved Oxygen	**Bay**	**Eastern Shore Tribs**	**Western Shore Tribs**	**James**	**York**	**Rappahannock**	**Potomac**	**Patuxent**
MD, g m^{-3}	-0.14	-0.45	-0.80	0.91	0.90	0.52	0.63	0.44
AMD, g m^{-3}	1.01	1.53	1.72	1.14	1.28	1.09	1.50	1.68
RD, %	13.3	17.8	18.6	13.3	16.7	13.6	20.9	21.7

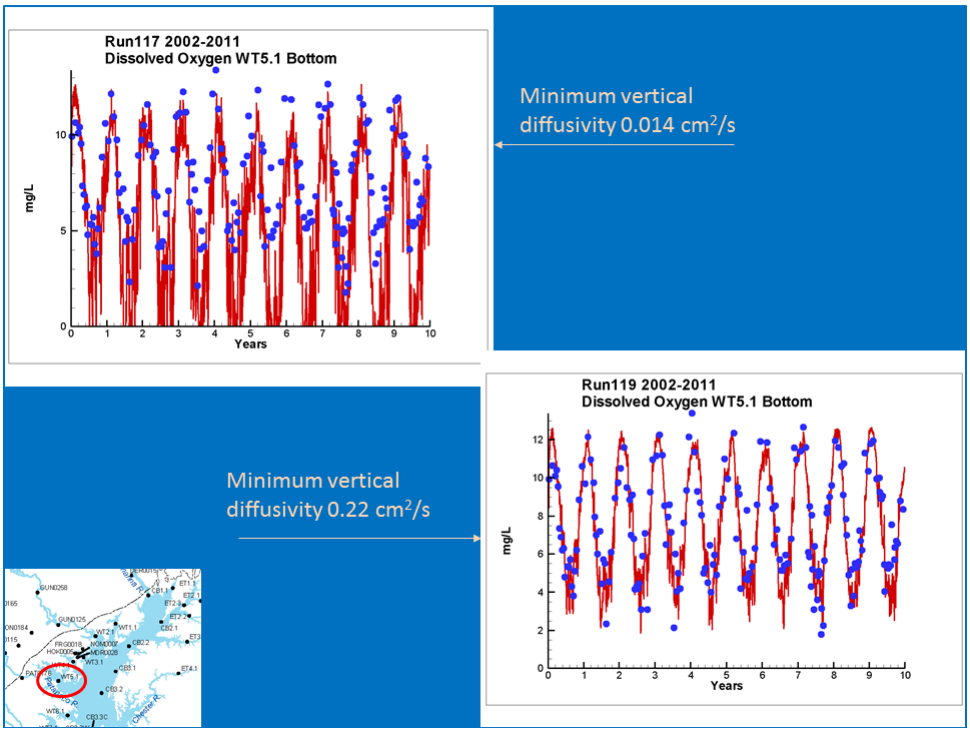

Figure 1. The effect on dissolved oxygen of increasing minimum vertical diffusivity from 0.014 $cm^2\ s^{-1}$ (CH3D) to 0.22 $cm^2\ s^{-1}$ (WQM).

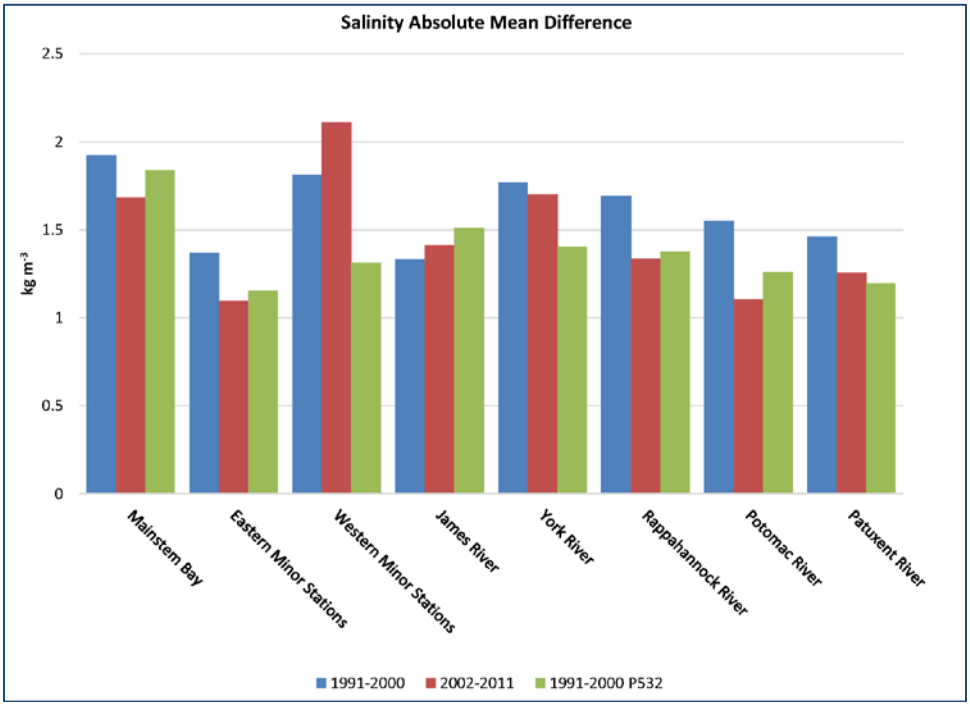

Figure 2. Salinity Absolute Mean Difference statistic.

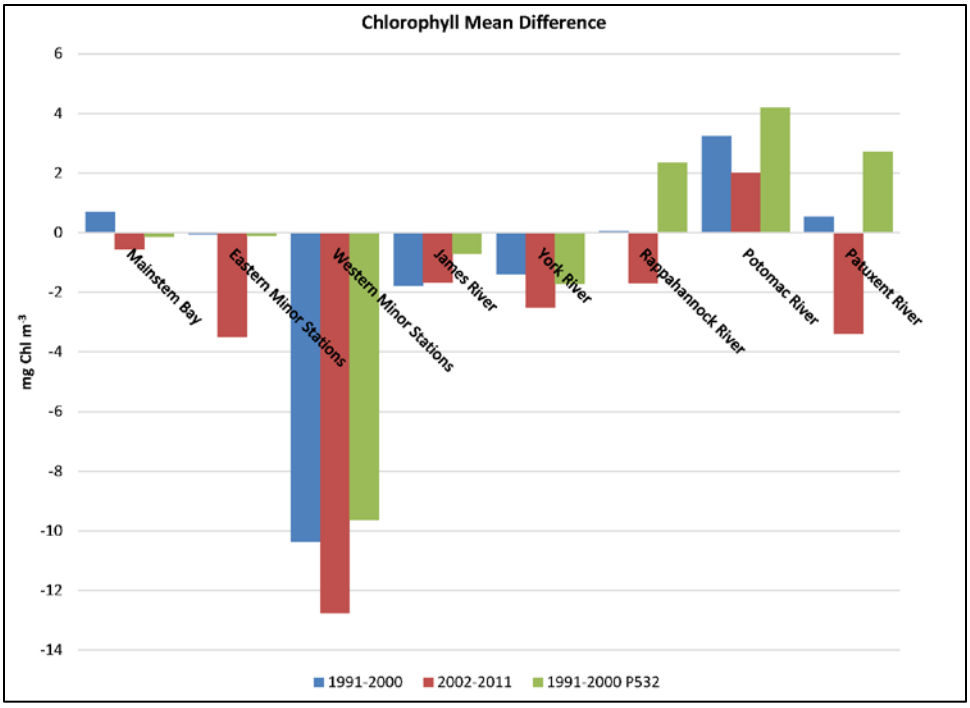

Figure 3. Chlorophyll Mean Difference statistic.

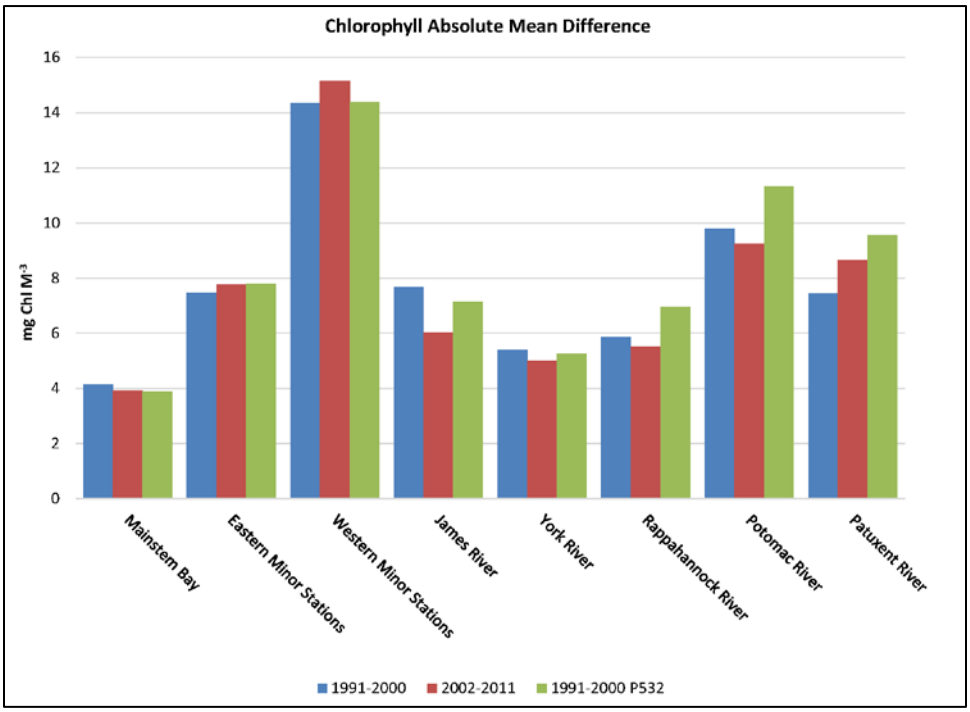

Figure 4. Chlorophyll Absolute Mean Difference statistic.

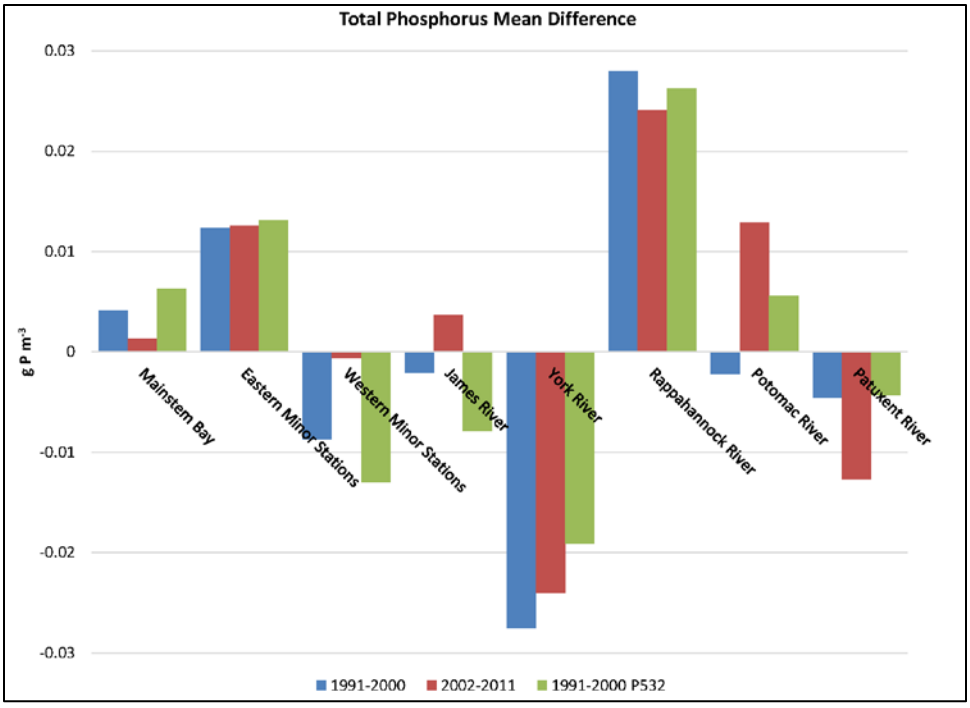

Figure 5. Total phosphorus Mean Difference statistic.

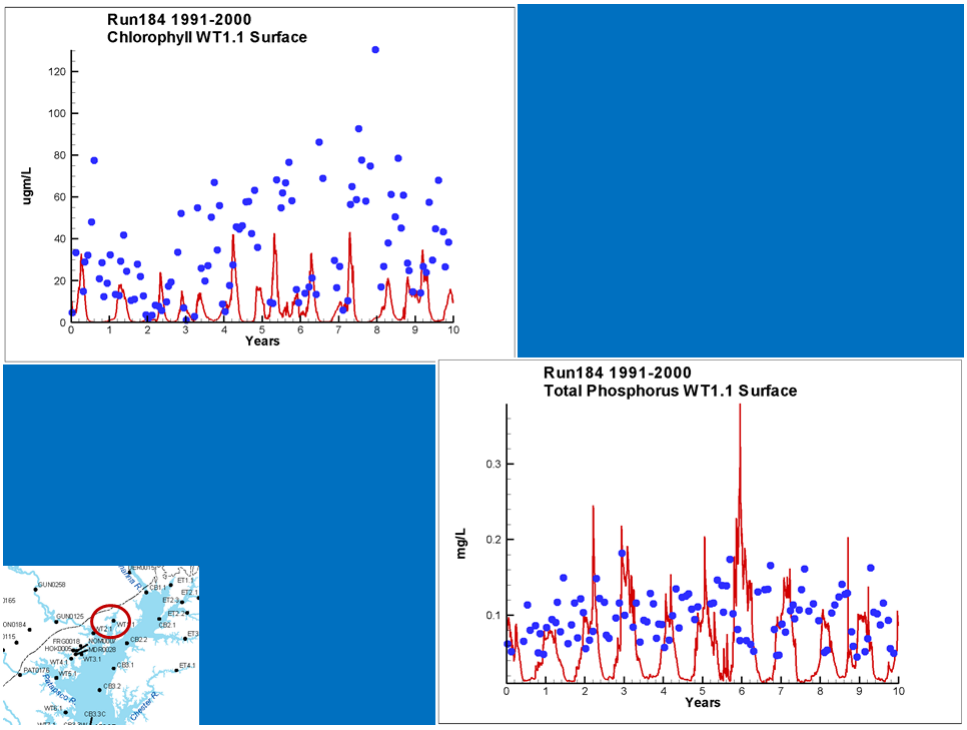

Figure 6. Computed chlorophyll and total phosphorus in the Bush River. Note the shortfall in computed total phosphorus.

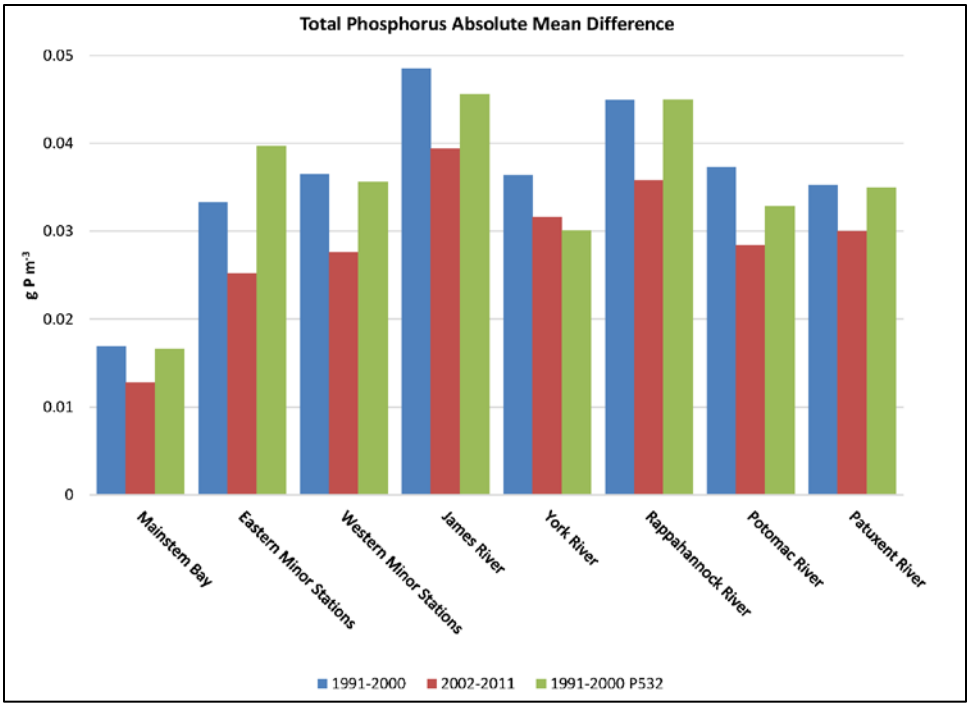

Figure 7. Total phosphorus Absolute Mean Difference statistic.

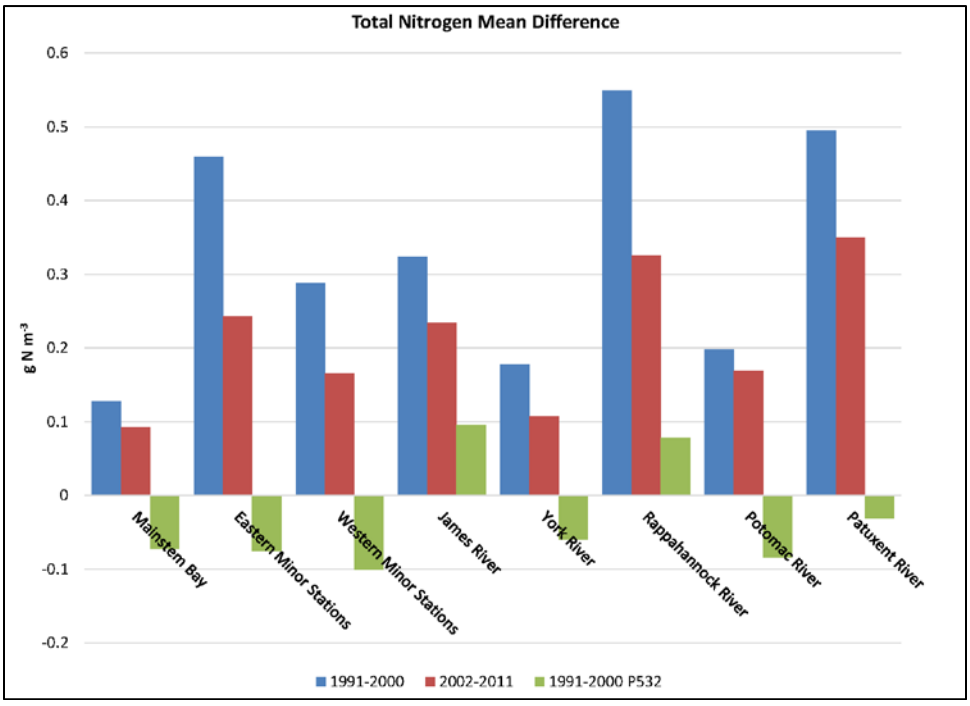

Figure 8. Total nitrogen Mean Difference statistic.

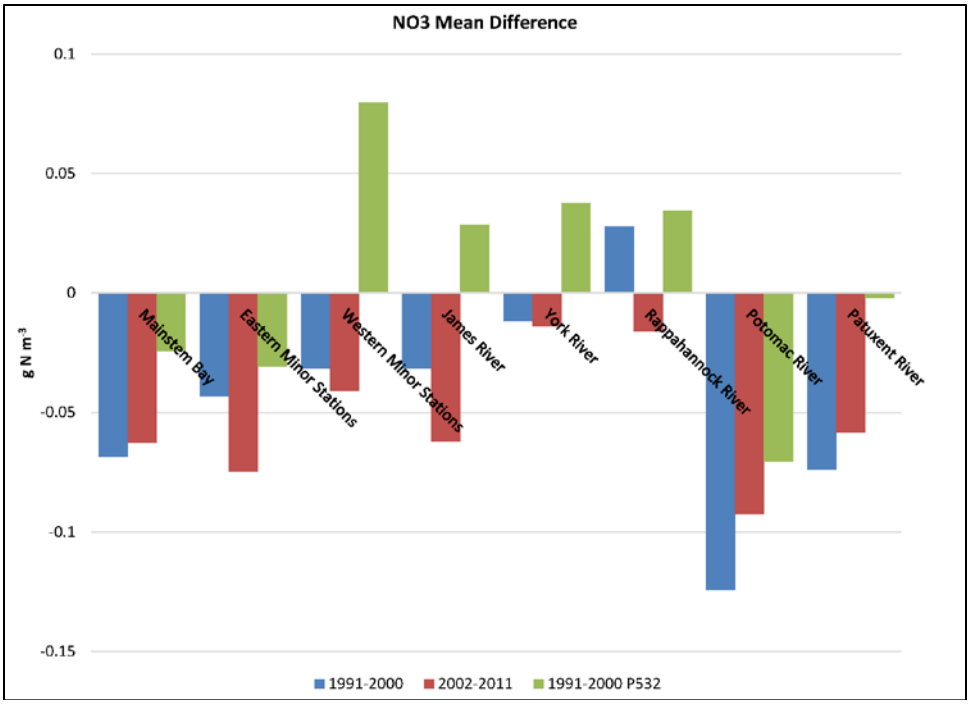

Figure 9. Nitrate Mean Difference statistic.

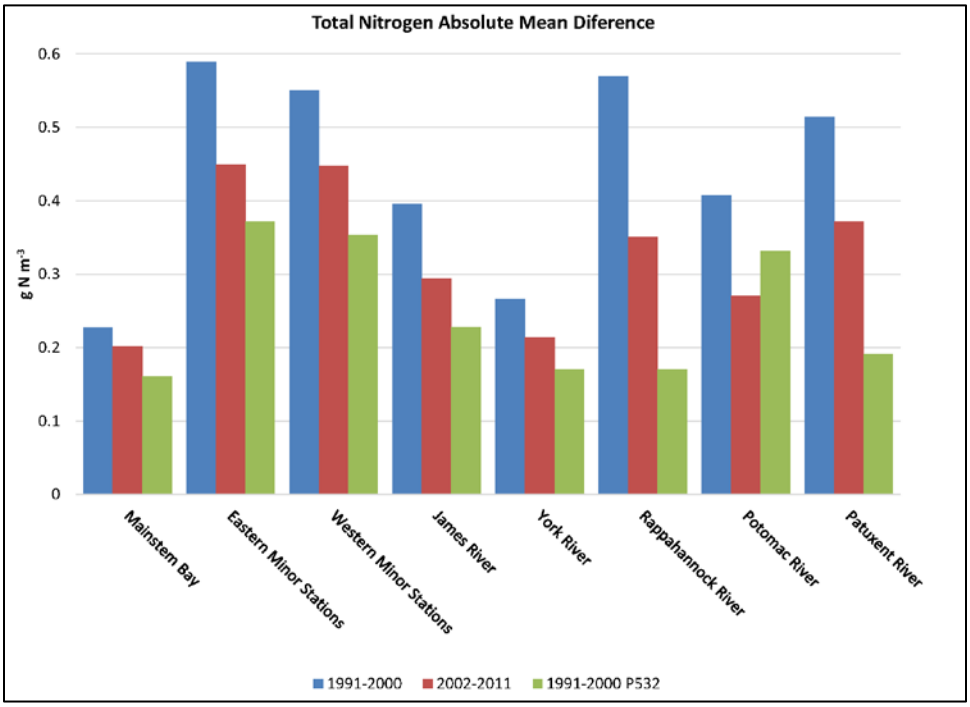

Figure 10. Total nitrogen Absolute Mean Difference statistic.

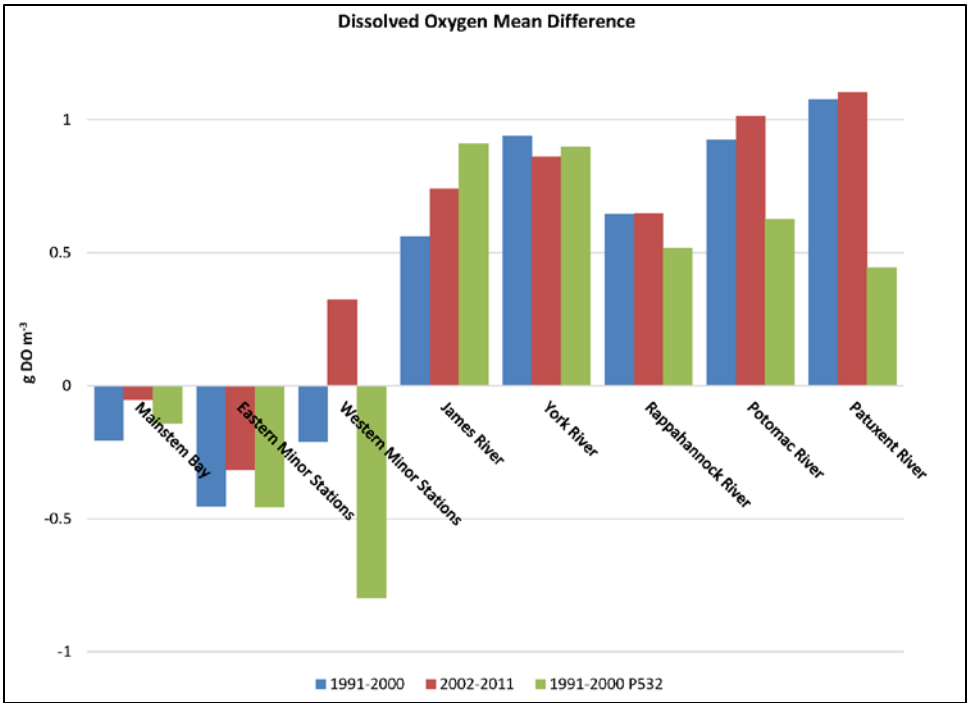

Figure 11. Dissolved oxygen Mean Difference statistic.

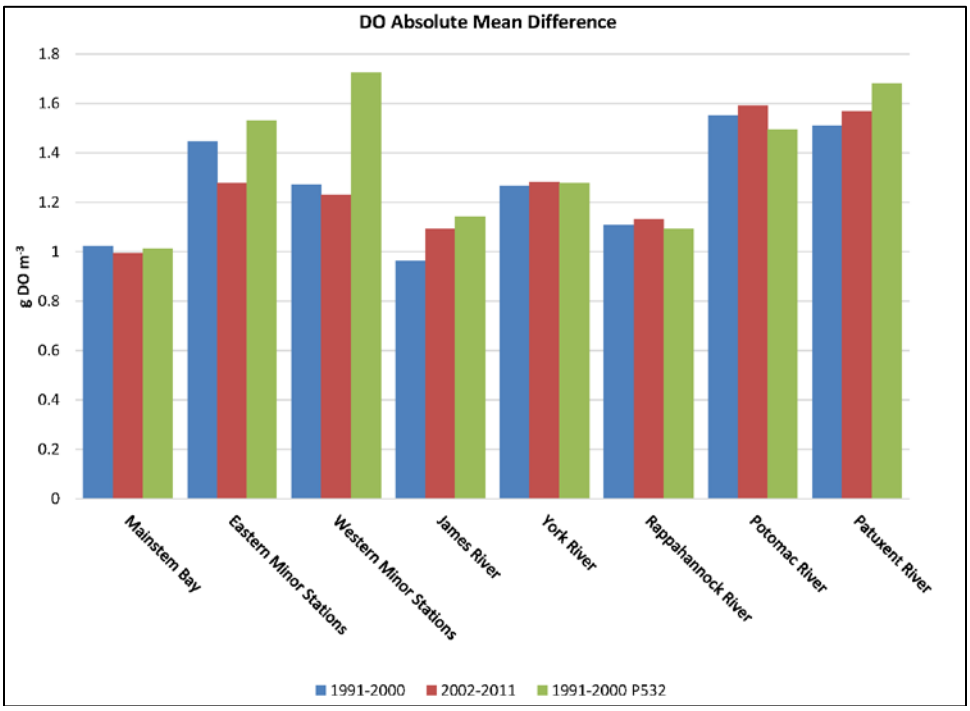

Figure 12. Dissolved oxygen Absolute Mean Difference statistic.

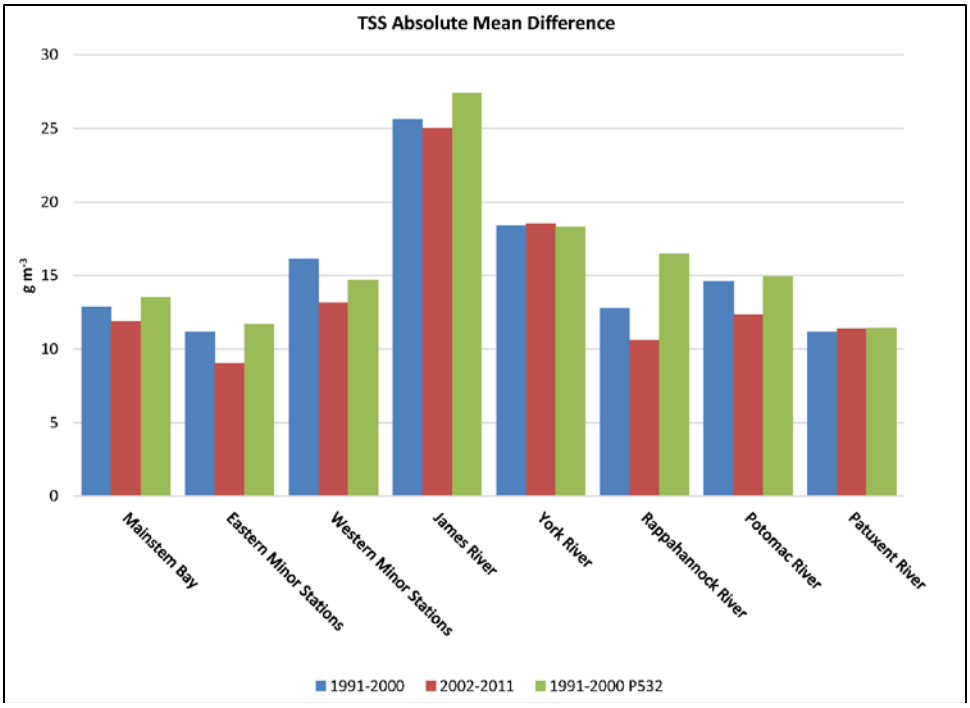

Figure 13. Total suspended solids Absolute Mean Difference statistic.

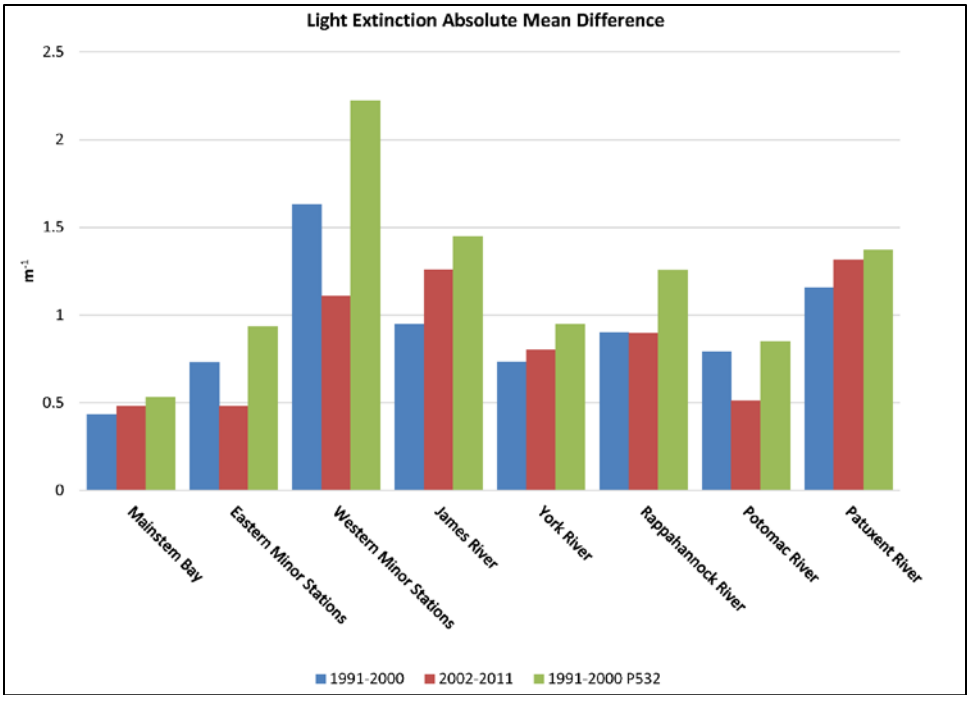

Figure 14. Light extinction Absolute Mean Difference statistic.